



**HAL**  
open science

## Gas-phase chemistry of organocopper compounds

Al Mokhtar Lamsabhi, Manuel Yáñez, Jean-Yves Salpin, Jeanine Tortajada

► **To cite this version:**

Al Mokhtar Lamsabhi, Manuel Yáñez, Jean-Yves Salpin, Jeanine Tortajada. Gas-phase chemistry of organocopper compounds. *PATAI'S Chemistry of Functional Groups*, Wiley, pp.279-346, 2009, 10.1002/9780470682531.pat0440 . hal-00514251v2

**HAL Id: hal-00514251**

**<https://hal.science/hal-00514251v2>**

Submitted on 18 Sep 2023

**HAL** is a multi-disciplinary open access archive for the deposit and dissemination of scientific research documents, whether they are published or not. The documents may come from teaching and research institutions in France or abroad, or from public or private research centers.

L'archive ouverte pluridisciplinaire **HAL**, est destinée au dépôt et à la diffusion de documents scientifiques de niveau recherche, publiés ou non, émanant des établissements d'enseignement et de recherche français ou étrangers, des laboratoires publics ou privés.

## **Gas-Phase Chemistry of Organo-Copper Compounds**

Al-Mokhtar Lamsabhi<sup>a</sup>, Jean-Yves Salpin<sup>b</sup>, Jeanine Tortajada<sup>b</sup> and Manuel Yáñez<sup>a</sup>

<sup>a</sup>Departamento de Química. Universidad Autónoma de Madrid. Cantoblanco. 28049-Madrid. Spain

<sup>b</sup> Université d'Evry Val d'Essonne – Laboratoire d'Analyse et Modélisation pour la Biologie et l'Environnement– CNRS – UMR 8587 – Bâtiment Maupertuis, Boulevard François Mitterrand, 91025 Evry, France

## I. Introduction

Organo-copper compounds play very important roles in chemistry and biochemistry, and they have received a great deal of attention as useful reagents or because they are basic components of proteins and enzymes. Among the former, the so-called blue copper proteins are particularly relevant because they exhibit high reduction potentials. Actually, for some proteins the presence of Cu(II) is required to interact with the appropriate peptides or other proteins to carry out their specific activity. Copper forms also part of oxidation enzymes such as catechol oxidase,<sup>1</sup> peptidylglycine  $\alpha$ -hydroxylating monooxygenase<sup>2</sup> or indophenoloxidase as well as of many other biomolecules like tyrosinase,<sup>3</sup> superoxide dismutase,<sup>4</sup> or copper amine oxidase<sup>5</sup> whose biochemical activity is directly related to the presence of this transition metal in different oxidation states. Not surprisingly, many efforts have been devoted to unravel the mechanisms associated with the biochemical activity of these systems, to determine which is the active site and what is the role played by the metal. Different approaches can be found in the literature with this common objective, but only two subsets can be considered gas-phase investigations, those based on the use of mass spectrometry techniques, and those based on computational models of non-solvated systems. Of course, most of the studies carried out on the proteins or enzymes themselves do not fall in this category, and neither do many other studies, based on the use of appropriate chemistry model systems in the condensed phase. However, a great deal of effort was devoted to understand the intrinsic behavior of these complicated systems, by investigating the interactions of some of its basic components with Cu(I) and Cu(II). In this respect it is important to mention that there are more and more evidences that, more often than expected, the behavior of biochemical systems in the physiological medium

is closer to that shown gas phase than to that shown in solution, reflecting the low polarity of the physiological medium. Good examples are provided by the acidities of uracil and uracil analogues.<sup>6,7</sup> The enhanced intrinsic acidity of the N1 site is consistent with the stability of anionic uracil in the active site of uracil-DNA glycosylase, which is, conversely, contrary to the expectation based on solution acidities.<sup>8,9</sup> Also, it has been found, for instance, that blue copper proteins show structures which are very close (within  $1.7 \text{ kcal mol}^{-1}$ ) to their optimal gas-phase geometries,<sup>10</sup> and that the effects of base stacking and hydrogen bonding on DNA duplexes are similar in gas phase and in solution,<sup>11</sup> although the latter dominate in the gas phase.

This research activity was carried out either through the use of mass spectrometry techniques, through the use of computational models or by a wise combination of both. In the sections which follow we shall present an overview of the reactivity of Cu(I) and Cu(II), the two oxidation states which are more relevant from the chemical viewpoint, with molecules of different size, and different characteristics. Since both oxidation states are present in biochemical media, a great deal of attention was paid, mainly through the use of different mass spectrometry techniques, to the interactions of these two metal ions with small or medium size systems, which are basic components of larger biochemical compounds or which constitute reasonable model compounds of larger and more complicated systems, in an effort to understand their mode of action. A review dealing with copper complexes of a variety of organic and bioorganic molecules experimentally generated by different ionization methods has been recently published, mainly focused on ternary complexes of Cu(II).<sup>12</sup> Hence, we shall not discuss in detail in this chapter this kind of complexes, and we will focus a little bit more on the use of ternary complexes to generate odd-electron ions of biomolecules. On the other hand, in order to keep the number of citations within

reasonable limits we will refer exclusively to papers published in the last ten years, although papers published before 1998 might be quoted if necessary.

Although, gas-phase experimental investigations involving species containing Cu(I) and Cu(II) are numerous, gas-phase experimental results on neutral organo-copper compounds are, on the contrary, very rare. The very few studies reported in the literature are reduced to infrared or photochemical investigations of some small species.<sup>13,14</sup> A section will be devoted to overview the spectroscopic and photochemical of organo-copper compounds and to the photofragmentations produced.

As mentioned above, a great deal of the information on bonding, structure, binding energies, catalytic effects, etc., comes from computational approaches, so we thought it convenient to include in this chapter a section devoted to analyze the performance of the different theoretical models available for the treatment of Cu containing systems as well as the problems which arise depending on the oxidation state of the metal.

Particular attention will be also paid to the coordination of Cu as a function of its oxidation state, because, this coordination sometimes dictates the behavior of many Cu-containing proteins or enzymes.

It is also common that metal cations such as Cu(II) when dissolved in polar liquids show Jahn-Teller distortions, which of course have important effects on its specific interaction with different kind of ligands. Hence, some attention will be also paid to this question.

## **II. Performance of different theoretical models**

Since many of the results on structure, bonding, coordination and other properties of organo-copper compounds to be discussed in forthcoming sections are

based or use computational techniques, we have considered pertinent to begin this chapter by presenting a brief overview on the performance of *ab initio* and density functional theory (DFT) calculations normally used to offer a rationale to the properties of these compounds. For more general and complete analyses of the performance of different computational techniques when dealing with molecular ions in the gas phase the reader is addressed to two general reviews published recently<sup>15,16</sup>, where *ab initio* molecular orbital theory, DFT, quantum Monte Carlo theory and the methods to calculate the rate of complex chemical reactions involving ionic species in the gas phase are analyzed.

Nowadays, it is well established that accounting for electron correlation effects is practically mandatory in any computational method aiming at a correct description of a chemical system. In the framework of the molecular orbital theory this is usually done by using the Møller-Plesset (MPn) perturbation theory, at different orders ( $n = 2, 3, 4, \dots$ ) or coupled cluster (CCSD(T)) approaches. Correlation effects are particularly important when dealing with transition metal ions in general and with Cu(I) and Cu(II) in particular, because they can be considered as highly-correlated systems with significant electron clustering. Therefore, models based on Hartree-Fock (HF) calculations are usually very unreliable. It has been unambiguously shown, for instance, that the HF method yields wrong coordination numbers. This is indeed the case for different mixed complexes between Cu(I) and water and ammonia, where the three-coordination is systematically preferred at the HF level<sup>17</sup>, whereas the inclusion of correlation effects reduces in all cases the level of coordination to two. Similarly, the fact that the HF approach exaggerates the electrostatic and polarization contributions to the stabilization energies results in wrong coordination numbers in  $\text{Cu}(\text{H}_2\text{O})_n^+$  ( $n = 3-6$ ) complexes. Whereas at the HF level the three-coordinated complexes were the most stable minima

for  $n = 3-5$  and the four-coordinated one for  $n = 6$ , the inclusion of electron correlation effects reduces the optimum coordination number to two in all cases.<sup>18</sup> For smaller clusters, in particular for the dehydrated system, the RHF method predicts the  $D_{2d}$  structure to be the only stable form of the complex, while MP2 and CCSD(T) methods predict a lower symmetry ( $C_2$ ) for its ground state. It has also been found that in molecular dynamic simulations based on QM/MM approaches, the inclusion of correlation effects leads to a significant improvement in the characterization of the Jahn-Teller effects observed<sup>19</sup> in the solvation of  $Cu^{2+}$ . Correlation effects are also important when evaluating relative binding energies of  $Cu^+$  to guanine and adenine, where in general, the HF values are too small because they do not account for the stabilizing intersystem correlation energy and do not describe properly the covalent character of the bonds between the metal and the base.<sup>20</sup> Similar findings have been reported for the interactions between  $Cu^+$  and DNA base pairs.<sup>21</sup>

Much less demanding than the MP2 or CCSD(T) methods to account for dynamical correlation effects are the different methods based on the DFT. Among the different methods based on the local density approximation (LDA) or the gradient generalized approximation (GGA), the most commonly used is the B3LYP hybrid functional which combines the Becke's three-parameter nonlocal hybrid exchange potential<sup>22</sup> with the nonlocal correlation functional of Lee, Yang and Parr.<sup>23</sup> This approach has been shown to yield reliable geometries for a wide variety of systems,<sup>24-28</sup> and its performance to describe  $Cu^+$  complexes has been also assessed in different studies. Luna et al.<sup>29</sup> showed that for  $Cu^+$ -nitrogen bases complexes this DFT approach was a very good alternative, as far as binding energies, vibrational frequencies, rotational constants and electron densities were concerned, to high-level *ab initio* methods such as G2 theory of CCSD(T) calculations. Almost simultaneously, in their

study of the complexes of  $\alpha$ -aminoacids with  $\text{Cu}^+$ , Hoyau and Ohanessian,<sup>30</sup> found that the agreement between B3LYP and MP2 optimized geometries was excellent, although the DFT approach places the  $\text{Cu}^+$  ion systematically closer to the basic site of the aminoacid. Later, Sodupe et al.<sup>31</sup> also found that the B3LYP method was very reliable for the study of  $\text{Cu}^+$  and  $\text{Cu}^{2+}$  complexes with glycine. Also importantly, Luna et al.<sup>32</sup> found that the B3LYP method was superior to G2 and other high-level *ab initio* approaches when trying to reproduce the  $\text{Cu}^+$  affinities of a wide set of neutral bases. Similarly, the B3LYP method was found to be superior to MP2 in reproducing the sequential binding energies of  $[\text{Cu}(\text{NH}_3)_n]^+$  ( $n = 1,2,3,4$ ) complexes<sup>33</sup> and the relative  $\text{Cu}^+$  ion affinities of glycine and alanine,<sup>34</sup> although the performance is slightly worse when dealing with absolute values.<sup>35</sup> Klippenstein and Yang<sup>36</sup> also found a reasonably good agreement between CCSD(T) and B3LYP  $\text{Cu}^+$  binding energies, although the latter are almost systematically about 4 kcal mol<sup>-1</sup> higher than the former. As we shall discuss later in a little more detail, Sodupe et al. found for different  $\text{Cu}^{2+}$ -complexes<sup>31,37,38</sup> that functionals with a larger amount of exact exchange than B3LYP, such as B3LYP, yielded results in close agreement with CCSD(T) values.

It is important to emphasize however that not always DFT and MP2 approaches yield the same optimized geometries for  $\text{Cu}^+$ -complexes. This is the case, for instance, for some aromatic compounds including benzene. DFT methods favor for benzene- $\text{Cu}^+$  complex the less symmetric ( $C_s$ )  $\eta^2$  structure, whereas the MP2 method yields as the ground state a  $C_{6v}$   $\eta^6$  conventional  $\pi$ -complex.<sup>39</sup> A similar behavior was reported for phenylsilane- $\text{Cu}^+$  and phenylgermane- $\text{Cu}^+$  complexes.<sup>40</sup> Also, while the MP2 method predicts a  $\eta^6$  conventional  $\pi$ -structure for the complexes of aniline and phenol with  $\text{Cu}^+$ , the B3LYP approach yields as global minima  $\eta^1$  complexes in which the metal ion is bonded to the *para* carbon atom.<sup>41,42</sup> More importantly, when correlation corrections are



included beyond second order by carrying out quadratic configuration interaction calculations (QCISD) the structures predicted by the DFT approach are clearly stabilized with respect to MP2 results. As a matter of fact, for benzene, QCISD/6-311G(d,p) calculations predict both the  $\eta^6$  conventional  $\pi$ -complex found at the MP2 level and the  $\eta^2$  structure found when the B3LYP approach is used, to be local minima of the potential energy surface (PES), the former being only slightly more stable. For phenol and aniline, both  $\eta^1$  and  $\eta^6$  structures are also found to be practically degenerate.<sup>41</sup> The origin of the stabilization of these lower symmetry structures in which the metal cation interacts specifically with a CC bond will be discussed later on, when analyzing the behavior of other unsaturated systems.

An added difficulty inherent to the theoretical treatment of transition metal ions is the existence of different states close in energy, so non-dynamical correlation effects may also be important, in which case single-reference methods, as most of the standard *ab initio* and density functional approaches become unreliable. For the particular case of Cu(I) this situation is aggravated by the fact that, very often, more than one solution is obtained in the HF calculations which is the origin of dramatic failures when the G2 approach is used to evaluate Cu(I) binding energies. As a matter of fact, when more than one HF solution exist none is a good representation of the wave function, and even high-correlated methods based on them become unreliable.<sup>43</sup> This is already the case when dealing with  $\text{CuH}^+$ , the simplest system containing  $\text{Cu}^+$ , where two different HF solutions can be found, leading to wrong descriptions of the ion even at the CCSD(T) level of theory.<sup>43</sup> The situation is even worse for  $\text{CuO}^+$  where up to three different HF solutions can be found.<sup>32</sup> The most dramatic consequence is that when the standard G2 procedure, as implemented in the Gaussian series of programs,<sup>44</sup> is used, both  $\text{CuH}^+$  and  $\text{CuO}^+$  are predicted to be unbound. For the particular case of  $\text{CuO}^+$ , this unphysical

result is due to the fact that the G2 standard procedure starts from an unstable HF wavefunction. In principle, such solutions can be discarded “a priori” by analyzing the stability of the HF wave function or by obtaining the right orbitals in the initial guess of the HF calculations.<sup>45</sup> Nevertheless, as we have mentioned above, when more than one HF solutions are found none of them is a good zeroth order wave function and as a consequence, even when the right orbitals are chosen, the G2 and CCSD(T) estimated binding energies are still off with respect to the experimental value by more than 15.5 and 14.3 kcal mol<sup>-1</sup>, respectively.<sup>45</sup>

It must be also taken into account that in Gn theories, the correlation energy is estimated by assuming additivity of partial contributions evaluated at different levels, by means of the MPn perturbation series which for Cu(I)-containing systems converges very slowly. As illustrated in Figure 1, already for the bare Cu<sup>+</sup> ion the MPn series up to fifth order presents significant oscillations, and these oscillations increase significantly when the basis set includes diffuse components and high angular momentum polarization functions.<sup>32</sup> This pathological behavior is typically found in systems which present a significant electron clustering,<sup>46</sup> and is not exclusive of Cu(I) containing systems, but it has been also found in other transition metal ions, such as, Ni<sup>+</sup>. For instance NiOH<sup>+</sup> or Ni(OH)<sub>2</sub><sup>+</sup> present two and four different HF solutions within 2.5 kcal mol<sup>-1</sup> energy gap, respectively.<sup>47</sup> Ni<sup>+</sup>(<sup>2</sup>D) presents also similar strong oscillations of the MPn perturbation terms.<sup>48</sup>

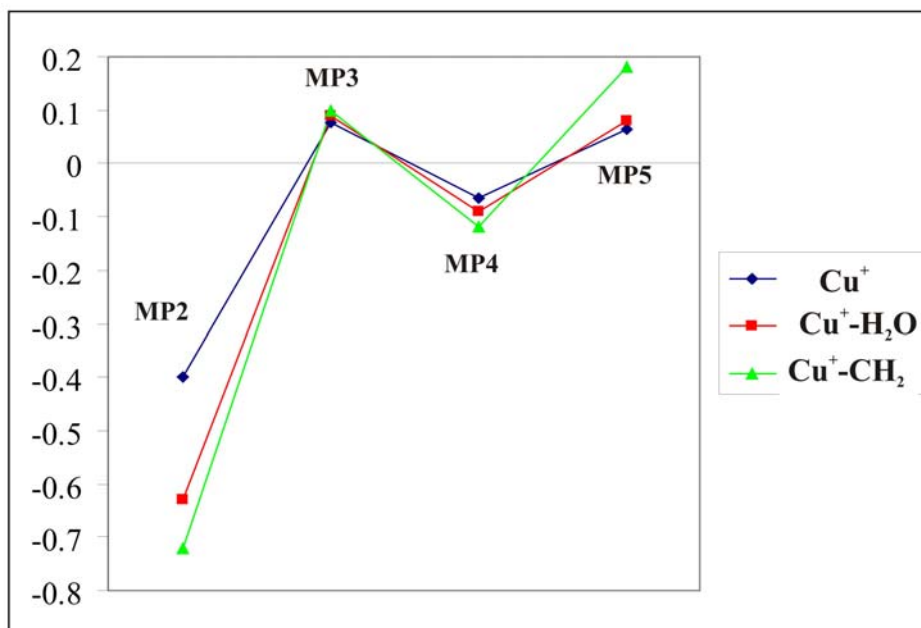


**Figure 1.** Electron correlation energies (hartrees) evaluated using the MPn ( $n = 2, 3, 4, 5$ ) perturbation series for  $\text{Cu}^+$  and its complexes with  $\text{H}_2\text{O}$  and  $\text{CH}_2$ , showing that this perturbative series converge very slowly for  $\text{Cu}^+$  containing systems. Values taken from ref. 32

Interestingly, the behavior of different density functional approaches is much more regular, and for those cases in which several HF solutions exist, only a unique solution is found when the density functional theory is used.<sup>43,47</sup> Furthermore, it has been shown that the B3LYP/6-311+G(2df,2p) calculations on B3LYP/6-311G(d,p) optimized geometries yielded Cu(I) binding energies in very good agreement with the known experimental values.<sup>32</sup> This is probably one of the reasons why most of the computational studies reported on Cu containing systems have been performed by using this DFT approach.

The situation is however slightly different as far as the next oxidation state of Cu is considered. On the one hand, and to the best of our knowledge no pathological behaviors have been described regarding *ab initio* calculations on Cu(II) complexes, in spite of the fact that Cu(II) is an open-shell species. On the other hand, there are some interesting differences with respect to Cu(I) concerning the performance of different

DFT approaches. It has been shown<sup>38</sup> using  $\text{Cu}(\text{H}_2\text{O})^{2+}$  as a suitable model system, that a correct description of its ground state depends significantly on the degree of mixing of the exact Hartree-Fock and DFT exchange functionals. MP2 and CCSD(T) calculations predicted for this complex a  $C_{2v}$  symmetry associated to a  ${}^2A_1$  state. This is not an unexpected result taking into account that the  $3d_z^2$  orbital is the one with larger overlap with  $\text{H}_2\text{O}$  and the larger this overlap the larger the metal-ligand repulsion is and therefore the less stable becomes the corresponding electronic state. This is nicely reflected in the Cu-O distance which follows the same trend as the electronic states stability:  ${}^2A_1 < {}^2B_1 < {}^2B_2 < {}^2A_2$ . In contrast, most of the different hybrid and non-hybrid functionals found as global minimum a  $C_s$  structure associated to a  ${}^2A'$  ground state, and only the BHLYP approach, where equal amounts of Hartree-Fock and DFT exchange are used, reproduced the CCSD(T) results. In fact, it was shown that within the  $C_{2v}$  symmetry the relative stabilities of the different electronic states is rather sensitive to the proportion of exact exchange introduced in the functional. The origin of this discrepancy is that both LDA and GGA functionals usually overestimate the stability of delocalized situations, as those associated with  $C_s$  structures in contrast with  $C_{2v}$  ones where the electron hole is more localized at the metal ion. This problem is significantly reduced by increasing the contribution of the exact exchange, explaining the good behavior of the BHLYP method. For some systems larger than  $\text{Cu}(\text{H}_2\text{O})^{2+}$  it was found that this effect is not very significant,<sup>49</sup> but it cannot be concluded that this will be, in general, the behavior to be expected. Hence, when dealing with Cu(II) compounds, it is convenient to verify if the results obtained are sensitive to the amount of exact exchange included in the functional.

It is important to note that, as indicated above, Cu(II) is an open-shell system and the possible spin contamination in the corresponding unrestricted treatment can be

in some specific cases important and it may render DFT calculations completely unreliable.<sup>50</sup>

### III. Ligand field spectroscopy and photofragmentation processes

Ligand-field spectroscopy has been considered traditionally a very useful technique in organometallic chemistry, but experiments are usually undertaken in the condensed phase. This implies that the solvent and the presence of a counter-ion significantly limit the knowledge one can gain on the structure of the chromophore from the spectral transitions. However, significant advances have been made in the last decade in the spectroscopy and photodissociation studies of size-selected metal ion complexes in the gas phase. Using a laser vaporization technique combined with a supersonic beam expansion,  $\text{Cu}^+$ -furan complexes were generated and analyzed by means of time-of-flight mass spectrometry techniques.<sup>51</sup> A ground-state binding energy of 37 kcal/mol for this complex<sup>51</sup> could be estimated from the photofragment spectra. Similarly, neutral Cu-benzene complexes,  $\text{Cu}_n(\text{benzene})_m$  were produced in the gas phase by using the laser vaporization method and characterized by mass spectrometry, photoionization spectroscopy, and chemical probe experiments.<sup>13</sup> Although, only the complexes with  $n = 1$  and  $m = 1, 2$  were generated their benzene-Cu binding energies could be measured. The values obtained, 0.18 and 0.22 eV, respectively are small and lower than those measured for early transition metals like Sc or Ti.<sup>13</sup> This is due to the fact that Cu has the  $d$  shell completely full, so no  $d-\pi$  interactions but repulsive interactions between the  $4s$  orbital and the benzene ligand should be expected.

Photodissociation experiments have also been reported for  $\text{Cu}^+$ -pyridine complexes.<sup>52</sup> These complexes were obtained by combining the laser ablation technique with a supersonic molecular beam. Although when this technique is used, up to five

pyridine molecules are coupled to  $\text{Cu}^+$ , only the photofragmentation of the monomer  $\text{Cu}^+$ -pyridine complex was investigated by irradiating with UV light in the 202-284.1 nm wavelength range. Even though one can reasonably expect the positive charge of the complex to be localized on the metal, since Cu has a lower ionization energy (7.72 eV) than pyridine (9.25 eV),<sup>53</sup> pyridine<sup>+</sup> was the only photoproduct detected in the experiments carried out. This means that photodissociative process induced intramolecular ligand-to-metal charge transfer.

Similar experiments on  $\text{Cu}^+$ -ketone (acetone, 2-butanone, 3-methyl-2-butanone and 2-pentanone) complexes showed<sup>54</sup> a significant different behavior to that outlined above for  $\text{Cu}^+$ -pyridine complexes. In this case the photofragmentation was produced by using UV radiation at 266 nm, which should correspond to ligand excitation. The first important finding is that no charged  $\text{L}^+$  fragments are observed for any of the ketones investigated, in clear contrast also with the behavior of  $[\text{Ag}(\text{acetone})]^+$  complex.<sup>55</sup> The same behavior was observed when the number of ligands is greater than 2, in which case the loss of neutral ligands to produce very stable  $[\text{CuL}_2]^+$  ions clearly dominates over bond cleavage processes within the ligand. Conversely, when the number of ligands is one or two there are significant differences between the different ketones as well as respect to  $\text{Cu}^+$ -pyridine complexes. For instance,  $[\text{Cu}(\text{acetone})]^+$  does not show any photodissociation, whereas 2-butanone and 2-pentanone lose both  $\text{CH}_3$  and the complementary alkyl group simultaneously or sequentially, indicating that 266 nm photons have enough energy to cleave two  $\alpha$  C-C bonds in the ligand. For 3-methyl-2-butanone the dominant dissociation process corresponds to the loss of  $\text{CH}_3$ . When the number of ligands is 2, with the only exception of 3-methyl-2-butanone, the dominant photofragment is  $[\text{CuLCO}]^+$ , which once more involves the cleavage of two  $\alpha$  C-C bonds. In  $[\text{Cu}(3\text{-methyl-2-butanone})]^+$  complexes only one metal-ligand bond is broken

and the dominant product is  $[\text{CuL}]^+$ . Very recently, a photofragmentation and theoretical study of  $[\text{Cu}-(\text{PhOH})(\text{PhO})]^+$  complex<sup>42</sup> showed that the phenolate anion interacts with the metal preferentially through the oxygen atom, which is accompanied by an electron transfer which locates the unpaired electron on the aromatic moiety. Furthermore, the bond strength between copper and the oxygen atom of the phenoxy radical is weakened by the presence of neutral phenol.

The spectroscopic information of complexes involving neutral Cu and organic ligands is almost inexistent, and we are only aware of the ZEKE (zero kinetic energy) photoelectron study of pyridine-Cu complex.<sup>14</sup> In this study, it was found that the ionization energy of the Cu-pyridine complex was 2.308 eV smaller than that of the free Cu atom, indicating a significant stabilization upon ionization. Using these data and the known binding energy for the  $\text{Cu}^+$ -pyridine complex, it was possible to obtain for the binding energy of the Cu-pyridine complex a value of  $5.5 \pm 2.4 \text{ kcal mol}^{-1}$ . However, this value was estimated using the first reported CID binding energy for the  $\text{Cu}^+$ -pyridine complex,<sup>56</sup> which is too low as compared with the one measured by means of photodissociation techniques<sup>52</sup> as well as to the new reported CID value.<sup>57</sup> If this new CID value is used instead, the Cu-pyridine binding energy amounts to  $9.5 \pm 2.4 \text{ kcal mol}^{-1}$  which is in reasonably good agreement with the B3LYP/6-311+G\*\* calculated value ( $12.1 \text{ kcal mol}^{-1}$ ).<sup>58</sup> Also interestingly, the shift in the ionization energy observed for Cu-pyridine complex with respect to  $\text{Cu}^{14}$  is larger than that measured using similar techniques,<sup>59</sup> for  $\text{CuNH}_3$ , which means that the  $\text{Cu}^+$ -pyridine binding energy is larger than the  $\text{Cu}^+$ - $\text{NH}_3$  one.

One of the difficulties associated with the spectroscopical investigation of  $\text{Cu}^{2+}$ -complexes is that the preparation in the gas phase of these doubly charged species is a challenge, because many of them are unstable with respect to charge transfer or to

proton loss. Nevertheless, even in these cases the ligand-field photochemistry of the resulting monocations offers important insights on their structure and reactivity. A paradigmatic example is offered by the study of Spence et al.<sup>60</sup> on the  $[\text{Cu}(\text{II})(\text{bpy})(\text{serine-H})]^{++}$  complex generated by means of electrospray ionization. In this study, the photodissociation of the serine moiety triggered by the excitation of a *d-d* transition is compared with the CAD of this ion complex, previously investigated by Turecek et al.<sup>61</sup> who proposed the scheme shown in Figure 2 to account for the four peaks observed on the CAD spectra. Ligand-field excitation of the aforementioned complex at 575 nm triggers photofragmentation reactions yielding three of the four products observed in CAD and metastable decomposition of  $[\text{Cu}(\text{II})(\text{bpy})(\text{serine-H})]^{++}$  complex, dissociation product (**5**) being absent. Although a detailed mechanism for the observed photofragmentations could not be established, the formation of products **2** and **3** follows the loss of  $\text{H}_2\text{CO}$ , whereas the formation of **4** follows the bond cleavage between Cu and the amino nitrogen of serine. Interestingly, the sum of the branching ratios for the formation of **2** and **3** (0.46) is comparable to that observed for CAD and metastable decomposition (0.44), which was taken as an indication that the barriers to elimination of formaldehyde and transfer of OH followed by the loss of  $\text{H}_2\text{CCHNH}_2\text{CO}_2$  must be rather similar and much lower than the photon energy (2.16 eV).



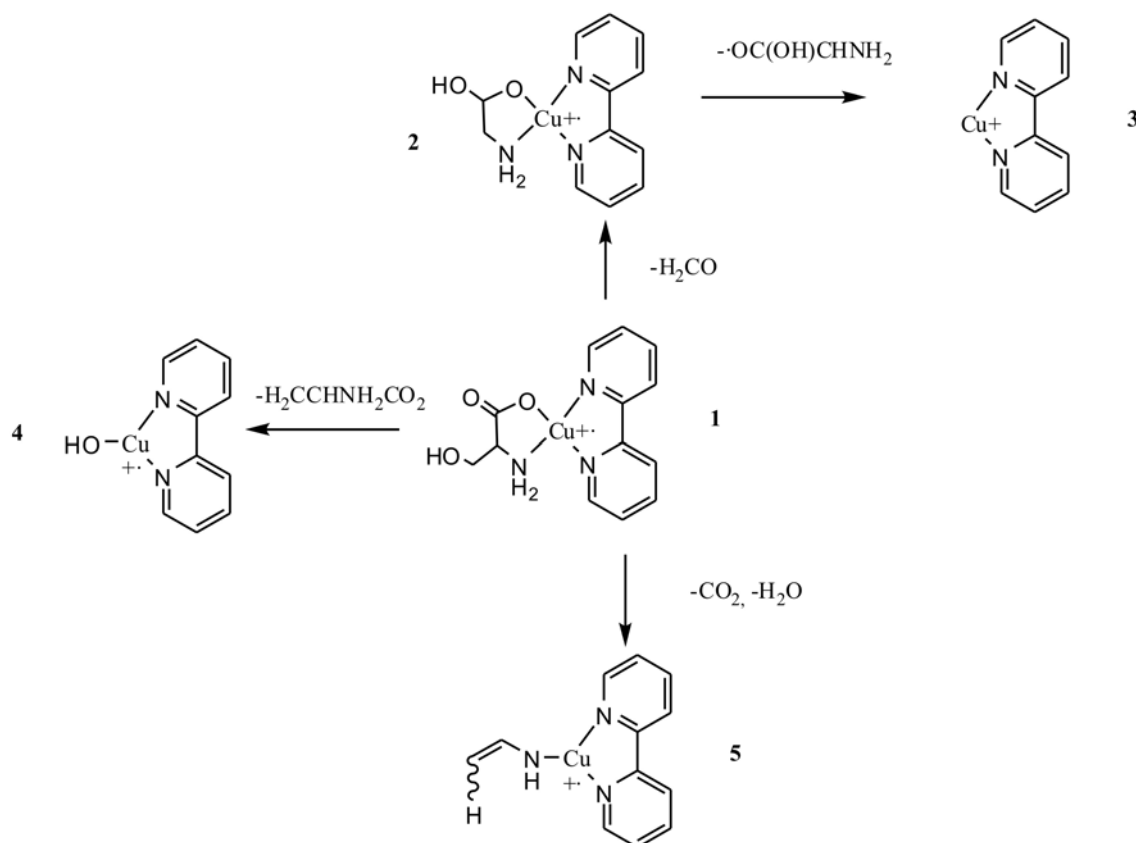


**Figure 2.** Reaction scheme mechanism proposed by Turecek et al.<sup>61</sup> for CAD of  $[\text{Cu}(\text{II})(\text{bpy})(\text{serine-H})]^+$  complex in the gas phase.

The advantage of being able to investigate transition metal ion complexes in which the metal is in a high oxidation state is that very often, as for Cu, this is the state in which they are found in solution or in the physiological medium. Hence, significant efforts have been devoted to the generation of  $\text{Cu}^{2+}$ -complexes in the gas phase. Although the number of the attempts that succeeded to do so are not much, it is important to discuss here the pioneering work of Stace and co-workers<sup>54,62-64</sup> who were able to produce  $[\text{Cu}(\text{pyridine})_n]^{2+}$  ( $n = 4-7$ ) and  $\text{Cu}[(\text{acetone})_n]^{2+}$  ( $n = 4-8$ ) complexes in the gas phase in order to study their photofragmentation. A detailed description of the modern experimental setup used by this group to study the photofragmentation of doubly charged species in the gas phase can be found in references<sup>65</sup> and<sup>66</sup>. The goal of these investigations, as those carried out on singly charged species, was to determine

whether *d-d* excitations within the metal ion can lead to metal-to-ligand charge transfer or whether the excitation of the ligand leads to a photofragmentation of the complex.  $[\text{Cu}(\text{pyridine})_4]^{2+}$  when UV irradiated at about 280 nm, which in principle can excite pyridine to either the  $S_1(n\pi^*)$  or the  $S_2(\pi\pi^*)$  state,<sup>67</sup> loses a neutral pyridine molecule, with practically no evidence of dissociative charge transfer. This is in clear contrast with the behavior observed<sup>54</sup> in the case of  $[\text{Cu}(\text{acetone})_4]^{2+}$  when light of 26 nm is employed. In this case, after excitation, the complex loses one neutral and one charged acetone molecule, the product of the reaction being a singly charged  $[\text{Cu}(\text{acetone})_2]^+$  species. This can be taken as an indication<sup>54</sup> that two acetone molecules are enough to stabilize a  $\text{Cu}^{2+}$  ion in the gas phase, while three molecules of pyridine are needed to produce a similar effect. The fragmentation of larger  $[\text{Cu}(\text{pyridine})_n]^{2+}$  complexes exhibit a pattern with very abrupt transitions yielding  $[\text{Cu}(\text{pyridine})_4]^{2+}$  as the dominant product, likely indicating a very large stability for this complex. Again the behavior of  $[\text{Cu}(\text{acetone})_n]^+$  systems when  $n \geq 5$  is different. For  $n = 5$  two acetone molecules are lost yielding a tri-coordinated  $[\text{Cu}(\text{acetone})_3]^+$  complex,<sup>54</sup> while no photodissociations were observed after excitation of this doubly charged species. It is also worth mentioning that the fragmentations undergone by  $[\text{Cu}(\text{acetone})_4]^{2+}$  under collision-induced dissociation (CID) conditions<sup>68</sup> differ from those observed upon UV irradiation, since after losing one neutral acetone molecule, a charge transfer process leads to two stable singly charged species, namely,  $[\text{Cu}(\text{acetone})]^+$  and  $[\text{Cu}(\text{acetone})_2]^+$ , pointing to quite different mechanism behind both kind of processes. When the ligand was 2-butanone, 2-pentanone and 3-methyl-2-butanone, the reactivity pattern was also different. For the latter no photofragmentations were detected under any circumstances. However, for the other two ketones, when the number of ligands around the metal ion was 5, one and two ligands were lost, the former process being, for both 2-butanone and

2-pentanone dominant. Also for the particular case of 2-butanone, a very small proportion of charge transfer leading to  $[\text{Cu}(2\text{-butanone})_3]^+$  singly charged ions was detected. For  $n = 6$ , only the loss of two neutral ketone molecules was observed.

The nature of the photofragments when  $[\text{Cu}(\text{pyridine})_n]^{2+}$  ( $n = 4-7$ ) are irradiated with visible light in the range of 450-1000 nm does not change with respect to that observed when UV light was used,<sup>62</sup> and a loss of neutral pyridine is observed, although the mechanism is certainly different. Using  $\text{Ar}_3^+$  as reference, the molar extinction coefficient for the transitions recorded around 600 nm, which corresponds to spin-allowed  $d-d$  transitions in Cu(II),<sup>69</sup> was  $100 \text{ L mol}^{-1} \text{ cm}^{-1}$ . This value is lower than that measured for Ag(II) complexes ( $500 \text{ L mol}^{-1} \text{ cm}^{-1}$ ) for which the charge transfer mechanism clearly dominates. Furthermore, the extinction coefficient estimated for  $[\text{Cu}(\text{pyridine})_4]^{2+}$  is in good agreement with the values reported for spin-allowed  $d-d$  transitions in Cu(II)-complexes in aqueous solutions.<sup>69-71</sup> They correspond to transitions from the  $d_{xz}$  and  $d_{yz}$  into the antibonding  $d_{x^2-y^2}$  and are very likely also responsible for the observed absorption spectra in the gas phase. For the smallest  $[\text{Cu}(\text{pyridine})_3]^{2+}$  complex investigated, it was found<sup>64</sup> that when irradiated in the same region, a weak signal associated with the loss of one charged pyridine unit was detected, leaving a stable  $[\text{Cu}(\text{pyridine})_2]^+$  ion. Interestingly, this finding is consistent with the results observed in CAD experiments carried out by the same group.<sup>65</sup> The same behavior has been observed for  $[\text{Cu}(\text{picoline})_n]^{2+}$  ( $n = 3-6$ ) complexes,<sup>64</sup> where  $[\text{Cu}(\text{picoline})_3]^{2+}$  photodissociates by losing a  $(4\text{-picoline})^+$  ion, whereas larger complexes just lose a neutral picolone molecule. However, the corresponding absorption bands appear slightly blue-shifted with respect to those of the corresponding pyridine complexes.

Although in recent years the number of studies on metal cation complexes using infrared multiphoton dissociation techniques (IRMPD) has grown dramatically, mainly

due to the availability of free-electron laser (FEL) facilities, very few of these efforts were focused on doubly charged complexes, and even less on  $\text{Cu}^{2+}$  containing systems. As a matter of fact we are only aware of the paper published by Wu et al.<sup>66</sup> in which the infrared multiphoton spectrum for  $[\text{Cu}(\text{pyridine})_4]^{2+}$  complexes was recorded. This technique is indeed an interesting complementary tool of visible or UV photofragmentations, even for systems with high binding energies. Although the energy required to dissociate a  $[\text{Cu}(\text{pyridine})_4]^{2+}$  complex into  $[\text{Cu}(\text{pyridine})_3]^{2+} + \text{pyridine}$  is as large as  $59.8 \text{ kcal mol}^{-1}$ , which is equivalent to the energy of about 21 IR photons, the available experimental setups can trigger the sequential absorption of up to 40 photons. In the IRMPD study of the  $[\text{Cu}(\text{pyridine})_4]^{2+}$  complex, a line-tunable  $\text{CO}_2$  laser over the range of  $910\text{-}1090 \text{ cm}^{-1}$  was used.<sup>66</sup> The assignment of the signals observed was guided through the use of DFT calculations, which showed that the only structure that was compatible with a band at  $1042 \text{ cm}^{-1}$ , accompanied by a much weaker one which is only detected when the laser power is increased, was a  $D_{4h}$  square-planar one,<sup>66</sup> (see Figure 3)

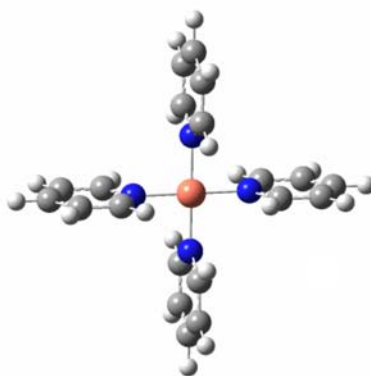


**Figure 3.**  $D_{4h}$  structure of the  $[\text{Cu}(\text{pyridine})_4]^{2+}$  complex.

These results are in line with previous DFT calculations which showed that indeed the  $D_{4h}$  structure is the ground state for  $[\text{Cu}(\text{pyridine})_4]^{2+}$  complexes, the  $D_{2h}$  and the  $D_{2d}$  conformers being at least  $14.3 \text{ kcal mol}^{-1}$  higher in energy.<sup>64</sup>

New IRMPD studies carried out by the same group on  $[\text{}^{63}\text{Cu}(\text{pyridine})_4]^{2+}$  at a laser power of 550mW, introduced some variations with respect to previous photodissociations using UV and visible light.<sup>66</sup> In these IR experiments there is a charge transfer, the dominant product being  $\text{C}_5\text{H}_5\text{N}^+$ . However, the fact that there is no complementary  $[\text{}^{63}\text{Cu}(\text{pyridine})_3]^+$  was interpreted<sup>66</sup> as the reaction pathway being sequential, so that the first step is the loss of neutral pyridine from  $[\text{}^{63}\text{Cu}(\text{pyridine})_4]^{2+}$ , the same reaction path observed in UV and visible photofragmentations, which is followed by the photoexcitation of  $[\text{}^{63}\text{Cu}(\text{pyridine})_3]^+$  to yield  $\text{C}_5\text{H}_5\text{N}^+$  and  $[\text{}^{63}\text{Cu}(\text{pyridine})_2]^+$ .

Finally it should be mentioned that some absorption spectra of Cu(II) complexes with bacteriochlorin<sup>72</sup> and texaphyrin<sup>73</sup> have been theoretically investigated in an effort to investigate the potential behavior of these molecules as photosensitizers in photodynamic therapy.

#### IV. $\text{Cu}^+$ and $\text{Cu}^{2+}$ binding energies

The number of experimental  $\text{Cu}^+$  binding energies is really scarce and even scarcer if one excludes inorganic compounds such as  $\text{NH}_3$ ,  $\text{H}_2\text{O}$ ,  $\text{H}_2\text{S}$  etc. A good compilation was published in 1996 by Freiser,<sup>74</sup> but after this compilation not many new values have been reported in the literature dealing with organic compounds, and most of the  $\text{Cu}^+$  binding energies known to date come from *ab initio* or DFT calculations. This is indeed the case as far as  $\text{Cu}^{2+}$  binding energies are concerned due to the difficulty in generating long-lived  $\text{Cu}^{2+}$ -complexes in the gas phase.

Since the development of what are usually called high-level *ab initio* methods, it was possible to obtain thermodynamic magnitudes within chemical accuracy ( $\pm 1$  kcal mol<sup>-1</sup>). Hence, very accurate *ab initio* calculations could be used to anchor gas-phase ion affinity scales, or to detect some anomalous experimental values. Cu<sup>+</sup> affinities present nice examples of both situations. In some other cases, theory was ahead of experiment predicting Cu<sup>+</sup> binding energies before they were experimentally known. Quite interestingly, in many cases these predictions were very accurate. This is the case, for instance, for a series of different aromatic compounds, whose experimental Cu<sup>+</sup> binding energies published in 2007<sup>75</sup> agreed very well with previous calculated values reported in 2004<sup>40</sup> and 2006.<sup>41</sup>

An absolute Cu<sup>+</sup> affinity scale for all aminoacids (see Table 1), was built up by combining a rather accurate CCSD(T) Cu<sup>+</sup> affinity value for glycine with the experimental relative scale reported by Cerda and Wesdemiotis<sup>76</sup> for all the aminoacids. This scale was expanded some years later by incorporating theoretical estimates for both the Cu<sup>+</sup> and Cu<sup>2+</sup> affinities of (glycyl)<sub>n</sub>glycine (n = 1-3) oligomers (see Table 1) obtained by means of B3LYP calculations.<sup>31</sup> These values differ slightly from those obtained previously by Shoeib et al.<sup>77</sup> using the same method but a smaller basis set. For both oxidation states of the metal, due to larger electrostatic interactions, the binding energies increase as the peptide chain becomes longer.<sup>31</sup> The gap between Cu<sup>+</sup> and Ag<sup>+</sup> binding energies in glycine (glycyl)<sub>n</sub>glycine series was also found to increase as the size of the ligand increases.<sup>77</sup>

Later on, new theoretical estimates of Cu<sup>+</sup> affinities of some  $\alpha$ -aminoacids were reported by the group of N. Russo<sup>34,35,78</sup> but these values did not differ substantially from those obtained by Hoyau and Ohanessian.<sup>30</sup> It is worth mentioning that in some of these studies Cu<sup>+</sup> was found to bind neutral bases systematically stronger than

$\text{Ag}^+$ .<sup>33,58,79</sup> Also, in some of these publications  $\text{Cu}^+$  affinities were found to be significantly larger than  $\text{Li}^+$  affinities.<sup>34,40,80</sup> Although in some cases this was attributed to simple differences in the electrostatic interactions between the metal cation and the base,<sup>34</sup> in forthcoming sections we will have the opportunity to show that the enhanced  $\text{Cu}^+$  affinities reflect a non-negligible covalent character in the  $\text{Cu}^+$ -ligand interactions.

**Table 1.** Affinities for  $\text{Cu}^+$  (in  $\text{kcal mol}^{-1}$ ) of  $\alpha$ -aminoacids<sup>a</sup> and some of its oligomers. The values within brackets correspond to  $\text{Cu}^{2+}$  binding energies

Amino acid	$\text{Cu}^+$ affinity	Amino acid	$\text{Cu}^+$ affinity
glycine	64.3 (68.1) <sup>b</sup> (68.6) <sup>c</sup> (67.1) <sup>d</sup> [214.8] <sup>b</sup> [205.2] <sup>d</sup> [242.7] <sup>e</sup>	tyrosine	72.5
alanine	65.9 (68.2) <sup>d</sup> [220.7] <sup>d</sup>	cysteine	72.9 [268.1] <sup>g</sup>
serine	67.4	glutamine	74.0
valine	67.9	methionine	74.6
leucine	68.4	tryptophan	75.7
isoleucine	68.6	histidine	77.6
threonine	68.8	lysine	>77.6
proline	69.1	arginine	>77,6
aspartic acid	69.3	$\text{GG}^{\text{f}}$	87.5 <sup>e</sup> (80.3) <sup>c</sup> [256.4] <sup>e</sup>
asparagine	70.9	$\text{GGG}^{\text{f}}$	97.5 <sup>e</sup> (94.8) <sup>c</sup> [301.7] <sup>e</sup>
glutamic acid	71.5	$\text{GGGG}^{\text{f}}$	104.7 <sup>e</sup> [338.1] <sup>e</sup>
phenylalanine	72.2		

<sup>a</sup> The values reported, except the values within parenthesis, were taken from ref. 30 and were obtained by combining an accurate theoretical estimate for the  $\text{Cu}^+$  affinity of glycine with the relative experimental scale reported in ref. 76.

<sup>b</sup> value obtained at the CCSD(T) level using B3LYP geometries taken from ref. 81

<sup>c</sup> Values obtained at the MP2(fc)/ 6-311++G(2df,2p)//B3LYP/DZVP level taken from ref. 77

<sup>d</sup> BHandHLYP/6-311++G\*\* calculated values taken from ref. 35

<sup>e</sup> B3LYP calculated values taken from ref. 31

<sup>f</sup> GG, GGG and GGGG stands for diglycine, triglycine and tetraglycine.

<sup>g</sup> B3LYP calculated value taken from ref. 78

$\text{Cu}^+$  affinities for biochemical systems other than  $\alpha$ -aminoacids or their oligomers have also been published, although most of them correspond to theoretical estimates. As a matter of fact, and to the best of our knowledge only the experimental  $\text{Cu}^+$  affinity of adenine has been reported.<sup>82</sup> B3LYP/6-311+G(2df,2p)  $\text{Cu}^+$  binding energies for uracil, thymine, cytosine, guanine and adenine were published by Russo et al.<sup>83</sup> (See Table 2). Those for uracil and all the thiouracil derivatives, at the same level, were also published by Lamsabhi et al.<sup>84</sup>. The agreement between the calculated<sup>83</sup> and the experimental values<sup>82</sup> for adenine is fairly good.

Not much experimental information is available either on  $\text{Cu}^+$  affinities to alkanes. Nevertheless, a compilation of B3LYP/6-31G\* calculated values for the first twelve members of the series, excluding heptane and nonane was reported in 2001,<sup>80</sup> showing a clear increase along the series which becomes clearly attenuated as the length of the chain increases (see Figure 4). A similar behavior was found for complexes with poly-ethylene glycols (PEG),<sup>80</sup> although the absolute binding energies are much larger. For both series of compounds the calculated  $\text{Cu}^+$  affinities are significantly larger than  $\text{Na}^+$  affinities, pointing to quite different bonding patterns as we shall discuss in forthcoming sections.



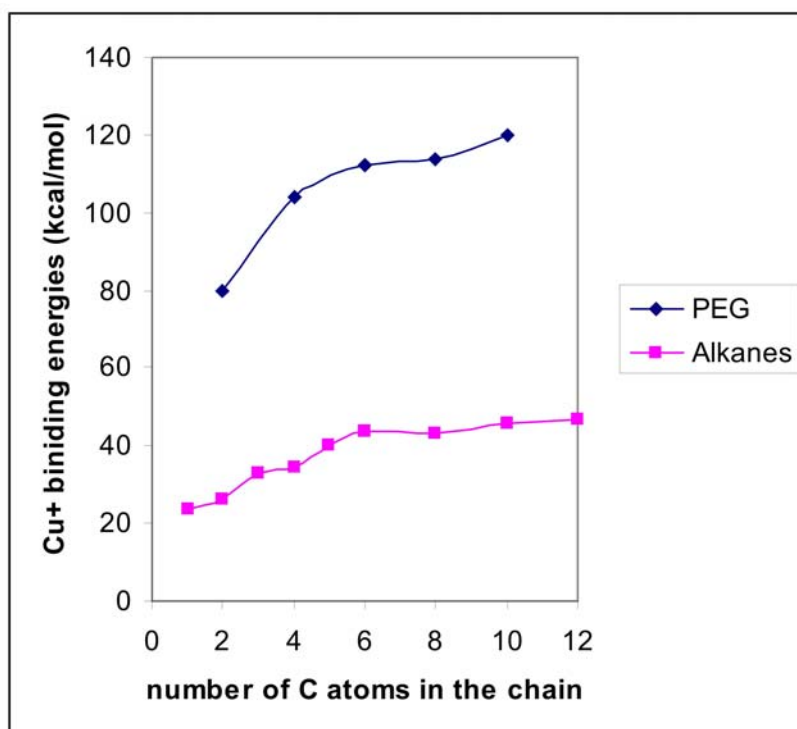


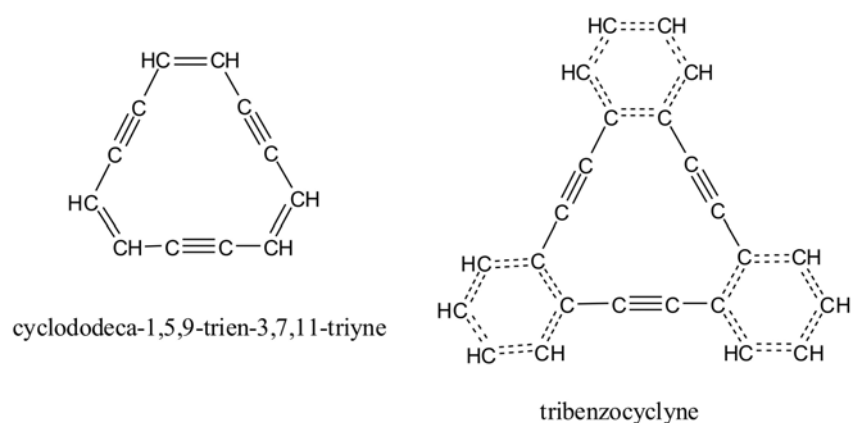
**Figure 4.** B3LYP/6-31G\*  $\text{Cu}^+$  binding energies for  $\text{Cu}^+$ -*n*-alkane and  $\text{Cu}^+$ -poly(ethylene glycol) (PEG) complexes as a function of the number of carbon atoms in the chain. Values taken from ref. 80

B3LYP/6-311+G(2df,2p)  $\text{Cu}^+$  affinities of small saturated and unsaturated bases containing N, P and As as active sites<sup>85-87</sup> show that unsaturated systems are systematically less basic than their saturated analogues. For methanimine ( $\text{H}_2\text{C}=\text{NH}$ ) only the nitrogen attached species was found to be stable, whereas for methylenphosphine ( $\text{H}_2\text{C}=\text{PH}$ ) and methylenarsine ( $\text{H}_2\text{C}=\text{AsH}$ ) both C- and heteroatom-attached species are local minima of the PES. For  $\text{H}_2\text{C}=\text{AsH}$  the carbon attached complex is the global minimum. For methyldynephosphine (HCP) and methyldynearsine (HCAs) only the carbon attached species have been found.<sup>85</sup> One year later, an experimental value for the  $\text{Cu}^+$  affinity of acetonitrile was reported.<sup>88</sup> As expected, this value was larger than that calculated for the unsubstituted parent compound (HCN)<sup>85</sup> and only slightly smaller than that predicted for methanimine.<sup>85</sup> It is worth noting that, although the same trend was found for their proton affinities, the

gap is significantly larger ( $17.2 \text{ kcal mol}^{-1}$ )<sup>53</sup> when the reference acid is a  $\text{H}^+$  than when it is a  $\text{Cu}^+$  ion ( $2.3 \text{ kcal mol}^{-1}$ ) (see Table 2).

In spite of the fact that the interactions between ethylene and transition metal ions received much attention because this compound is a good prototype to understand the behavior of unsaturated organic ligands in bond-activation process and catalysis, its experimental  $\text{Cu}^+$  affinity is still not known with precision. In 1990, Fisher and Armentrout<sup>89</sup> published a lower bound for the  $\text{Cu}^+$ -ethylene binding energy of  $23 \text{ kcal mol}^{-1}$  which is about half the value estimated by using reasonably accurate quantum chemistry methods.<sup>90</sup> This motivated a revision of the aforementioned experimental value using mass spectrometry techniques in which an equilibrium between  $(\text{H}_2\text{O})\text{Cu}^+$  or  $(\text{NH}_3)_n\text{Cu}^+$  ( $n = 1,2$ ) and  $(\text{C}_2\text{H}_4)\text{Cu}^+$  was tried to be established. Combining the calculated  $\text{NH}_3\text{-Cu}^+$  binding energy<sup>91</sup> with the fact that according to the aforementioned experiments the bond dissociation energy of  $\text{NH}_3\text{-Cu}^+$  exceeds that of  $\text{C}_2\text{H}_4\text{-Cu}^+$  at least by  $6 \text{ kcal mol}^{-1}$ , a more realistic experimental value for the ethylene  $\text{Cu}^+$  affinity of  $44\text{-}50 \text{ kcal mol}^{-1}$  was proposed.<sup>90</sup> Later on, using guided-ion beam mass spectrometry techniques, the mono- and the bis-ethylene complexes with  $\text{Cu}^+$  were studied by collisionally dissociating the complex ions with xenon.<sup>92</sup> The new  $\text{Cu}^+$  affinity so obtained ( $42 \pm 3 \text{ kcal mol}^{-1}$ ), was not far from the previous experimental range. Posterior theoretical estimates obtained at the CCSD(T) and B3LYP levels,<sup>36</sup> are in reasonably good agreement with this new experimental range (see Table 2). Also surprisingly, and to the best of our knowledge, no precise experimental  $\text{Cu}^+$  affinities have been reported for acetylene. However, the CCSD(T) and B3LYP estimates are reasonably close and within the range  $40\text{-}44 \text{ kcal mol}^{-1}$ ,<sup>36</sup> although an older MP2 value is slightly lower ( $36.2 \text{ kcal mol}^{-1}$ ).<sup>93</sup> The new B3LYP estimated value for the  $\text{Cu}^+$  affinity for benzene reported in the aforementioned publication<sup>36</sup> was in very good agreement with a previous value

obtained using the variable reaction coordinate transition state theory.<sup>94</sup> Also, estimates for the  $\text{Cu}^+$  affinity of coronene, cyclododeca-1,5,9-trien-3,7,11-triyne and tribenzocyclyne (see scheme 1), which are interesting ligands in organometallic chemistry, were reported.<sup>94</sup> The  $\text{Cu}^+$  affinity of coronene was predicted to be 5 kcal mol<sup>-1</sup> larger than that of benzene, reflecting the larger polarizability of the former. However, tribenzocyclyne binds  $\text{Cu}^+$  almost twice as strongly as benzene, because the corresponding  $\text{Cu}^+$  complex is planar, with the metal cation inserted directly into the ligand cavity, fact that had been postulated before by Dunbar et al.<sup>95,96</sup>



**Scheme 1**

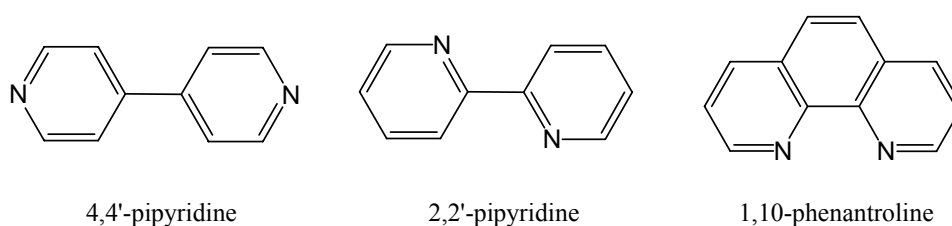
As expected, the  $\text{Cu}^+$  affinities measured for pyridine and pyrimidine are larger than that of benzene<sup>75,97</sup> (see Table 2), but for the former the reported values differ significantly depending on the experimental procedure used to obtain them, the binding energy measured in photodissociation experiments (65.5 kcal mol<sup>-1</sup>)<sup>52</sup> being much higher than the one obtained by means of threshold collision-induced dissociation experiments (58.7±2.4 kcal mol<sup>-1</sup>).<sup>56</sup> The reported calculated values do not solve completely this dichotomy because the MP2 estimates are closer to the CID experiments (57.8 kcal mol<sup>-1</sup>), whereas the B3LYP estimates (65.5 kcal mol<sup>-1</sup>)<sup>58</sup> agree

better with the values obtained in photodissociation experiments. More recent CID measurements<sup>57</sup> yield a value ( $62.7 \text{ kcal mol}^{-1}$ ) which seems to support both the value obtained in photodissociation experiments and by B3LYP calculations. For imidazole, the agreement between the experimental values obtained in collision-induced dissociation experiments and the B3LYP/6-311+G(2d,2p) calculated values is very good. Interestingly, in parallel with their behavior in protonation processes, imidazole was found to be more basic than pyridine when  $\text{Cu}^+$  is the reference acid (see Table 2). However, the gap between the  $\text{Cu}^+$  affinities is more than three times larger than the gap between the corresponding proton affinities. Conversely, pyrimidine, which is a weaker base than pyridine in protonation process<sup>53</sup> was predicted to be slightly more basic<sup>98</sup> than pyridine when the reference acid is  $\text{Cu}^+$ , if for the pyridine  $\text{Cu}^+$  affinity the CID value is adopted.<sup>56</sup> However, if either the photodissociation value<sup>52</sup> or the new CID<sup>57</sup> are used, pyridine would still be more basic than pyrimidine with respect to  $\text{Cu}^+$ , which seems to support these last two estimates. Luna et al. have shown<sup>85</sup> for different series of organic bases the existence of a rough correlation between  $\text{Cu}^+$  affinities and proton affinities, however, these correlations depend significantly in the nature of the basic site. Hence, the correlations found for P- and As- containing bases present similar slopes, but very different from that found for the corresponding N-containing analogues. This seems to point out to significant dissimilarities between proton and  $\text{Cu}^+$  association processes, even if in the latter the covalent character, which is very important in the former, is not negligible.

Recently, a compilation of the  $\text{Cu}^+$  affinities of a large series of aromatic compounds obtained by means of threshold collision-induced dissociation techniques has been published.<sup>75</sup> It is worth mentioning that several of these experimental values, namely those of phenol, toluene, aniline were in very good agreement with calculated

values obtained at the B3LYP level and reported in the literature several years in advance.<sup>40,41</sup> As indicated in a previous section, the  $\text{Cu}^+$  binding energy to furan was measured by means of photodissociation techniques and the experimental value is very well reproduced by CCSD(T) calculations.<sup>51</sup>

Of particular interest are the comparisons of the  $\text{Cu}^+$  affinity of dimethoxyethane (DXE)<sup>99</sup> and dimethylether (DME)<sup>100</sup> and those of pyridine, 4,4'-bipyridine, 2,2'-bipyridine and 1,10-phenanthroline (see Scheme 2), which illustrate the chelating effect when the metal ion interacts with bidentate ligands. Since DXE is bidentate it binds more strongly to  $\text{Cu}^+$  than DME. However, while the second DME molecule binds to  $\text{Cu}^+$  slightly more strongly than the first one, the second DXE is bound much weakly than the first one. As we shall discuss later on, this is related to the fact that for  $\text{Cu}^+$  dicoordination is strongly favored through the participation of *sd* hybrids, which reduces metal ligand repulsion. This is also consistent with the fact that  $\text{Cu}^+$  binds a second DXE molecule much more strongly than the third and fourth DME ligands.



**Scheme 2**

2,2'-bipyridine and 1,10-phenanthroline exhibit very strong binding as compared to pyridine or 4,4'-bipyridine, because the latter behave as monodentate ligands, while the former yields chelated complexes in which  $\text{Cu}^+$  is simultaneously bound to the two ring nitrogens. This means that although the *trans* isomer is by far the most stable structure of 2,2'-bipyridine, the interaction with  $\text{Cu}^+$  triggers an internal rotation around the single

bond connecting both aromatic rings in order to facilitate the interaction of the metal ion with both N atoms. This is also reflected in the incremental binding energies of these systems as we shall discuss at the end of this section.

A compilation of DFT calculated interaction energies between  $\text{Cu}^{2+}$  and typical bidentate ligands, namely, ethyl xanthate, ethyl trithiocarbonate, dithiobutyric acid, ethyl dithiocarbamate, diethyl dithiocarbamate, diethylphosphinecarbodithioic acid and diethoxyphosphinecarbodithioic acid showed<sup>101</sup> that the stronger interactions occur for dithiocarbamates, in agreement with their ability as powerful collectors.<sup>102</sup> The  $\text{Cu}^{2+}$  binding energies to dimethyl dithiocarbamate were also calculated at the DFT level.<sup>103</sup>

Table 2.  $\text{Cu}^+$  affinity (in  $\text{kcal mol}^{-1}$ ) of different organic compounds

Compound	$\text{Cu}^+$ affinity	Compound	$\text{Cu}^+$ affinity
uracil	59.9 <sup>a</sup> ; 54.8 <sup>b</sup>	vinylarsine	53.9 <sup>o</sup>
2-thiouracil	63.2 <sup>b</sup>	ethynylphosphine	55.3 <sup>p</sup>
4-thiouracil	65.9 <sup>b</sup>	ethynylarsine	51.2 <sup>p</sup>
2,4-dithiouracil	67.1 <sup>b</sup>	methylidynephosphine	47.0 <sup>n</sup>
thymine	60.0 <sup>a</sup>	methylarsine	58.5 <sup>n</sup>
cytosine	80.2 <sup>a</sup>	methylenarsine	51.3 <sup>n</sup>
guanine	88.0 <sup>a</sup>	methylidynearsine	51.8 <sup>n</sup>
adenine	70.3±2.5 <sup>c</sup> ; 69.0 <sup>a</sup>	dimethylether	44.3±2.8 <sup>q</sup>
methane	23.6 <sup>d</sup>	dimethoxyethane	63.1±1.8 <sup>r</sup>
ethane	26.0 <sup>d</sup>	benzene	52±5 <sup>s</sup> ; 50.6 <sup>t</sup> ; 51.9±1.4 <sup>u</sup> ; 50.3 <sup>v</sup>
propane	32.9 <sup>d</sup> ; 28.3 <sup>e</sup>	toluene	52.7 <sup>s</sup> ; 52.3±2.2 <sup>u</sup>
butane	34.5 <sup>d</sup>	phenylsilane	51.8 <sup>w</sup>
pentane	40.4 <sup>d</sup>	phenylgermane	52.9 <sup>w</sup>
hexane	43.6 <sup>d</sup>	phenol	52.1 <sup>x</sup> ; 50.3±2.8 <sup>u</sup>

octane	43.2 <sup>d</sup>	aniline	59.8 <sup>x</sup> ; 60.2±2.5 <sup>u</sup>
decane	46.0 <sup>d</sup>	benzaldehyde	52.2 <sup>x</sup>
dodecane	47.0 <sup>d</sup>	benzoic acid	55.9 <sup>x</sup>
ethylene glycol	79.6 <sup>d</sup>	trifluormethyl benzene	41.7 <sup>x</sup>
acetonitrile	57.0 <sup>f</sup>	pyridine	58.7±2.4 <sup>y</sup> ; 65.5 <sup>z</sup> 57.8 <sup>aa</sup> ; 65.7 <sup>bb</sup> ; 62.7 <sup>cc</sup>
ethylene	44-50 <sup>f</sup> ; 45.4 <sup>g</sup> ; 42.2 <sup>h</sup> 46.5 <sup>e</sup> ; 43.4 <sup>i</sup> ; 42.0±3 <sup>j</sup>	4,4'-dipyridine	63.0 <sup>dd</sup>
acetylene	40.3 <sup>h</sup> ; 43.9 <sup>e</sup>	2,2'-dipyridine	88.5 <sup>ee</sup>
ethylsilane	40.8 <sup>i</sup>	1,10-Phenanthroline	94.4 <sup>ff</sup>
ethylgermane	42.9 <sup>i</sup>	pyrimidine	59.6±2.3 <sup>gg</sup>
prop-1-ene	47.8 <sup>i</sup>	imidazole	68.7±1.7 <sup>hh</sup>
vinylsilane	46.0 <sup>i</sup>	furan	37 <sup>ii</sup> 37.6 <sup>jj</sup>
vinylgermane	47.6 <sup>i</sup>	Fluorobenzene	43.8±1.1 <sup>u</sup>
prop-1-yne	48.9 <sup>k</sup>	Chlorobenzene	46.5±1.1 <sup>u</sup>
ethynylsilane	47.2 <sup>k</sup>	Bromobenzene	50.7±1.8 <sup>u</sup>
ethynylgermane	50.3 <sup>k</sup>	Iodobenzene	52.8±1.8 <sup>u</sup>
methylamine	59.8 <sup>l</sup>	anisole	56.5±2.1 <sup>u</sup>
methanimine	59.3 <sup>l</sup>	N-methylaniline	63.8±2.5 <sup>u</sup>
hydrogen cyanide	50.0 <sup>l</sup>	N,N-dimethylaniline	55.6±2.8 <sup>u</sup>
acetonitrile	57.0 <sup>m</sup>	pyrrole	57.2±3.0 <sup>u</sup>
methylphosphine	63.4 <sup>n</sup>	N-methylpyrrole	63.9±1.8 <sup>u</sup>
methylenphosphine	52.9 <sup>n</sup>	indole	60.6±2.1 <sup>u</sup>
ethylamine	62.3 <sup>o</sup>	naphthalene	55.3±2.1 <sup>u</sup>
ethylphosphine	65.7 <sup>o</sup>	coronone	59.7 <sup>v</sup>
ethylarsine	61.0 <sup>o</sup>	cyclododeca-1,5,9-trien-3,7,11-triyn	92.4 <sup>v</sup>

vinylamine	62.8 <sup>o</sup>	tribenzocyclyne	107.5 <sup>v</sup>
vinylphosphine	62.2 <sup>o</sup>	<i>Bis</i> (2,2'-bipyridine)	38.8 <sup>kk</sup>

<sup>a</sup>B3LYP/6-311+G(2df,2p) calculated value at 0 K taken from ref.. 83

<sup>b</sup>B3LYP/6-311+G(2df,2p) calculated value at 298 K taken from ref. 84

<sup>c</sup>Experimental value taken from ref. 82

<sup>d</sup>B3LYP calculated values taken from ref. 80

<sup>e</sup>B3LYP calculated value taken from ref. 36

<sup>f</sup>Experimental estimate taken form ref. 90

<sup>g</sup>CCSD(T) calculated value taken form ref. 90

<sup>h</sup>CCSD(T) calculated value taken from ref. 36

<sup>i</sup>B3LYP/6-311+G(2df,2p) calculated value taken from ref. 104

<sup>j</sup>Experimental value taken from ref. 92

<sup>k</sup>B3LYP/6-311+G(2df,2p) calculated value taken from ref.105

<sup>l</sup>B3LYP/6-311+G(2df,2p) calculated value taken from ref. 29

<sup>m</sup>Experimental value taken from ref. 88. The values for Cu<sup>+</sup>(CH<sub>3</sub>CN)<sub>2</sub>, Cu<sup>+</sup>( CH<sub>3</sub>CN)<sub>3</sub>, Cu<sup>+</sup>( CH<sub>3</sub>CN)<sub>4</sub>, Cu<sup>+</sup>( CH<sub>3</sub>CN)<sub>5</sub> are: 56.6, 16.6, 11.2 and 5.0 kcal mol<sup>-1</sup>, respectively

<sup>n</sup>B3LYP/6-311+G(2df,2p) calculated value taken from ref . 85

<sup>o</sup> B3LYP/6-311+G(2df,2p) calculated values taken from ref .86

<sup>p</sup> B3LYP/6-311+G(2df,2p) calculated value taken from ref .87

<sup>q</sup>Experimental value taken from ref. 100. The values for Cu<sup>+</sup>(DME)<sub>2</sub>, Cu<sup>+</sup>(DME)<sub>3</sub>, Cu<sup>+</sup>(DME)<sub>4</sub> are: 57.2, 16.4, and 18.0 kcal mol<sup>-1</sup>, respectively

<sup>r</sup>Experimental value taken from ref. 99. The value for Cu<sup>+</sup>(DXE)<sub>2</sub> is 43.1 kcal mol<sup>-1</sup>

<sup>s</sup>Experimental value taken from ref. 97

<sup>t</sup>Value estimated using the variable reaction coordinate transition state theory taken from ref. 94

<sup>u</sup>Experimental values taken from ref. 75

<sup>v</sup>B3LYP calculated values taken from ref. 36

<sup>w</sup>B3LYP/6-311+G(2df,2p) calculated value taken from ref. 40

<sup>x</sup>B3LYP/6-311+G(3df,2p) calculated value taken from ref. 41

<sup>y</sup>Experimental value taken form ref. 56

<sup>z</sup>Experimental value taken from ref. 52

<sup>aa</sup>G2 calculated values taken form ref. 52

<sup>bb</sup>B3LYP calculated value taken from ref. 58. In the same reference a Cu binding energy of 12.1 kcal mol<sup>-1</sup> is also reported.

<sup>cc</sup>Experimental value taken from ref. 57. The values for Cu<sup>+</sup>(pyridine)<sub>2</sub>, Cu<sup>+</sup>(pyridine)<sub>3</sub>, Cu<sup>+</sup>(pyridine)<sub>4</sub> are: 56.5±2.1, 19.7±0.5, and 14.4±0.6 kcal mol<sup>-1</sup>, respectively.

<sup>dd</sup>Experimental value taken from ref. 57. The values for Cu<sup>+</sup>(4,4-dipyridyl)<sub>2</sub>, Cu<sup>+</sup>(4,4-dipyridyl)<sub>3</sub> are: 55.6±2.5, 19.7±0.5, and 15.1±0.4 kcal mol<sup>-1</sup>, respectively.

<sup>ee</sup>Experimental value taken from ref. 57. The value for Cu<sup>+</sup>(2,2-dipyridine)<sub>2</sub> is: 56.8±2.3 kcal mol<sup>-1</sup>.

<sup>ff</sup>Experimental value taken from ref. 57. The value for Cu<sup>+</sup>( 1,10-phenanthroline)<sub>2</sub> is: 55.7±3.0 kcal mol<sup>-1</sup>.

<sup>gg</sup>Experimental value taken from ref. 98

<sup>hh</sup>Experimental value taken form ref. 106. The values for Cu<sup>+</sup>(imidazole)<sub>2</sub>, Cu<sup>+</sup>(imidazole)<sub>3</sub>, Cu<sup>+</sup>(imidazole)<sub>4</sub> are: 61.5±2.2, 19.1±0.6, and 15.2±0.5 kcal mol<sup>-1</sup>, respectively

<sup>ii</sup>Experimental value taken from ref. 51

<sup>jj</sup>CCSD(T) calculated value taken from ref. 51



<sup>kk</sup>B3LYP calculated value taken from ref. 33

### A. Role of Agostic-type interactions on Cu<sup>+</sup> binding energies

Particularly interesting are the enhanced Cu<sup>+</sup> affinities of silicon and germanium saturated and unsaturated compounds. The calculated Cu<sup>+</sup> affinity of propane is in line with the values reported for methane, but surprisingly those calculated for ethylsilane and ethylgermane are almost twice as large<sup>104</sup> (see Table 2). Also some unexpected Cu<sup>+</sup> affinities were reported for the corresponding unsaturated compounds. The Cu<sup>+</sup> affinity for propene is, as expected, only slightly larger than that estimated for ethylene, but surprisingly the Cu<sup>+</sup> affinities for vinylsilane and vinylgermane are similar to that of propene. Analogously, ethynylsilane and ethynylgermane exhibit Cu<sup>+</sup> affinities rather close or even slightly higher than propyne<sup>105</sup> (See Table 2). The behavior of the analogous aromatic derivatives is similar and phenylsilane and phenyl germane were predicted to be as basic as toluene with respect to Cu<sup>+</sup>.<sup>40</sup>

The enhanced Cu<sup>+</sup> affinity exhibited by ethylsilane and ethylgermane is due to the fact that the metal cation prefers to bond the terminal SiH<sub>3</sub> and the GeH<sub>3</sub> groups rather than the terminal methyl group. The global minimum of the propane-Cu<sup>+</sup> complex corresponds to a structure in which Cu<sup>+</sup> interacts simultaneously with both terminal CH<sub>3</sub> group<sup>104,107</sup> (See Figure 5). Conversely, although for ethylsilane and ethylgermane, the analogous structures in which Cu<sup>+</sup> interacts with the CH<sub>3</sub> and the XH<sub>3</sub> simultaneously, are also local minima of the potential energy surface, the global minima correspond to complexes in which the metal cation interacts exclusively with the XH<sub>3</sub> group (X = Si, Ge) (See Figure 5). The important finding is, however, that the latter structures are significantly more stable than the former. An analysis of the bonding, using second order orbital analysis within the natural bond orbital (NBO) formalism,<sup>108</sup> shows the existence of a charge donation from the  $\sigma_{X-H}$  (X = C, Si, Ge) bonding orbital towards the empty *4s* of the metal and a back-donation from the occupied *d* orbitals of

the metal into the  $\sigma^*_{X-H}$  ( $X = C, Si, Ge$ ) antibonding orbital of the organic moiety. These interactions are particularly strong when  $X$  is not very electronegative, so that a  $X^{\delta-}H^{\delta+}$  polarity is expected. This kind of interactions resemble closely the agostic bonds defined by Brookhart and Green<sup>109</sup> to account for the effects of transition metals on the C-H bond of organic ligands, and therefore they have been named as agostic-type interactions.



**Figure 5.** B3LYP/6-311G(d,p) optimized geometries corresponding to the global minima of the propane-, ethylsilane- and ethylgermane- $Cu^+$  complexes, respectively, taken from ref. 104.

The unexpected high  $Cu^+$  affinities exhibited by the unsaturated and aromatic analogues: vinylsilane, vinylgermane, ethynylsilane and ethynylgermane, and the phenyl derivatives, are also a direct consequence of the stabilizing effect of the aforementioned agostic-type interactions. For the unsaturated and aromatic hydrocarbons, propene, propyne and toluene, the most stable conformation of the  $Cu^+$  complexes in the gas phase correspond to conventional  $\pi$ -complexes (See Figure 6), in which the bonding is usually described in terms of Dewar-Chatt-Duncanson model,<sup>110,111</sup> which was quantitatively analyzed for the case of  $Cu^+$ -ethylene complexes by Ziegler and Rauk.<sup>112</sup> According to this model the metal ion interacts with the  $\pi$ -system, through a donation of charge from  $\pi_{CC}$  bonding orbitals of the organic moiety towards the empty  $4s$  orbital of the metal and a backdonation from the occupied  $d$

orbitals of the metal towards the  $\pi_{CC}^*$  antibonding orbitals of the organic moiety, as illustrated in Figure 7.

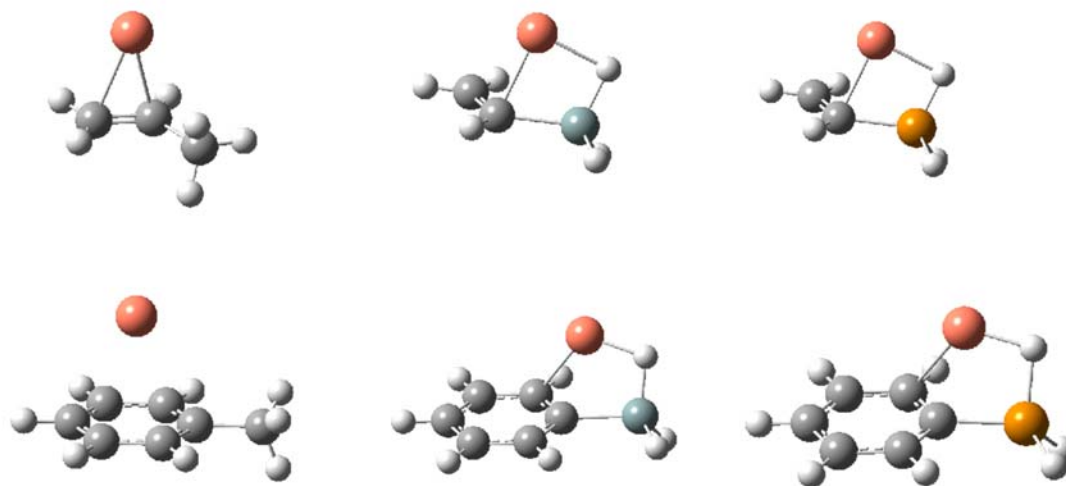


**Figure 6.** B3LYP/6-311G(d,p) optimized geometries corresponding to the global minima of the propene-, vinylsilane-, vinylgermane-, toluene-, phenylsilane, and phenylgermane- $\text{Cu}^+$  complexes, respectively, taken from ref. 104 and 40

Conversely, for Si- and Ge-containing compounds, the most stable structure corresponds to a non-conventional complex in which a typical three-center-two-electron bond is formed through the interaction of a  $p$  orbital of the C atom, a  $d$  orbital of the metal and the  $s$  orbital one of the H atoms of the  $\text{XH}_3$  ( $\text{X} = \text{Si}, \text{Ge}$ ) group (see Figure 8)

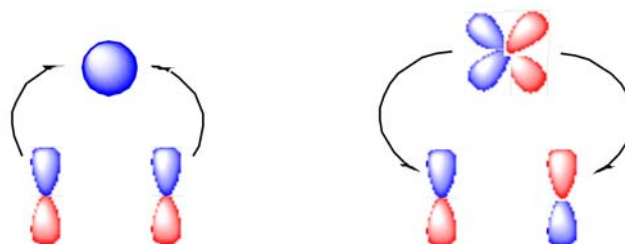


**Figure 7.** Orbital interactions associated with conventional  $\pi$ -complexes between  $\text{Cu}^+$  and unsaturated carbon compounds.

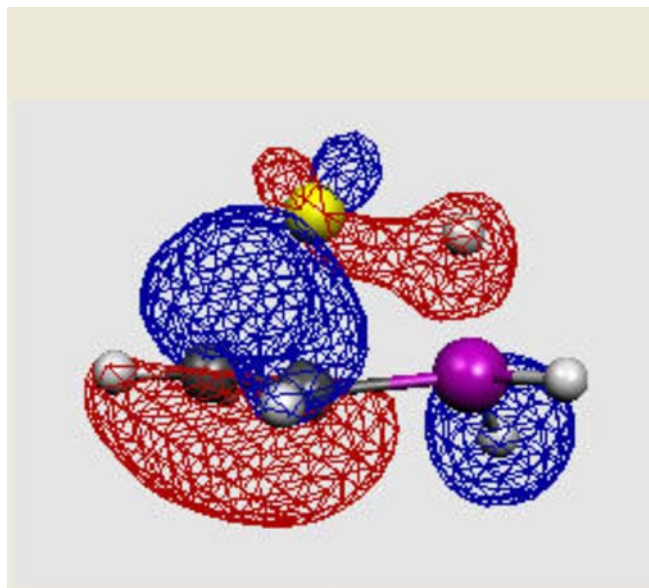


**Figure 8.** Molecular orbital of the complex vinylsilane- $\text{Cu}^+$  showing the overlap between a  $d$  orbital in Cu with the  $\pi_{\text{CC}}$  orbital and  $s$  orbital of one of the H of the  $\text{SiH}_3$  group.

The existence of these agostic-type interactions leads to a significant activation of the X-H (X = Si, Ge) bond which participates in the interaction, because the depopulation of the  $\sigma_{\text{XH}}$  bonding orbital and the population of the  $\sigma^*_{\text{XH}}$  antibonding orbital leads necessarily to a significant weakening of this linkage. This is clearly reflected in a significant lengthening of the bond which becomes 0.11-0.15 Å longer than the X-H bonds that do not interact with the metal. This weakening has also a dramatic effect on the infrared spectra of these species. These differences are clearly seen when the spectrum of the conventional  $\pi$ -complex of vinylsilane, taken as a suitable example, is compared with that of the corresponding non-conventional  $\pi$ -complex. As illustrated in Figure 9, the infrared spectrum of the non-conventional  $\pi$ -complex presents two strong absorption bands at about  $1700\text{ cm}^{-1}$  and  $1200\text{ cm}^{-1}$ , respectively which are not observed for the conventional  $\pi$ -complex. They correspond to the Si-H stretching and the Si-H bending modes, respectively, of the SiH bond directly interacting with the metal. Due to

the weakening triggered by the agostic interaction the former appears red-shifted by about  $600\text{ cm}^{-1}$  and the latter blue-shifted by about  $400\text{ cm}^{-1}$ .

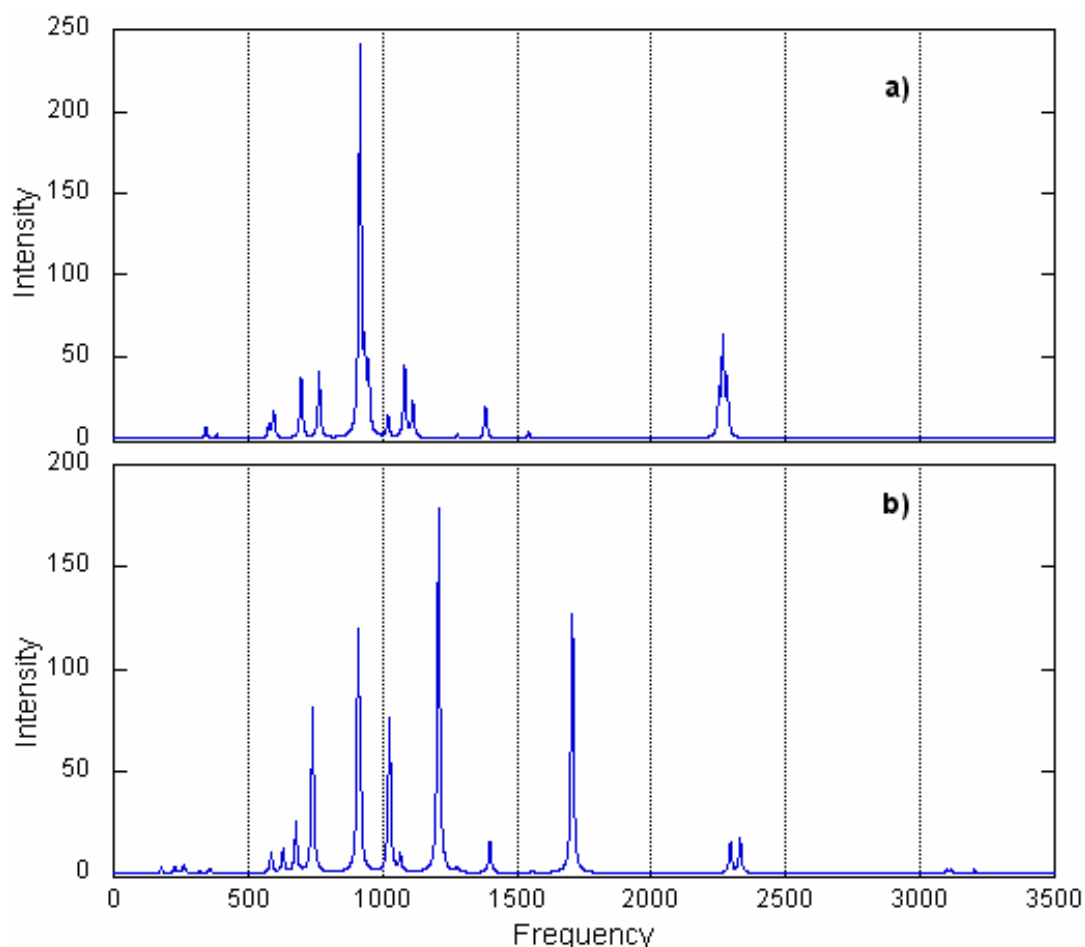


**Figure 9.** Infrared spectra for the **a)** conventional  $\pi$ -complex and **b)** non-conventional  $\text{Cu}^+$ - vinylsilane complexes, calculated at the B3LYP/6-311G(d,p) level. Frequencies are in  $\text{cm}^{-1}$  and intensities in  $\text{KM mole}^{-1}$ .

## B. Binding Energies of Solvated $\text{Cu}^+$ and $\text{Cu}^{2+}$ ions

To finish this section it is convenient to indicate that some efforts have also been addressed to investigate the effects that the solvation of  $\text{Cu}^+$  and  $\text{Cu}^{2+}$  may have on their binding energies, as well as to the measuring of incremental binding enthalpies with different organic ligands.<sup>88,106,113</sup> For obvious reasons most of these efforts concentrate

on the interactions with systems of biochemical relevance. For  $[\text{Cu}^+(\text{H}_2\text{O})_5\text{Guanine}]^+$  complexes, the most stable conformers always correspond to bisligated Cu ions bonded to one water molecule and to N7 of guanine, the binding energies being in the range  $75\text{-}83\text{ kcal mol}^{-1}$ .<sup>114</sup> This implies a decrease with respect to the binding energy

of the bare metal ion of about 5-13 kcal mol<sup>-1</sup>. When the metal cation is in its higher Cu(II) oxidation state, a clear attenuation of the bonding energy as a function of the number of water molecules around the metal is also observed<sup>115</sup> as illustrated in Figure 10. Hence, while the binding energy of guanine to a bare Cu<sup>2+</sup> ion amounts to 302 kcal mol<sup>-1</sup>, addition of one water molecule leads to a reduction of ca. 70 kcal mol<sup>-1</sup>. When two and three water molecules are added the calculated decreases are 143 and 180 kcal mol<sup>-1</sup>, respectively. When the maximum number of coordinated water molecules (5) is reached, the overall decrease is ca. 212 kcal mol<sup>-1</sup>.<sup>115</sup> Similar findings have been reported for complexes involving [Cu(H<sub>2</sub>O)<sub>3</sub>]<sup>2+</sup> and guanine or GGG triplets.<sup>116</sup> The replacement of water by guanine leads to a stabilization of the complex of about 24.3 kcal mol<sup>-1</sup>. This stabilization amounts to 35-45 kcal mol<sup>-1</sup> when water is replaced by TGGG or CGGG triplets. The interaction of hydrated Cu<sup>2+</sup> ions with guanine and an anionic phosphate group was also studied through the use of DFT methods.<sup>117</sup>

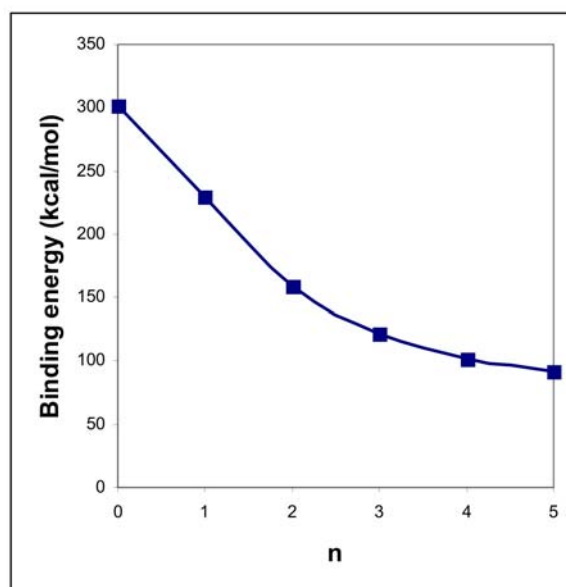


**Figure 10.** Binding energy of [Cu(H<sub>2</sub>O)<sub>n</sub>(guanine)]<sup>2+</sup> complexes as a function of the number of water molecules (n).

One typical signature as far as  $\text{Cu}^+$  sequential binding enthalpies is concerned is that the values measured or calculated for the second ligand are nearly equal or even slightly larger than those obtained for the first ligand. This is indeed the case when dealing with  $\text{Cu}^+(\text{dimethyl ether})_n$ ,  $\text{Cu}^+(\text{methanol})_n$  and  $\text{Cu}^+(\text{acetone})_n$  ( $n = 1-4$ ) complexes, where the  $\text{Cu}^+$  bond dissociation energy for  $n = 2$  are about  $2.0 \text{ kcal mol}^{-1}$  larger than that measured for  $n = 1$ .<sup>100,118,119</sup> This bonding enhancement is well reproduced by CCSD(T)<sup>113</sup> and DFT calculations,<sup>118,119</sup> and is a consequence of the hybridization of the  $d_z^2$  and  $4s$  orbitals of the metal which leads to a significant reduction of the Pauli repulsion between the metal cation and the ligand in the corresponding linear arrangement. Consistently with this explanation, for the three kinds of complexes the binding of the third ligand implies a dramatic decrease (about  $40 \text{ kcal mol}^{-1}$  for dimethyl ether,  $28 \text{ kcal mol}^{-1}$  for methanol and  $34 \text{ kcal mol}^{-1}$  for acetone) of the interaction energy. The situation is similar when the ligands are acetonitrile,<sup>88</sup> imidazole<sup>106</sup> or pyridine<sup>57</sup> with the only difference that the binding energy of the second ligand is, in these cases, slightly smaller than that of the first ligand (see Table 2). A particular case is represented by 2,2'-bipyridine and 1,10-phenanthroline, where the change in the  $\text{Cu}^+$  binding energies on going from complexes with one ligand to complexes with two ligands is significantly large ( $31$  and  $39 \text{ kcal mol}^{-1}$ , respectively),<sup>57</sup> reflecting the fact that in the complex with only one ligand the metal ion is already bisligated. Accordingly, the electrostatic contributions to the binding decrease sharply because the chelating ligands provide two donor interactions such that the charge retained by  $\text{Cu}^+$  decreases quite significantly. On the other hand, the addition of the second ligand yields a structure in which the coordination number of the metal ion is 4, which is accompanied by a significant increase in the repulsion between the two ligands.

## V. Coordination

Different evidences seem to be consistent with the idea that copper coordination preferences in Cu-containing enzymes could play a significant role in their biological functions, and therefore the preferred coordination of copper, and its dependence on its oxidation state was the subject of many studies. There are also evidences of the effect of the coordination geometry on the gas-phase reactivity of four-coordinated Cu(II) ion complexes. In the gas-phase reactions of ammonia with  $\text{Cu}(\text{EN}-(\text{py})_2)^{2+}$ ,  $\text{Cu}((\text{en})-(\text{phen})_2)^{2+}$ ,  $\text{Cu}((\text{phen})_2)^{2+}$  (EN = 1,6-bis(2-pyridyl)-2,5-triazahexane; en = ethylenediamine; phen = 1,10-phenanthroline) the reactivity of the four coordinate complexes strongly depends on the nature of the ligand. When EN-(py)<sub>2</sub> is the ligand the rate constant is about half that measured when (en)(phen)<sub>2</sub> is the ligand. Even more significant is the change observed when two phen ligands are bound to the metal ion, because in this case no significant addition of NH<sub>3</sub> was observed.<sup>120</sup>

### A. Coordination in complexes with one ligand

It is interesting to discuss in the first place, what should be the expected coordination when the metal ion interacts with only one ligand. We have already discussed in the section devoted to analyze the performance of various theoretical models, the different coordination patterns exhibited by Cu<sup>+</sup> when the base is a benzene derivative. Of particular interest are the situations which arise when the ligand presents two or more basic sites. We have already discussed several cases in which the metal forms chelated structures when the base presents more than one basic site, however, it is important to emphasize that not always a chelated structure is found to be the global minimum of the PES of bidentate or polydentate bases. Glycine and urea are two suitable examples. Both bases present as possible basic sites a carbonyl group, an amino group, and in the case of glycine,



in addition of a hydroxyl group. However, whereas glycine leads to a bisligated complex<sup>30</sup> in which  $\text{Cu}^+$  interacts with the carbonyl oxygen and with the amino N (see Figure 11) in urea this conformer lies  $12.9 \text{ kcal mol}^{-1}$  higher in energy than the global minimum<sup>121</sup> in which  $\text{Cu}^+$  interacts exclusively with the carbonyl oxygen. This can be understood if one takes into account that in urea the amino nitrogen lone-pair conjugates with the carbonyl group and is not available to interact with the metal. It is worth noting however that the attachment of  $\text{Cu}^+$  to the carbonyl group is not linear, as it is the case for alkali ions, pointing to different bonding patterns as we shall discuss later. The same behavior is found for uracil<sup>83,84</sup> and thymine complexes.<sup>83</sup> Also for 2-, 4- and 2,4-thiouracil, the  $\text{Cu}^+$  adducts are monocoordinated  $\text{Cu}^+$  complexes in which the metal ion is attached preferentially to the sulfur atom. It is also interesting to indicate that any attempt to find a tricoordinated glycine- $\text{Cu}^+$  complex in which the metal interacts with both oxygen atoms and with the nitrogen atom failed,<sup>30</sup> as all these structures collapsed to the bisligated global minimum. The situation is different however as far as the complexes with serine and cysteine are concerned. In these two cases the global minimum corresponds to conformers in which  $\text{Cu}^+$  interacts with the amino nitrogen, the carbonyl oxygen and the alcohol oxygen in serine, or the thiol sulfur in cysteine (See Figure 11).

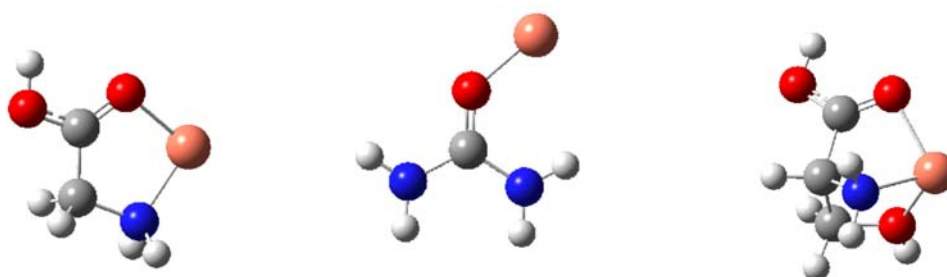


**Figure 11.** Optimized geometries of glycine, urea and serine- $\text{Cu}^+$  complexes

This propensity to yield high coordinated complexes reflects the importance of polarization interactions and depends on the flexibility of the base to adequately orient

its lone pairs towards the metal. We have already mentioned the case of 2,2'-bipyridine where the association with the metal is preceded by an internal rotation around the single bond connecting both aromatic rings in order to favor the interaction of both ring nitrogens with the metal ion. Also in the case of serine and cysteine, the neutral base undergoes a rearrangement to favor the interaction of the three basic sites with the metal ion, which implies little energy. Conversely, the concomitant interaction with the OH group of the carboxylic group would require a strong distortion and the breaking of the intramolecular hydrogen bond between this group and the carbonyl oxygen, and therefore this interaction does not occur. This is corroborated by the fact that the complexes between diglycine and triglycine with  $\text{Cu}^+$  always correspond to bisligated structures in which the metal ion is chelated to the terminal amino group and the carbonyl oxygen, and all attempts to produce tricoordinate complexes were not successful.<sup>31,77</sup> Conversely, for  $\text{Ag}^+$  tri- (in the case of diglycine) and tetra-coordinate (in di and triglycine) structures are the most stable.<sup>77</sup> It should also be emphasized that for diglycine, triglycine and tetraglycine the complexes with a structure similar to that shown in Figure 11 for glycine- $\text{Cu}^+$ , are not the global minimum of the potential energy surface because  $\text{Cu}^+$  prefers a linear coordination environment rather than an angular one. As already explained in previous sections, associated with the linear arrangement a significant reduction of the Pauli repulsion between the metal cation and the ligand takes place, through the formation of  $sd$  hybrids<sup>122-124</sup> (See Figure 12). Conversely, in an angular arrangement the hybridization involves necessarily, by symmetry reasons, the  $4p$  and the  $d_{xz}$  orbital, and due to the higher energy of the  $4p$  orbitals the hybridization is less effective and the repulsion decrease smaller.<sup>31</sup> We will find again a similar conformation in many complexes in which  $\text{Cu}^+$  interacts with two or more ligands.



**Figure 12.** B3LYP optimized geometries for the global minima of the diglycine-, triglycine- and tetraglycine- $\text{Cu}^+$  potential energy surfaces taken from ref. 31

The structure of the glycine complexes does change dramatically when  $\text{Cu}^+$  is replaced by  $\text{Cu}^{2+}$  since, although the global minimum still corresponds to a bisligated structure, in this case the metal ion interacts with the  $\text{CO}_2^-$  terminus of the zwitterionic form of glycine<sup>81</sup> (see Figure 13). A similar behavior has been found when the structure of  $\alpha$ -alanine- $\text{Cu}^+$  complex is compared with that of  $\alpha$ -alanine- $\text{Cu}^{2+}$ .<sup>35</sup> Changes are apparently less significant when dealing with urea and uracil,<sup>49,125</sup> where the replacement of  $\text{Cu}^+$  by  $\text{Cu}^{2+}$  triggers a noticeable opening of the C-O-Cu angle, which for uracil becomes very close to  $180^\circ$ . More importantly  $\text{Cu}^{2+}$  association leads to a significant symmetry change in the urea moiety, where one of the C-N bonds becomes sizably shorter than the other one<sup>49</sup> (see Figure 13). Conversely, attachment of  $\text{Cu}^{2+}$  to thiourea yields a nearly symmetric structure in which  $\text{Cu}^{2+}$  binds to the sulfur atom practically in the plane which bisects the NCN angle,<sup>49</sup> the CSCu angle being  $109.7^\circ$  (see Figure 13). Similar CSCu bending arrangements are also found for thiouracil derivatives.<sup>125</sup>

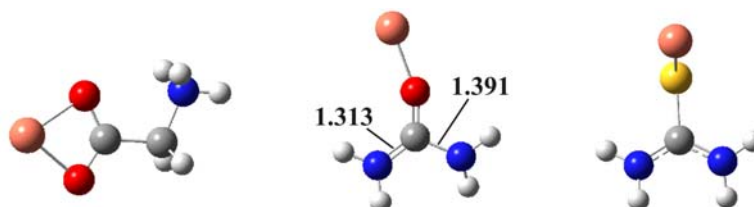


**Figure 13.** B3LYP optimized geometries of the  $\text{Cu}^{2+}$  complexes with glycine, taken from ref. 10, urea and thiourea, taken from ref. 49

These significant dissimilarities between  $\text{Cu}^+$  and  $\text{Cu}^{2+}$  complexes when interacting with one ligand reflect completely different bonding patterns.<sup>81,125</sup> As pointed out by Bertrán et al.<sup>81</sup> the ionization potential of  $\text{Cu}^+$  (20.8 eV) is much larger than that of most of the aforementioned organic bases, and certainly larger than that of glycine (9.38 eV), urea (10.27 eV), thiourea (8.5 eV) or uracil (9.2 eV),<sup>53</sup> so one may expect  $\text{Cu}^{2+}$  to be able to oxidize the base so that the  $\text{Cu}^{2+}$  complexes would behave more like  $\text{Cu}^+$ -base<sup>+•</sup> than like  $\text{Cu}^{2+}$ -base systems. This is mirrored in the corresponding electron densities.  $[\text{Cu-uracil}]^{2+}$  complexes can be actually viewed as  $\text{Cu}^+$ -uracil<sup>+</sup> complexes, not only because the uracil moiety bears a net positive charge very close to unity, but because the spin density, which in a  $\text{Cu}^{2+}$  complex should be located on the metal (with a  $d^9$  configuration), is located on the organic moiety. The same electron distribution was observed in  $[\text{Cu-thiouracils}]^{2+}$ <sup>125</sup> and  $[\text{Cu-urea}]^{2+}$  complexes.<sup>49</sup> As we shall discuss in detail in forthcoming sections, the oxidative capacity of  $\text{Cu}^{2+}$  is one of its specific signatures and dictates many of the properties of Cu(II)-containing systems. Actually, the fact that the global minimum of the  $[\text{glycine-Cu}]^{2+}$  complex corresponds to a  $\eta^2\text{-O,O}$  structure of the zwitterionic isomer indicates that  $\text{Cu}^{2+}$  association strongly favors a proton transfer from the carbonylic group towards the amino group.<sup>126</sup> This was also observed in cysteine- $\text{Cu}^{2+}$  interactions<sup>78</sup> where the association with  $\text{Cu}^{2+}$  triggers a proton transfer from the S-H group towards the amino group, the global minimum of the  $[\text{cysteine-Cu}]^{2+}$  complex being a bisligated structure in which Cu interacts with the carbonyl oxygen and the sulfur atom of this zwitterionic form.<sup>78</sup> It is important to mention that the charge transfer from the base towards the metal ion seems to be strongly favored in monodentate complexes, whereas for bidentate structures the spin density is more delocalized, as found for glyoxilic acid oxime- $\text{Cu}^{2+}$  interactions.<sup>37</sup>

## B. Coordination in complexes with more than one ligand

When Cu(I) or Cu(II) interact with more than one ligand, it seems well established that Cu(I) prefers lower coordination numbers than Cu(II).<sup>4</sup> Actually, different studies confirmed a preference for Cu(I) to be bisligated, whereas Cu(II) is usually found in tetracoordinated planar structures. So, even though it is usually assumed that  $d^{10}$  metal ions should form tetrahedral complexes,<sup>127</sup> this is not always the case when dealing with  $\text{Cu}^+$ . We have already indicated the preference of Cu(I) to yield complexes in which Cu is linear or nearly bound to two active sites of a polydentate base, whenever the base is flexible enough to favor these linear arrangements. When two or more ligands interact with the metal ion this is indeed the kind of coordination usually found. Obviously, this is the arrangement in  $\text{Cu}^+(\text{pyridine})_2$  complexes<sup>128</sup> as well as in the neutral counterpart,  $\text{Cu}(\text{pyridine})_2$ , although in the latter the Cu-N distances are larger because of the increase of the Pauli electron repulsion between the N lone-pair and the  $4s$  electron of the metal. This preference of Cu(I) for dicoordination is nicely reflected in the solvation patterns exhibited by  $\text{Cu}^+$  in  $\text{Cu}^+(\text{H}_2\text{O})_n$  ( $n = 2, 4, 6$ ) clusters.<sup>129</sup> At the MP2 and CCSD(T) levels of theory, the  $\text{Cu}^+(\text{H}_2\text{O})_2$  cluster is predicted to be a  $\text{C}_2$  structure (See figure 14).<sup>130</sup> When a third water molecule is added, the lowest energy structure corresponds to that depicted in Figure 14, in which the third water molecule forms hydrogen bonds with one in the first shell. Analogously, the most stable structure for  $\text{Cu}^+(\text{H}_2\text{O})_4$  clusters can be viewed as the result of the solvation of the  $\text{C}_2$  dimer. That is, two water molecules are covalently bonded to the metal, while the other two interact with the first-shell water molecules through the formation of hydrogen bonds, acting as proton acceptors (see Figure 14). Also consistently, the global minimum of the  $\text{Cu}^+(\text{H}_2\text{O})_6$  has only two water molecules in the first shell linearly bound to the metal, while the other four solvate these two acting as proton acceptors (see figure 14).

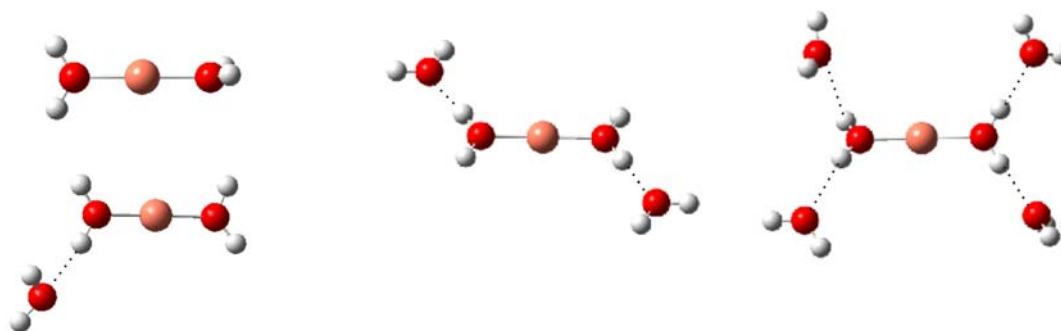


**Figure 14.** Structure of the global minima for  $\text{Cu}^+(\text{H}_2\text{O})_n$  ( $n = 2,3,4,6$ ) taken from refs.130 and 129 showing the preference of  $\text{Cu}^+$  to form linear L-Cu-L' arrangements when interacting with several ligands.

This bonding pattern is also found in many complexes between  $\text{Cu}^+$  and organic ligands. For instance, in the  $\text{Cu}^+(\text{imidazole})_2$  complexes Cu is linearly coordinated to the two bases. Furthermore, when a third imidazole molecule is added it interacts through hydrogen bonds with one of the imidazoles of the first shell, whereas the local minima in which the three ligands are in the first solvation shell is predicted to be  $4.4 \text{ kcal mol}^{-1}$  higher in energy.<sup>106</sup> Similarly, in the global minimum for the  $\text{Cu}^+(\text{imidazole})_4$  complex only two imidazole molecules are directly connected to the metal, while the structures with three and four ligands in the first solvation shell are predicted to be  $6.3$  and  $11.5 \text{ kcal mol}^{-1}$  less stable, respectively. In  $\text{Cu}^+(\text{dimethyl ether})_2$  again the ground state correspond to a nearly linear bisligated complex. In this case, when a third ligand is added, it does not solvate one of the ligands of the first shell because in this case there is no possibility of forming hydrogen bonds, but the structure of the complex corresponds to a distorted T-type arrangement, in which the third ligand is much weakly bound than the other two (see Figure 15).

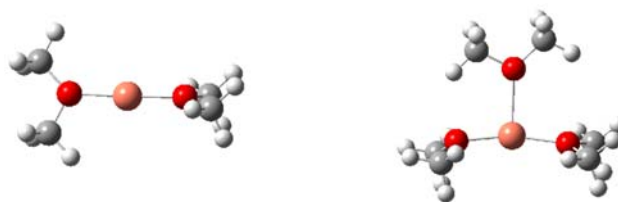


**Figure 15.-** CCSD(T) optimized geometries for the  $\text{Cu}^+(\text{dimethyl ether})_n$  ( $n = 2, 3$ ) complexes taken from ref. 113

A similar bonding pattern was obtained at the B3LYP/DZVP level for complexes formed by the interaction of glycine- $\text{Cu}^+$  ions with CO, water and ammonia.<sup>131</sup>

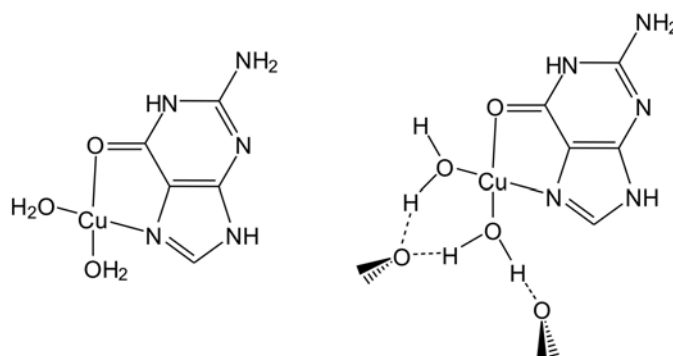
Whereas Cu(I) prefers in general di-coordinated structures, Cu(II) yields quite stable tetra-coordinated complexes, and when the coordination number is six, there is a significant Jahn-Teller effect which forces two of the ligands to be much less tightly bound than the other four. This happens, for example, in complexes between Cu(II) and acetone.<sup>132</sup> These complexes were generated in the gas phase by a technique able to produce complexes of a controlled size. Each complex is first produced as a neutral Cu-solvent species, which is subsequently ionized by electron impact. The data obtained for  $[\text{Cu}(\text{acetone})_n]^{2+}$  complexes show a maximum abundance when the number of ligands is four, accompanied by a rapid decline in the abundance when  $n$  increases. On the other hand the results show no evidence of a stable octahedral unit when  $n = 6$ , due to a strong Jahn-Teller effect leading to a distorted octahedral structure in which two ligands are weakly bound. Very interestingly, however, when the ligand is ethylene, the maximum in intensity is observed for  $n = 3$ .<sup>132</sup> This was interpreted in terms of donations and back-donations between the CC  $\pi$ -system and the metal, because the optimum number of  $\pi$ -bonded ligands would be three, through the interaction of  $d_{xy}$ ,  $d_{xz}$  or  $d_{yz}$  orbitals with the  $\pi_{cc}^*$  antibonding orbital.<sup>132</sup> The same experimental technique was used to investigate the coordination of Cu(II) to different alcohols, namely, methanol, ethanol, 1-propanol, 2-propanol, different ketones (acetone, butanone, pentanone, 2,4-

pentadione) and other organic bases such as pyridine, pyrazine, tetrahydrofuran, dioxane, benzene, benzonitrile, and ethylenediamine.<sup>65</sup> The intensity distributions recorded for the interactions with acetone, pyridine, tetrahydrofuran, and acetonitrile are clearly dominated by a very intense  $[\text{CuL}_4]^{2+}$  unit, followed by a rapid decline in the intensity measured for complexes of larger size. Furthermore, in  $[\text{CuL}_4]^{2+}$  complexes containing acetone, 2-butanone or 2-pentanone, the charge transfer reaction leads to the loss of two ligands to form  $[\text{CuL}_2]^+$  complexes. The situation is different for alcohol ligands. For 1- and 2-propanol both Cu(II) complexes exhibit intensity maxima at  $n = 4$  as for the case of the aprotic solvent mentioned above. However, for ethanol and methanol up to eight ligands can be gathered around the metal because of the ability to form hydrogen bonds between the ligands in the first shell and those in the second one. In fact, as shown by Bérces et al.,<sup>133</sup> in the case of methanol, four ligands are located in the first solvation shell in a square-planar distribution, with other four connected to the first ones via hydrogen bonds. On going to ethanol there is a downward shift in maximum intensity to  $n = 6$ , with  $[\text{CuL}_4]^{2+}$  becoming more prominent. The association with benzene constitutes a special case since  $[\text{Cu}(\text{C}_6\text{H}_6)_2]^{2+}$  is the only ion observed, suggesting that the structure corresponds, very likely to a sandwich-like arrangement in which the metal dication is centrally located between both aromatic rings.

In  $[\text{Cu}(\text{pyridine})_n]^{2+}$  ( $n = 4, 6$ ) complexes,<sup>64</sup> when  $n = 4$  the ground state corresponds to a  $D_{4h}$  structure, but the ground state of the hexamer, can be viewed as the result of associating to the  $D_{4h}$  tetramer, two additional ligands in an overall octahedral arrangement. However, while the Cu-N distance for four ligands is 1.95 Å, for two of them is 3.72 Å, showing a clear Jahn-Teller distortion, similar to the one found in clusters in which  $\text{Cu}^{2+}$  is solvated by water,<sup>19,134-137</sup> ammonia<sup>135,138</sup> or water and ammonia molecules simultaneously.<sup>19,135,139,140</sup> This preference for tetra-coordination in



the case of Cu(II) complexes was also observed in clusters between GGG (G=glycine) and hydrated Cu<sup>2+</sup> ions.<sup>116</sup> Even in complexes between glycine and Cu<sup>2+</sup>(H<sub>2</sub>O)<sub>4</sub>, where the coordination around the metal ion is forced to be five, one of the water ligands is always far away from it, or moves to the second solvation shell.<sup>141</sup> Very recently, the structures of complexes between guanine and hydrated Cu(II) were reported.<sup>115</sup> The B3PW91/6-31+G(d) optimized geometries showed that the global minimum of the diaqua system corresponds to a four-coordinated complex, in which the metal forms a chelated structure with the base and interacts simultaneously with the two water molecules (see scheme 3). Importantly however, when two more water molecules are added, the coordination of the metal ion does not change, and as illustrated in scheme 3, the two new water ligands form hydrogen bonds with the water molecules of the first shell.<sup>115</sup>

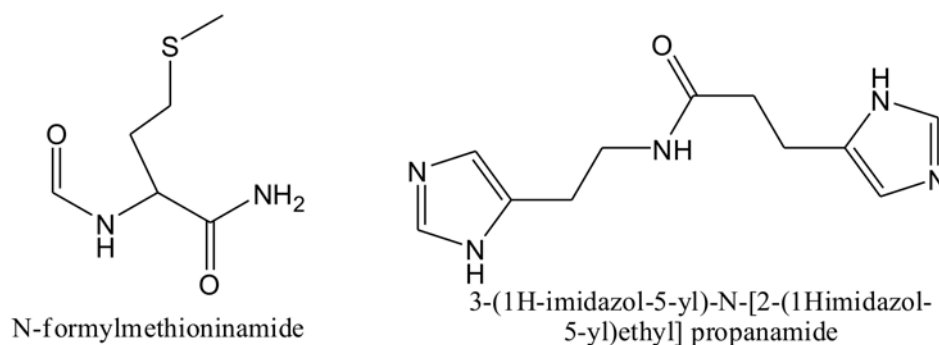


**Scheme 3**

Even in the case of copper-bound proteins, where the rigidity imposed by the protein backbone may prevent ligand exchange or ligand loss, Cu(I) shows a clear preference to yield dicoordinated species.<sup>4,142,143</sup> Two thorough theoretical studies of the Cu(I) and Cu(II) binding sites for a His-His peptide model,<sup>4,142</sup> using 3-(1H-imidazol-5-yl)-N-[2-(1Himidazol-5-yl)ethyl] propanamide) (**L**) as a suitable model system (see scheme 4), showed a preference of Cu(II) to yield tetracoordinated complexes, forming in general

distorted square planar structures. Since this modelling was carried out by taking into account the specific solvation of the metal cation by water molecules, it was found that Cu(II) releases water molecules when the histidines and the backbone get involved in the coordination sphere, in order to keep the coordination number equal to four.<sup>142</sup> A more recent study using the same model compound<sup>4</sup>, showed that a reduction of the metal was accompanied by a decrease in the coordination number to three or two. As a matter of fact, it was found that lowering the coordination number of Cu(I) from four to three or two was favored irrespective of the identity of the ligand lost.

Actually, in the most stable complex between Cu(I) and compound **L**, the metal ion forms two linear bonds with the N atoms of the imidazole rings. A third Cu(I)-O very weak interaction in the stem position leads to a distorted T geometry.



**Scheme 4**

In a systematic investigation of the bonding of Cu(II) and Cu(I) to a N-formylmethioninamide(NFMET) (see Scheme 4)<sup>143</sup> as a suitable methionine model peptide, analogous results were found. Hence, in general tetracoordinated Cu(II)-NFMET complexes were found to be more stable than those with higher coordination numbers. However, for Cu(I)-NFMET the tricoordinate complexes were more stable than the tetracoordinated ones.

### C. Coordination of Cu(II) in Blue Proteins

The coordination of Cu(II) in blue proteins has received a particular attention, because it seems well established that coordination dictates their oxidation capacity, i.e. their role as electron-transfer proteins as well as other of their properties. As a matter of fact, mononuclear copper proteins have been usually classified into two types, which differ clearly in the coordination of Cu(II). In the so-called “normal” proteins Cu(II) exhibits two different arrangements depending on the coordination number, tetragonal or elongated octahedral due to a typical Jahn-Teller effect. In contrast, in blue proteins Cu(II) is usually surrounded by a trigonal coordination sphere involving two histidine nitrogen atoms and a cysteine thiolate group. Our knowledge on the coordination of Cu(II) in blue proteins comes essentially from theoretical modeling using small systems. A quite simple model, in which Cu(II) interacts with two or three ammonia molecules and with a SH<sup>-</sup>, SH<sub>2</sub> or S(CH<sub>3</sub>)<sub>2</sub> ligands, permitted to gain some insight into the origin of these preferences for a trigonal coordination.<sup>144</sup> This model clearly reproduced the unusually short Cu-cysteine and the unusually long Cu-methionine bond lengths. Methionine occupies an axial position in the protein and leads to an unfavorable interaction with the doubly occupied *d* orbital of the metal ion. At the same time the model clearly showed the stabilizing role played by the thiolate ligand because of its soft character that gives covalent Cu-S bonds, stabilizing the trigonal arrangement around the metal. In a posterior analysis,<sup>10</sup> it was concluded that for small and hard ligands the tetragonal structure around Cu(II) was the most stable, while for large, soft, and polarizable ligands trigonal and tetragonal coordinations are very close in energy, although in complexes like Cu(NH<sub>3</sub>)<sub>2</sub>(SH)(SH<sub>2</sub>)<sup>+</sup> the trigonal structure is more stable showing the important role played by methionine in this kind of proteins, as a consequence of the large amount of charge transferred from the ligand to the copper ion, whose charge becomes rather close to +1.

More sophisticated models, in which  $S(CH_3)_2$  and  $CH_3CONH_2$  ligands simulate the effects of methionine and glutamine residues, respectively, and  $CH_3CONH(CH_2)_2$ -imidazole simulates the effect of the backbone amide group, were used<sup>145</sup> to gain insight into the coordination of a series of blue copper proteins such as azurine, or stellacyanin (see Figure 16). The main conclusion of this analysis was that the axial ligands had a rather small influence on the reduction potentials of these proteins, which seems to depend essentially on the solvent accessibility to the copper site and on the orientation of the protein dipoles around the metal.

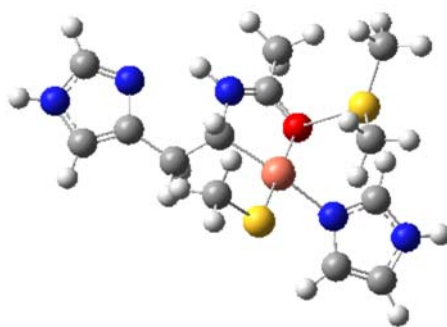


**Figure 16.** Model complex used in ref. 145 to model blue copper proteins

QM/MM calculations<sup>146</sup> were also reported for azurin, plastocyanin and stellacyanin in which the QM region, which contains complexes similar to those described in the previous paragraph, was treated at the DFT level of theory, whereas the rest of the protein was described using molecular mechanic approaches. This model reproduces the trends in the relative values of the redox potentials for plastocyanin and stellacyanin, suggesting that the much smaller value found for stellacyanin is associated with much shorter Cu-O distance in the oxidized form.

## VI. Bonding

### A. Bonding in Cu<sup>+</sup> complexes

It has been usually assumed that the interaction of Cu<sup>+</sup> with neutral systems is essentially electrostatic, but more and more evidences indicate that covalent contributions are not at all negligible. This covalency is reflected both in the binding energies and in the structures of the Cu<sup>+</sup> complexes, through the contribution of dative bonds from the ligand to the *4s* empty orbital of the metal and back-donations from occupied *d* orbitals of the metal into empty antibonding orbitals of the base.<sup>39-41,90,104,105,112,147</sup>

We have already discussed in preceding sections, that these interactions were the origin of the enhanced stability of non-conventional  $\pi$ -complexes between Cu<sup>+</sup> and unsaturated or aromatic derivatives of silicon and germanium. We will emphasize here the significant differences between Cu<sup>+</sup> and alkali metal ions, where the interactions are dominantly electrostatic. The differences in bonding are clearly illustrated in Figure 17 which shows the energy density contour maps for the conventional  $\pi$ -complexes of Li<sup>+</sup> and Cu<sup>+</sup> with phenylgermane.<sup>40</sup> It should be reminded here that negative values of the energy density<sup>148</sup> indicate that the potential energy density dominates over the kinetic energy density as in covalent bonds and vice-versa, a positive value of the energy density indicates that the kinetic energy density term dominates as in typical ionic bonds.

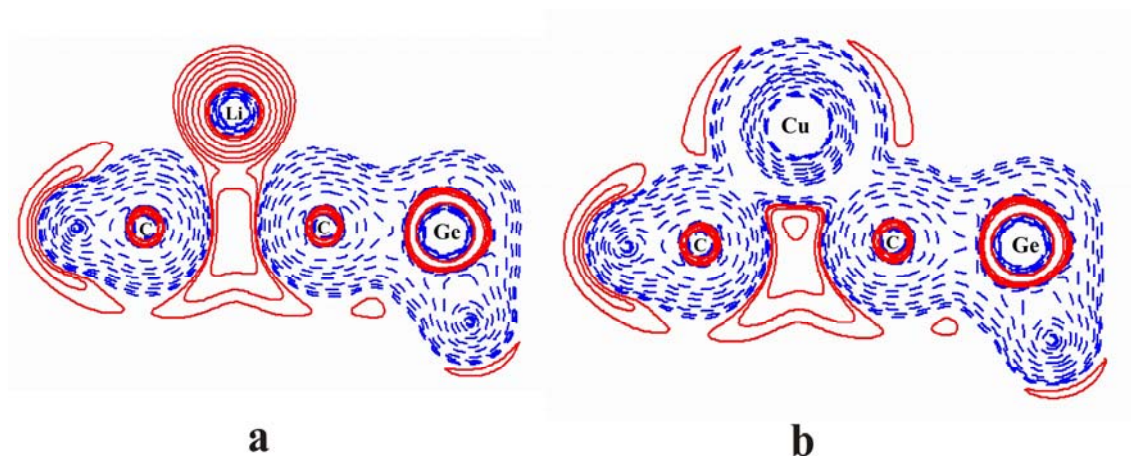


**Figure 17.** Energy density contour maps for the phenylgermane- $\text{Li}^+$   $\pi$ -complex (**a**) and phenylgermane- $\text{Cu}^+$  (**b**) conventional  $\pi$ -complex. The energy density has been plotted in a plane perpendicular to the aromatic ring and containing the substituted and the *para* carbon atoms, as well as the metal ion.

Figure 17 shows that in the phenylgermane- $\text{Li}^+$  and phenylgermane- $\text{Cu}^+$  conventional  $\pi$ -complexes the metal ion sits on the electronic hole of the aromatic ring, but whereas the energy density is clearly positive between the metal cation and the base for the  $\text{Li}^+$  complex, for  $\text{Cu}^+$  it is negative, providing evidence that this interaction has a non-negligible covalent character. This is coherent with the interaction energies between the  $\sigma_{\text{C1C6}}$ ,  $\sigma_{\text{C2C3}}$  and  $\sigma_{\text{C4C5}}$  occupied orbitals of the base toward the  $4s$  empty orbital of Cu (15, 14, and 13 kcal mol<sup>-1</sup>, respectively) calculated using a second order NBO perturbation analysis and those from filled  $d$  orbitals of the metal and the corresponding antibonding orbitals of the base (7, 6, 5 kcal mol<sup>-1</sup>, respectively).<sup>40</sup> The depopulation of the  $\sigma_{\text{C1C6}}$ ,  $\sigma_{\text{C2C3}}$  and  $\sigma_{\text{C4C5}}$  bonding orbitals and the concomitant population of the  $\sigma^*_{\text{C1C6}}$ ,  $\sigma^*_{\text{C2C3}}$  and  $\sigma^*_{\text{C4C5}}$  antibonding ones, results in a lengthening (0.018 Å, in average) of all the CC bonds of the aromatic ring, whose stretching frequencies appear shifted to the red by ca. 36-51 cm<sup>-1</sup>.<sup>40</sup> Of course, these kinds of interactions are not possible in  $\text{Li}^+$  complexes where the first empty  $2s$  orbital lies very high in energy. The situation is not different when dealing with saturated compounds.<sup>147</sup>

As shown in Figure 18 for complexes of  $\text{Li}^+$  and  $\text{Cu}^+$  with germane, again the energy density is positive between the metal ion and the base in the case of  $\text{Li}^+$ , but clearly negative when the metal ion is  $\text{Cu}^+$ .

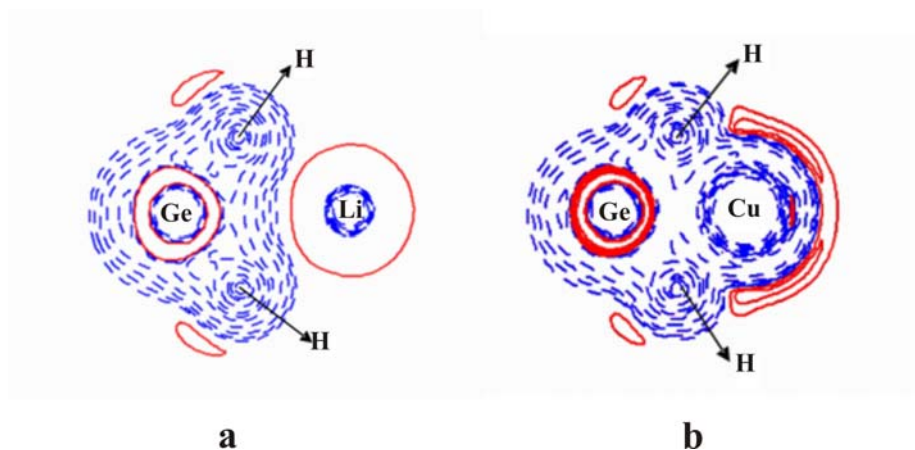


**Figure 18.** Energy density contour maps for the germane- $\text{Li}^+$  (a) and germane- $\text{Cu}^+$  (b) complexes. The energy density has been plotted in a plane containing the silicon atom, as well as the two hydrogen atoms interacting with the metal ion.

The non-negligible covalent character of  $\text{Cu}^+$ -complexes is mirrored in binding affinities which are, in average, 1.3 times larger than the corresponding  $\text{Li}^+$  affinities.<sup>40</sup> Similar behavior was reported for guanine and adenine  $\text{Cu}^+$  complexes when compared with the corresponding  $\text{Li}^+$  ones.<sup>20</sup> Finally, it is worth mentioning that besides electrostatic terms, the energy employed in the deformation of the ligand is crucial to rationalize the stability trends of different complexes.<sup>31,81</sup>

### B. Bonding in $\text{Cu}^{2+}$ complexes

The most significant characteristic of the bonding in  $\text{Cu(II)}$  complexes is the oxidation undergone by the ligand with the result that both, the spin density and the electron deficiency is concentrated in it.<sup>4,31,42,81,101,115,116,125,149-151</sup> A similar oxidation effects has been reported for  $\text{Cu(III)}$  complexes<sup>93</sup> where the metal does not have a  $d^8$  electronic configuration explaining why, quite unexpectedly, the Cu-L distances are uniformly longer in  $\text{Cu(III)}$  complexes than in their  $\text{Cu(I)}$  analogues.<sup>93</sup>

As it could be anticipated, the more coordinated the metal is the less oxidized the ligands are.<sup>115</sup> For instance, while in  $\text{Cu}^{2+}$ -guanine complexes reduction of  $\text{Cu(II)}$  to  $\text{Cu(I)}$  takes place and the spin density on the metal is almost zero, when the number of water molecules solvating the metal increases this effect decreases dramatically and the spin density on Cu (0.72) is again closer to unity.<sup>115</sup> Interestingly, the same conclusion was reached when dealing with complexes in which only one (polydentate) ligand interacts with the metal.<sup>31,37</sup>

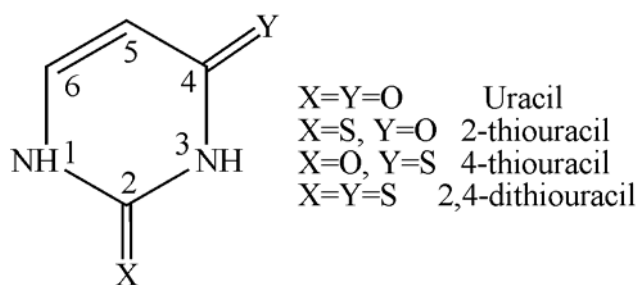
The aforementioned oxidation of the ligand enhances its intrinsic acidity which facilitates its deprotonation.<sup>150,152</sup> This explains why in general  $[\text{Cu-L-H}]^+$  monocations are readily detected in the gas phase instead of the corresponding  $[\text{Cu-L}]^{2+}$  doubly charged species.<sup>151</sup>  $\text{Cu(II)}$  has also a clear tendency to oxidize aminoacids and peptides. For instance,  $[\text{Cu(II)}(2,2'\text{-bipyridine})(\text{AA-H})]^+$  complexes (where AA is an aminoacid) lead to the loss of  $\text{CO}_2$  followed by further radical-driven fragmentation of the resulting  $\text{Cu(I)}$  complex.<sup>61,153,154</sup> Similarly, CID experiments carried out on  $[\text{Cu}(2,2'\text{-bipyridine})(\text{Arg})]^{2+}$  and  $[\text{Cu}(\text{His})_2]^{2+}$  complexes lead to the formation of  $[\text{Arg-CO}_2]^+$  and  $[\text{His-CO}_2]^+$  radical cations, what was taken as an evidence of the formation of arginine and histidine radical cations as transient species.<sup>153,155</sup> Similar results were reported for complexes between  $\text{Cu(II)}$  and histidine containing peptides, as we will see in the section dealing with the reactivity of copper ions with biomolecules. On the other hand, the reduction of  $\text{Cu(II)}$  to  $\text{Cu(I)}$  is the basic mechanism behind the electron-transfer role of blue copper proteins,<sup>10,144</sup> whereas the oxidation capacity of  $\text{Cu(II)}$  is also the driven force of proton-transfer reactions within base pairs.<sup>156,157</sup> Experiments conducted in the gas phase<sup>158</sup> showed significant differences in the bonding of  $\text{Cu(II)}$  with respect to  $\text{Ag(II)}$  and  $\text{Au(II)}$ .



## VII. $\text{Cu}^+/\text{Cu}^{2+}$ reactions with small organic bases

Over the past decades, a great body of studies on gas-phase reactions of bare  $\text{Cu}^+/\text{Cu}^{2+}$  cations with small molecules containing prototypical bonds (e.g., N-H, C-H, C-C, O-H), have been performed.<sup>159-168</sup> In this section we will present an overview of the most significant results reported in the period of time covered in this chapter.

The interaction of  $\text{Cu}^+$  with carbonyl compounds has been widely studied in the literature. The binding energy has been measured or calculated for a large set of compounds as has been discussed in preceding sections. For  $\text{Cu}^{2+}$  the deprotonation usually accompanying the association of this doubly charged metal to organic compounds makes the measurement of binding energies practically impossible since the species experimentally accessible is the singly-charged deprotonated complex. As a matter of fact, as we have already noted when discussing the bonding, it appears that the most significant difference in reactivity between both copper oxidation states, is the oxidation capacity of Cu(II). The interaction of  $\text{Cu}^+/\text{Cu}^{2+}$  with thiouracils derivatives (see Scheme 5) provides a good example for these differences<sup>84,125,150</sup>. While  $\text{Cu}^+$  interaction occurs preferentially with one and oxygen or a sulfur lone pair,  $\text{Cu}^{2+}$  interacts preferentially with the two oxygen lone pairs simultaneously. In the first case, the attachment of the metal occurs at the most basic site which is the heteroatom at C4. For  $\text{Cu}^{2+}$  the interaction is preferred at the oxygen atom independently of its position. This was explained by a greater affinity of  $\text{Cu}^{2+}$  towards carbonyl than towards the thiocarbonyl group<sup>125</sup>, even though in general thiocarbonyl derivatives exhibit a gas-phase basicity larger than their carbonyl analogues.<sup>169,170</sup>



**Scheme 5**

To the best of our knowledge there are no studies dealing with the reactivity of uracil and thiouracil derivatives towards  $\text{Cu}^+$ . However, as these compounds can be viewed as formed by two different groups, formamide and urea or their thio derivatives, the reactivity patterns of uracils and thiouracils might be considered similar to those of formamide and urea or thiourea, if one excludes ring effects which are only present in the former and which will be discussed in next sections. Luna *et al.* have reported<sup>171</sup> a nice experimental and theoretical study on the fragmentation of formamide- $\text{Cu}^+$  complexes in the gas phase. In a preliminary study the isomerization of formamide using different levels of theory was analyzed in order to estimate its affinity towards  $\text{Cu}^+$  and to locate the most basic centers.<sup>172</sup> Subsequently, by means of Chemical Ionization-Fast-Atom Bombardment (CI-FAB) mass spectrometry techniques, the dissociation products of the formamide- $\text{Cu}^+$  complex were investigated, the main precursors for these fragmentations being the oxygen and the nitrogen attached species. The exploration of the PES at the B3LYP/6-311+G(2df,2p)//B3LYP/6-311G(d,p) level of theory revealed that  $\text{OCCu}^+$  and  $\text{CuNH}_3^+$ , which were the most abundant fragments observed by Mass Analyzed Ion Kinetic (MIKE)-CAD spectra, may be produced through three different mechanisms. If the O-attached complex is assumed to be the precursor, the reaction should overcome, as a first step, an activation barrier of about 93.4 kcal/mol associated with a 1,2 hydrogen shift from carbon to nitrogen, (see figure 19). A similar energetic barrier, ca. 95.7 kcal/mol, corresponding to a 1,2 hydrogen

transfer from carbon to oxygen is the first step when the same fragments are produced if the N-attached complex is considered to be the precursor for the unimolecular fragmentation. The calculated activation barrier is higher (about 104.9 kcal/mol see figure 20) if a direct hydrogen transfer from the CH group to the amino one is envisaged.

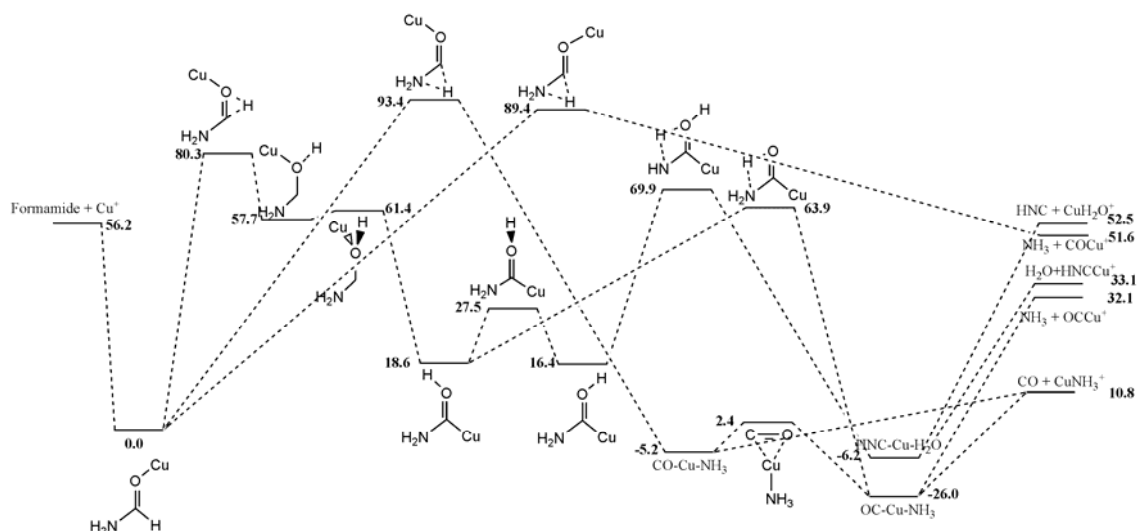


**Figure 19.** Energy profile of the unimolecular reactivity of the oxygen-attached formamide- $\text{Cu}^+$  complex.

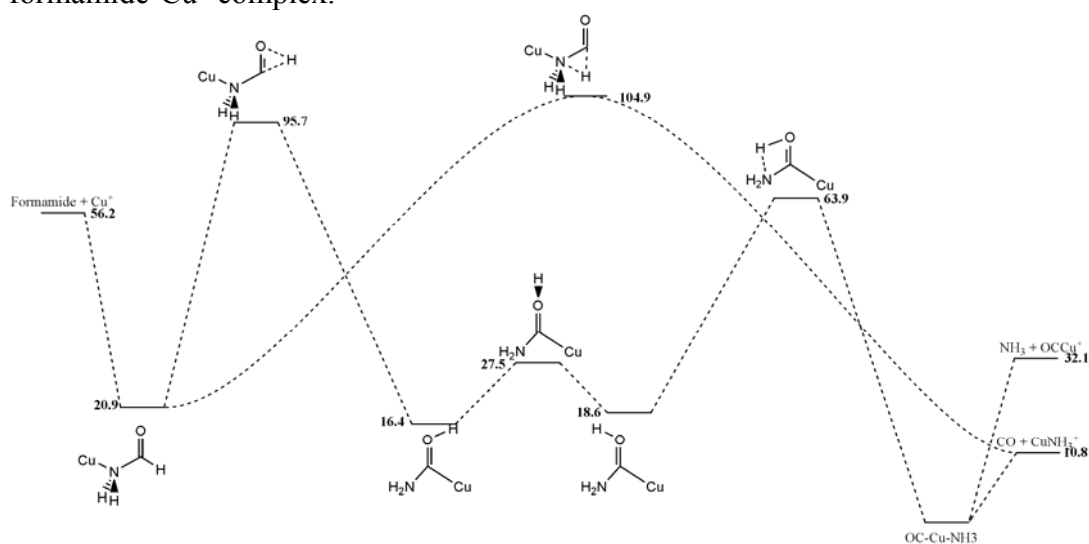


**Figure 20.** Energy profile of the unimolecular reactivity of the nitrogen-attached formamide- $\text{Cu}^+$  complex.

In the case of urea, two amino groups are available for the interaction with the metal ion. The effects of this second amino group are reflected in both the interaction

patterns of copper and the nature of the fragments obtained in gas-phase unimolecular decompositions, because new fragments can be generated when dealing with urea, which are not possible when the base is formamide. For instance, while the loss of ammonia leads to  $\text{COCu}^+$  in the case of formamide- $\text{Cu}^+$  reactions, in urea- $\text{Cu}^+$  reactions the same process produces a  $\text{HNCOCu}^+$  ion, which is the most abundant one.<sup>121,173</sup> The DFT calculated PESs showed a quite different mechanism in both cases. While in urea- $\text{Cu}^+$  reaction, ammonia is formed through a 1,3-Hydrogen transfer between both amino groups, for formamide- $\text{Cu}^+$  reactions, this is a three-steps process, the former being a 1,2-H shift from the C-H group towards the carbonyl oxygen, which is subsequently transferred to the amino group by means of a 1,3-H shift. Furthermore, the  $\text{HNCOCu}^+$  fragment is only produced from the O-attached adduct as precursor. In both reactions a high intensity peak corresponding to the  $\text{CuNH}_3^+$  ion is observed with origin in the N-attached complex. In both cases the barriers are lower than the entrance channel which indicates that these mechanisms are thermodynamically favored (see figure 21).

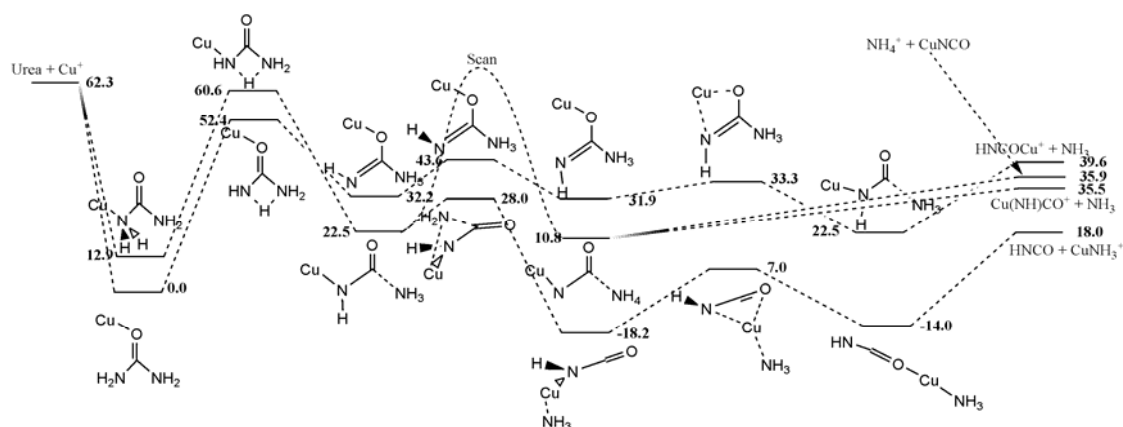
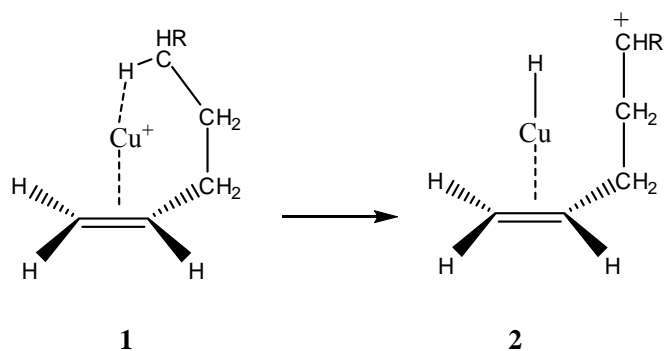


**Figure 21.** Energy profile associated with the unimolecular reactivity of the urea- $\text{Cu}^+$  system

In the reaction of formamide with copper, it is to be mentioned that the loss of water was found to be a quite favorable process whereas such a process was not

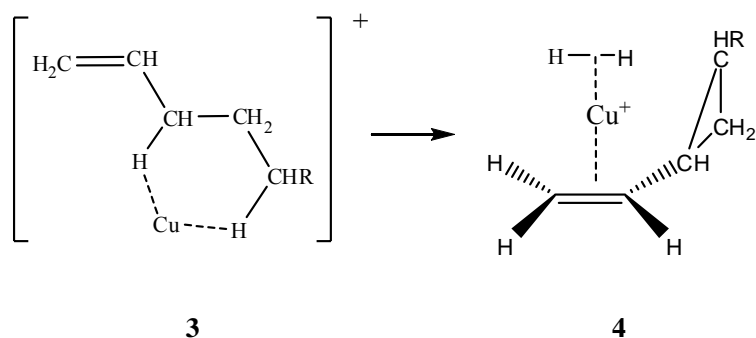
observed for urea. A theoretical survey of the corresponding PES showed that for formamide a double hydrogen transfer towards the carbonyl oxygen atom is feasible, a first one from the nearest carbon and a second one from the amino group<sup>171</sup>. However, for urea-Cu<sup>+</sup> these hydrogen transfers to oxygen do not compete with those taking place between the two amino groups which ultimately lead to the loss of NH<sub>4</sub><sup>+</sup>.<sup>121</sup> Interestingly, this is not the case when the carbonyl group is replaced by an isoelectronic NH group as in the case of guanidine-Cu<sup>+</sup> complexation<sup>174</sup> where the loss of NH<sub>4</sub><sup>+</sup> was not observed in the mass spectra. It is worth noting, however, that this is the only significant difference between guanidine-Cu<sup>+</sup> fragmentations and urea-Cu<sup>+</sup> ones. For instance, if we take into account that the difference between urea and guanidine molecule is the replacement of the oxygen by a NH group, the loss of HNCO observed in urea-Cu<sup>+</sup> reactions<sup>121</sup> appears as the loss of HNCNH in guanidine-Cu<sup>+</sup> ones<sup>174</sup>. In both cases the dominant product of the reaction was ammonia.

Another aspect to be emphasized on the Cu<sup>+</sup> reactivity is that the metal cation can act as a hydrogen carrier for the loss of H<sub>2</sub>. For urea- and formamide-Cu<sup>+</sup> systems the experimental results do not provide any indication of such a loss. However, in 2-propanol-Cu<sup>+</sup>,<sup>175,176</sup>, ethylenediamine-Cu<sup>+</sup>,<sup>177</sup> and alkenes-Cu<sup>+</sup> reactions,<sup>178</sup> the loss of H<sub>2</sub> molecule was systematically observed with different intensity. All the theoretical studies which aimed at explaining the dissociation of H<sub>2</sub> in these complexes pointed to the role of copper as a carrier. Concerning the alkenes-Cu<sup>+</sup> complexes, the attachment of the metal cation to  $\pi$ -system forces a coiling of the alkyl chain which favors the formation of a hexa-coordinated intermediate (form **1** in scheme 7) which eventually evolves to yield form **2** which could be a good precursor for the loss of H<sub>2</sub>.



Scheme 7

However, much more stable complexes, as species **3** (see Scheme 8), can be formed when the metal ion interacts simultaneously with two C-H bonds of the alkyl chain, through typical agostic-type interactions, already discussed in detail in preceding sections of this chapter. The activation of both C-H bonds lead to the formation of structure **4** (see Scheme 8) which finally dissociates by losing  $\text{H}_2$



Scheme 8

The most favorable process in the reactions between  $\text{Cu}^+$  and alkenes corresponds, however, to the loss of one olefin molecule. This happens, as proposed by Fordham *et al.*<sup>179</sup>, through a pseudo-insertion mechanism, in which form **1**, where the alkyl chain coils up to enhance its interaction with the metal cation, plays an important role. From **1**, and for the particular case of pentene, two different unimolecular dissociation processes leading to  $\text{C}_2\text{H}_4 + [\text{H}_3\text{C}-\text{CH}=\text{CH}_2-\text{Cu}]^+$  and to  $\text{C}_2\text{H}_6 + [\text{H}_2\text{C}=\text{CH}_2-\text{Cu}]^+$  are possible, the former being more favorable due to the larger  $\text{Cu}^+$  binding energy to  $\text{H}_3\text{C}-\text{CH}=\text{CH}_2$ .

The loss of H<sub>2</sub> in Cu<sup>+</sup>-2-propanol reactions was investigated by Cheng *et al.*<sup>176</sup>, by means of B3LYP/6-311+G(d,p) calculations. Two different mechanisms would be compatible with the experimental observations of Huang *et al.*<sup>175</sup> where the most abundant fragment is Cu-[C<sub>3</sub>H<sub>6</sub>O]<sup>+</sup>. One of them would yield 2-propenol-Cu<sup>+</sup> while the other would produce acetone-Cu<sup>+</sup>. In both cases, the 2-propanol-Cu<sup>+</sup> complex loses a hydrogen molecule. The most favorable mechanism was the one schematized in Figure 21 where acetone-Cu<sup>+</sup> appears as the product ion. The exit channel is reached via a C-OH metal insertion followed by a hydrogen shift. It can be viewed that, also in this case, copper acts as carrier of the hydrogen molecule to yield the acetone-Cu<sup>+</sup> fragment and the energy barriers involved in this mechanism are below the entrance channel. Note that the C-H insertion mechanism was found energetically unfavorable and consequently was discarded.

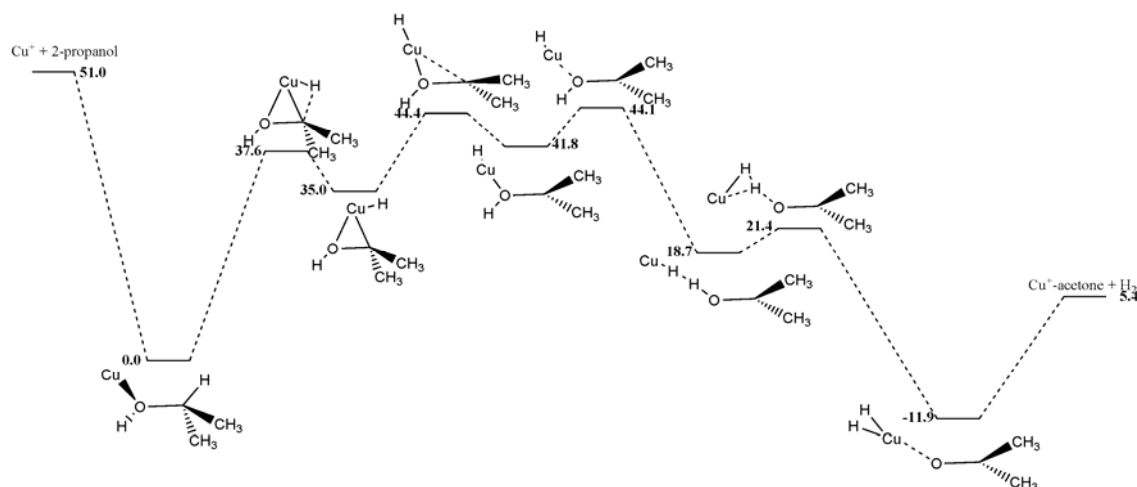


**Figure 21.** Energy profile associated with the unimolecular decomposition of the 2-propanol-Cu<sup>+</sup> complex

For ethylenediamine-Cu<sup>+</sup> reaction, Alcamí *et al.*<sup>177</sup> also showed the active role played by copper in the H<sub>2</sub> loss. In this case also the activation energies remain below the entrance channel all along the route from the initial Cu<sup>+</sup> adduct to the products. (see Figure 22)

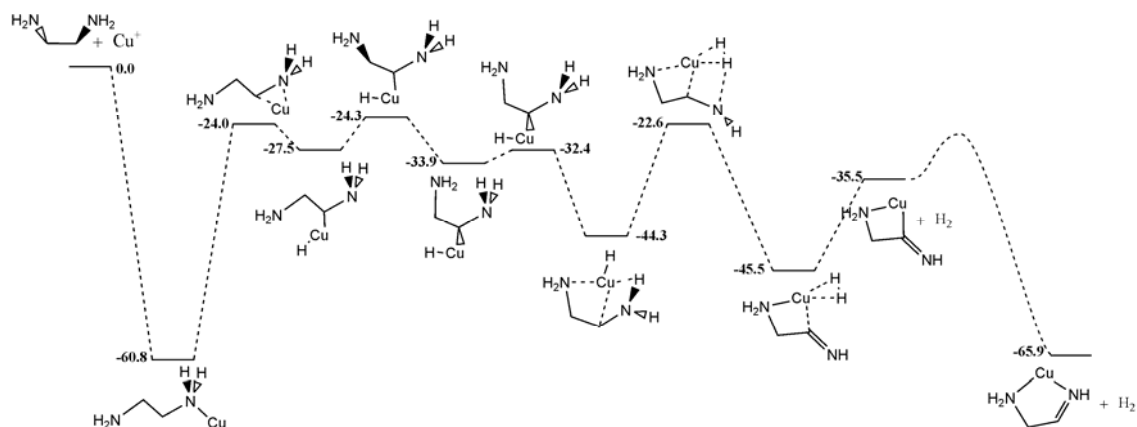


**Figure 22.** Energy profile associated with the unimolecular decomposition of the ethylenediamine- $\text{Cu}^+$  complex.

$\text{Cu}^{2+}$  reactivity is dominated by its oxidation capacity already mentioned when discussing its bonding. Accordingly, and unlike inorganic molecules<sup>180</sup>, the doubly charged complexes resulting from the association of  $\text{Cu}^{2+}$  to any typical organic base have not been experimentally observed by the experimental techniques available to date, since an immediate deprotonation of the system takes place and only the singly charged deprotonated copper complex is detected. Hence,  $\text{Cu}^{2+}$  reactivity is rather similar in many aspects to that of  $\text{Cu}^+$ , since what is usually observed is the fragmentation of the singly charged species produced upon deprotonation of the doubly charged complexes.<sup>125,150,181</sup> Hence, not surprisingly the fragmentation of uracil- $\text{Cu}^{2+}$  complexes, to be discussed in a forthcoming section, follows similar patterns to those observed for instance in the fragmentation of formamide- $\text{Cu}^+$  and urea- $\text{Cu}^+$  complexes.

The most significant difference between formamide- $\text{Cu}^+$  and urea- $\text{Cu}^+$  with respect to uracil- $\text{Cu}^{2+}$  reactions is the loss of  $\text{NCO}^\bullet$  radical which is only observed for the latter reflecting as we shall discuss later on the important role played in this case by  $\pi$ -type complexes.



## **VIII. Gas-phase reactivity of copper(I) and copper(II) ion towards molecules of biological relevance**

As already mentioned in the introduction, copper plays a significant role in different biochemical processes. For example, in the mechanism of action of several enzymes, it is the cofactor of redox reactions involving molecular oxygen, and it is involved in antibody production.

Gas-phase studies on the interaction of copper with small model molecules is of great interest because the knowledge of their intrinsic properties can provide important clues to understand the behavior of more complicated systems of biological importance. These studies have received much more attention since the introduction of fast atom bombardment (FAB), laser desorption, and electrospray ionization (ESI) as methods of forming such complexes in the gas phase.

### **A. Reactivity with amino acids and peptides**

A typical example is the study of the reactivity of copper ions towards amino acids and peptides, and numerous studies involving either of the aforementioned ionization methods have been published during the last decade. These studies can be divided into two categories. The first one corresponds to the direct examination of "binary" mixtures of copper salts and amino acids or peptides, and will be first described. The second category deals with the generation of ternary complexes by using an auxiliary organic ligand which occupies some coordination sites in the copper ion, and thus directs the coordination of the biomolecule.

#### ***1. Binary mixtures***

Gas-phase interaction between Cu(I) ions and the simplest amino acid, namely glycine, have been first studied by Plasma Desorption Mass Spectrometry.<sup>182</sup> Complexes of interest were generated in a plasma desorption ion source by bombarding a mixture of glycine and cupric salts by fission fragments of <sup>252</sup>Cf. Regardless of the copper salt used, the resulting adducts are of the type M<sup>+</sup>Cu<sup>+</sup>. Copper in its cuprous oxidation state [Cu(I)] is indeed exclusively observed, not only for glycine but also for the other nine amino acids considered in this study (Val, Phe, Tyr, Trp, His, Asp, Asn, Glu, Gln). Under metastable conditions, the unimolecular decomposition of the [Cu-glycine]<sup>+</sup> complex is characterized by the predominant elimination of a 46u [H<sub>2</sub>C, O<sub>2</sub>] fragment. Noteworthy, this fragmentation is commonly observed both cationized and protonated amino acids. This elimination may correspond either to the loss of formic acid, HCOOH, or to the consecutive loss of H<sub>2</sub> and CO<sub>2</sub>, or H<sub>2</sub>O and CO. Use of deuterated amino acids suggested that most probable mechanism involves the consecutive elimination of water and carbon monoxide, likely leading to the formation of a metal-cationized imine.

The Cu<sup>+</sup>/glycine system has been recently reinvestigated by combining electrospray ionization tandem mass spectrometry and DFT calculations.<sup>183</sup> Collisional activation experiments were carried out on [<sup>63</sup>Cu-glycine]<sup>+</sup> ions (*m/z* 138). Again, the most favorable dissociation process corresponds to the formation of [Cu<sup>+</sup>·HN=CH<sub>2</sub>]<sup>+</sup> concomitant to the elimination of [H<sub>2</sub>C, O<sub>2</sub>]. Total H/D exchange of the acidic hydrogens showed that the hydrogen atoms eliminated in the 46 u are labile hydrogens. In order to rationalize these experimental findings, authors explored the potential energy surfaces associated with this system. As mentioned before in this chapter and confirming previous theoretical studies, the most stable form of copper-glycine involves metal chelation between the nitrogen atom and the oxygen atom of the carbonyl group.

Several mechanisms were considered to account for the fragmentations observed, involving either metal insertion into covalent bonds (C-C, C-O) or dissociative attachment whereby the metal ion catalyzes the fragmentation by its distant electronic influence. It was shown that the formation of  $[\text{Cu}\cdots\text{HN}=\text{CH}_2]^+$  is exclusively associated with the loss of  $(\text{H}_2\text{O}+\text{CO})$  as elimination of other neutral species such as  $\text{HCOOH}$ ,  $\text{C}(\text{OH})_2$  and  $\text{H}_2+\text{CO}_2$  imply energy barriers located higher in energy than the decationization energy and therefore are not competitive. The dissociation proceeds through mechanisms involving copper insertion into the C-C and C-OH bonds. It may either start with insertion into the C-C bond, followed by insertion into the C-OH bond (Figure 23), or these two elementary steps may occur in the reverse order.

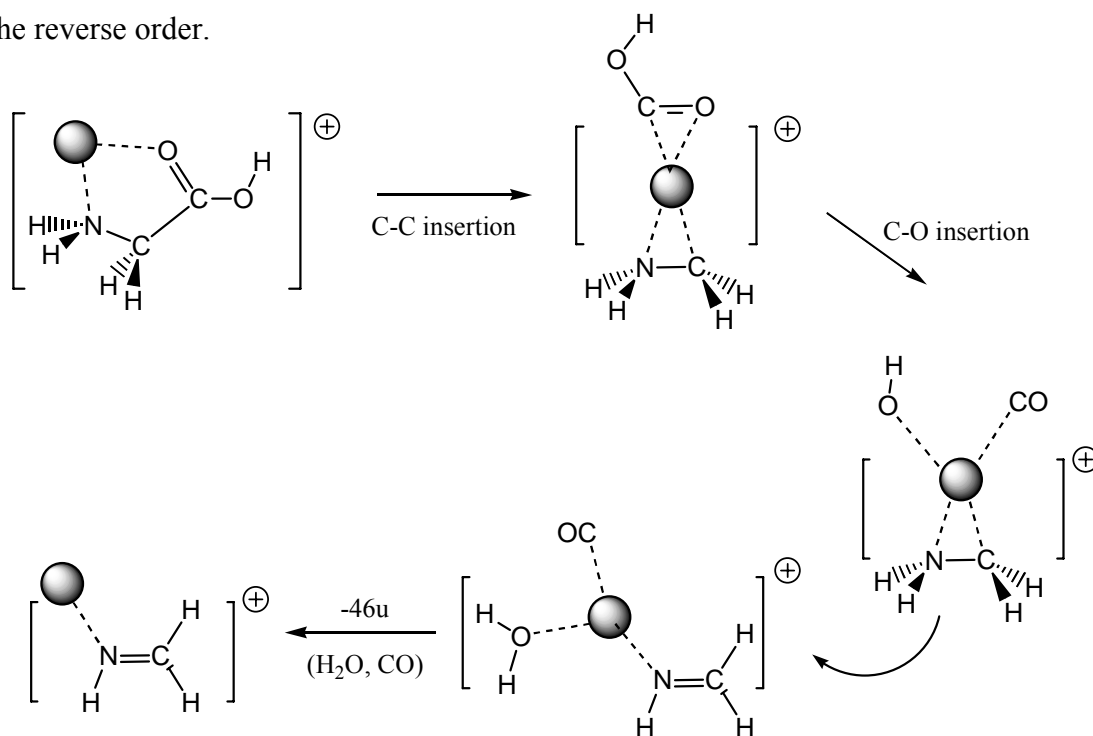


**Figure 23.** Most favorable mechanism proposed for the elimination of 46u from the  $[\text{Cu-glycine}]^+$  complex.

This elimination of 46u is in fact commonly observed for various amino acids, and notably the four aromatic amino acids histidine, tryptophan, tyrosine and phenylalanine.

<sup>155,182,184</sup> However, the reactivities of glycine and of these amino-acids also differ. For

example, elimination of  $\text{CO}_2+\text{NH}_3$  is systematically observed and is the main fragmentation for the  $[\text{Cu-His}]^+$  complex.<sup>184</sup> An additional characteristic fragmentation detected at high collision energies corresponds to the loss of a 137u consistent with a  $[\text{Cu,C}_2,\text{O}_2,\text{N,H}_4]$  group, and leading to the ionized side chain  $\text{R}^+$ . The observed losses are found to be very similar for all the aromatic systems and only differ in their relative intensities. They do not involve cleavage within the amino acid side chain, in agreement with other previous metal cation–amino acid studies.<sup>77,185</sup> Given these similarities, Rimola et al.<sup>184</sup> have only investigated theoretically the  $[\text{Cu-Phe}]^+$  system. The most stable structure corresponds to the metal cation interacting with the aromatic ring, the amine nitrogen and the carbonyl oxygen. The exploration of the various potential energy surfaces showed that the observed eliminations are produced from insertion of the metal cation either into the backbone C-C bond of Phe (losses of 46u) or into the C-R bond (losses of 137u). Concerning the latter process, it has been demonstrated that the direct elimination of a  $\text{HOOC-CH-NH}_2\text{Cu}$  moiety is favored over the consecutive loss of  $\text{CuCOOH}$  and  $\text{CH}_2=\text{NH}$ .

In addition to the  $[\text{Cu-AA}]^+$  species, complexes of general formula  $[\text{Cu(AA)-H}]^+$  can also be generated by decreasing the cone voltage of an electrospray interface. This was observed for histidine.<sup>155</sup> Expectedly, the gas-phase reactivities of  $[\text{Cu-His}]^+$  and  $[\text{Cu(His)-H}]^+$  complexes are different. Upon collision, the latter species not only expels a  $[\text{C}_2,\text{O}_2,\text{H}_3,\text{N}]$  entity but also yields the immonium  $\text{I}_{\text{His}}$ , as fragment ion. Based on thermochemical estimates, the formation of these two particular ions has been interpreted as elimination of  $\text{CO}_2$ , immediately followed by loss of formalimine and the neutral metal, respectively. Note that for zinc and copper the decarboxylated complexes appeared unstable (not observed) while they are detected in significant abundance for other metal ions such as  $\text{Ni}^{2+}$ ,  $\text{Co}^{2+}$  and  $\text{Fe}^{2+}$ . In the literature, the

decarboxylation is usually interpreted as a radical-like mechanism involving reduction of the metal (Figure 24). Note that the elimination of formaldimine implies the insertion of the metal within the amino acid side-chain.

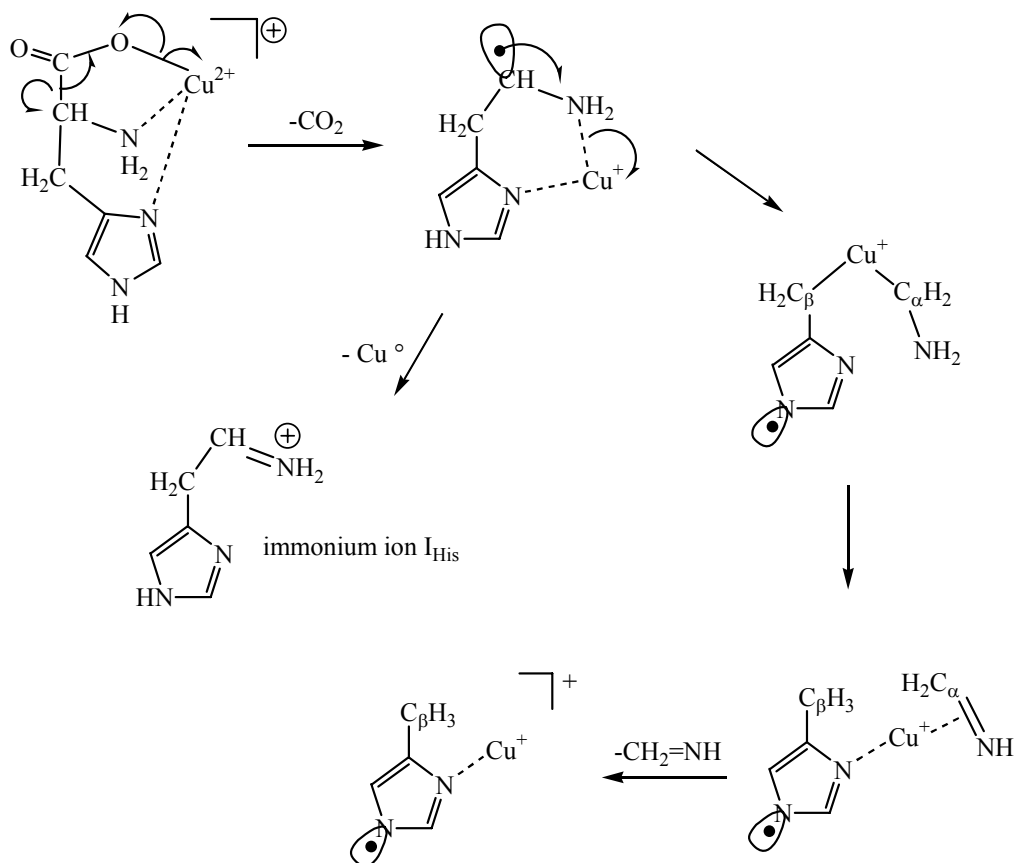


**Figure 24.** Mechanism proposed for the characteristic fragmentations of the  $[\text{Cu}(\text{His})\text{-H}]^+$  complex.

Adopting mild source/interface conditions also allows the formation of multiply charged and solvated ions by electrospray. As a matter of fact, with such conditions and by using water as solvent, Seto and Stone<sup>186</sup> managed to generate stable and relatively abundant  $[\text{Cu}(\text{gly})(\text{H}_2\text{O})]^{2+}$ ,  $[\text{Cu}(\text{gly})(\text{H}_2\text{O})_2]^{2+}$  and  $[\text{Cu}(\text{gly})_2]^{2+}$  complexes in the gas phase, even if the major ion in the spectrum is that of protonated glycine,  $\text{GlyH}^+$ . On the other hand, these authors did not manage to produce in the source the complex in which the copper dication interacts with a single glycine molecule, but this behavior under ESI is typical of this metal, as mentioned before. It is worth noting that a doubly charged

species isobaric to the  $[\text{Cu}(\text{gly})]^{2+}$  ion was detected in the CAD spectra of  $[\text{Cu}(\text{gly})(\text{H}_2\text{O})]^{2+}$  and  $[\text{Cu}(\text{gly})(\text{H}_2\text{O})_2]^{2+}$ , strongly suggesting that the  $[\text{Cu}(\text{gly})]^{2+}$  is indeed stable thermodynamically.

The unimolecular reactivity of the doubly charged complexes is characterized by two kinds of product ions, depending on whether a charge reduction occurs during the fragmentation. If one examines the CID spectra of the  $[\text{Cu}(\text{gly})(\text{H}_2\text{O})]^{2+}$  species, one can see that there is a preference for loss of neutral water rather than neutral glycine, in agreement with the fact that glycine should have the higher enthalpy of association.

An interesting fragment ion in the MS/MS spectrum of  $[\text{Cu}(\text{gly})_2]^{2+}$  is the loss of water. The postulated mechanism for the formation of this ion is the elimination of a molecule of water in an intracomplex condensation reaction, leading to the formation of a peptide bond between the two glycine residues, the dipeptide remaining attached to the metal. Even if there is no experimental evidence in the gas phase supporting this assumption, it is worth mentioning that such a reaction occurs in aqueous solutions containing a Cu(II) salts and glycine.<sup>187,188</sup>

Chiral assignments are of great interest because the chemical or biological activity of a substance often depends on its stereochemistry. While condensed-phase techniques such as NMR, circular dichroism and chromatography are widely used to study enantioselective intermolecular interactions, increasing attention is being paid to gas-phase techniques, in particular mass spectrometry. Chiral recognition by mass spectrometry has been made possible through the use of the well-known kinetic method,<sup>189,190</sup> which was initially developed by R.G. Cooks for the determination of thermochemical values such as gas-phase basicities, metal ion affinities or ionization energies of organic compounds.<sup>191</sup> Recently, the kinetic method has been successfully applied to the chiral recognition of *D*- and *L*- amino acids by analysis of the kinetics of

competitive fragmentations of trimeric copper(II)-bound complexes.<sup>192</sup> Singly charged cluster ions of general formula  $[\text{Cu}(\text{II})(\text{AA})_n - \text{H}]^+$  ( $\text{AA} = \text{amino acids}, n = 2, 3, 4$ ) can be generated easily in the gas phase by electrospray ionization of  $\text{Cu}(\text{II})$ -amino acid mixtures. CID experiments showed that dimeric clusters ions ( $n=2$ ) dissociate according to  $\text{CO}_2$  loss. In contrast, heterotrimeric cluster ions appeared to have two singly bound ligands (Figure 25), as attested by the MS/MS spectra of  $[\text{Cu}(\text{AA}1)_2(\text{AA}2) - \text{H}]^+$ , resulting solely in the formation of dimeric cluster ions by elimination of either  $\text{AA}1$  or  $\text{AA}2$ .

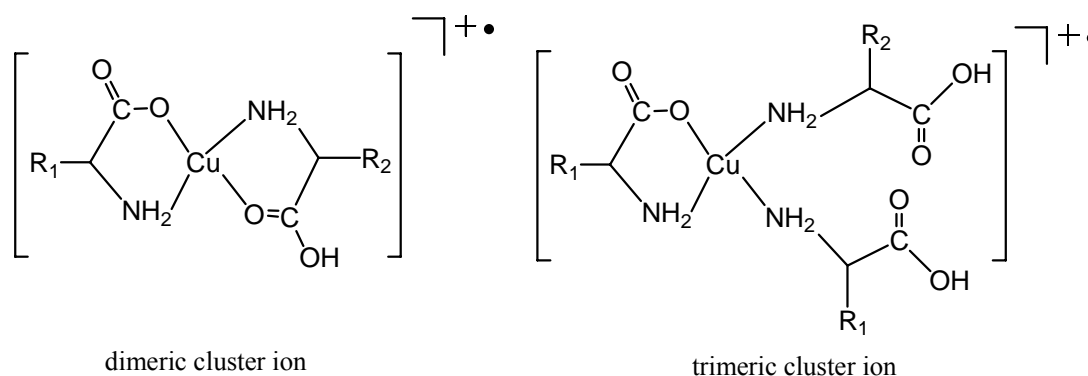
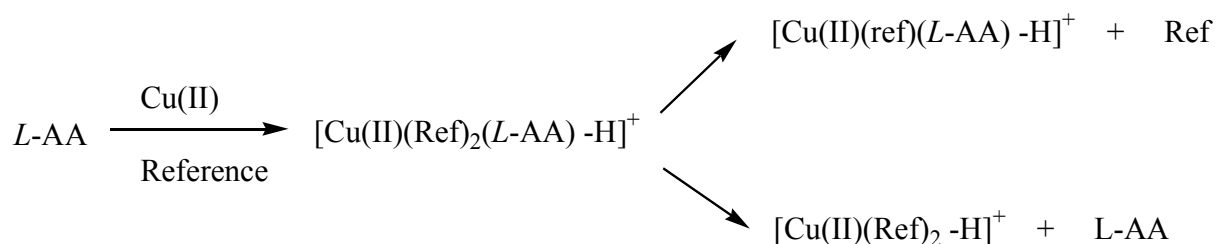
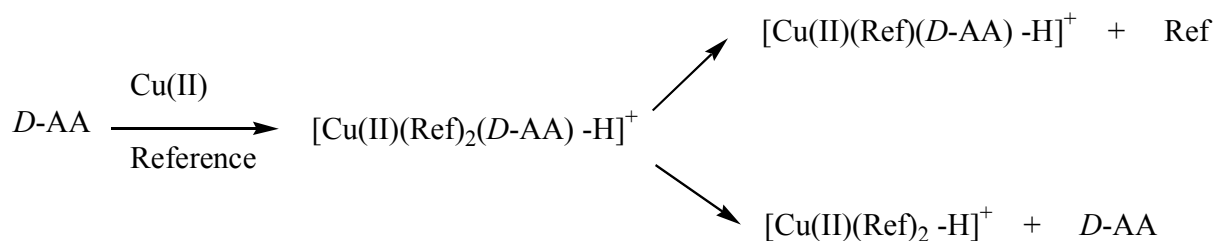


**Figure 25.** Coordination scheme of copper in binary and ternary cluster ions

Six amino acids (AA) were studied i.e. Tyr, Leu, Met, Phe, Thr, Asp. By using L-proline as reference and by assuming that only the monoligated aminoacids can be lost, the singly charged trimeric cluster ions  $[\text{Cu}(\text{II})(\text{L-proline})_2(\text{AA}) - \text{H}]^+$  were mass selected and collisionally excited in a quadrupole ion trap, where they are dissociated competitively to form the dimeric complexes  $[\text{Cu}(\text{II})(\text{L-proline})(\text{AA}) - \text{H}]^+$  and  $[\text{Cu}(\text{II})(\text{L-proline})_2 - \text{H}]^+$  by the loss of the neutral reference, or the amino acid AA studied, respectively.



with  $r_L = I([\text{Cu(II)}(L\text{-proline})(L\text{-AA})\text{-H}]^+) / I([\text{Cu(II)}(L\text{-proline})_2\text{-H}]^+)$ ,



and  $r_D = I([\text{Cu(II)}(L\text{-proline})(D\text{-AA})\text{-H}]^+) / I([\text{Cu(II)}(L\text{-proline})_2\text{-H}]^+)$ .

The difference in stability of the fragment ions  $[\text{Cu(II)}(L\text{-proline})(\text{AA})\text{-H}]^+$ , due to the two enantiomeric forms of the AA, results in differences in the corresponding product ion abundances, measured relative to the abundance of  $[\text{Cu(II)}(\text{ref})_2\text{-H}]^+$ . The two abundance ratios  $r_L$  and  $r_D$  allow evaluating the "chiral resolution factor R", equal to  $r_D/r_L$ . The data obtained revealed that amino acids with an aromatic side chain shows a very high chiral effect ( $R \gg 1$ ), while aliphatic amino acid are characterized by R values very close to 1.

Additional experiments demonstrated for aromatic amino acids the quantitative nature of the chiral distinction achieved by the kinetic method. Proline mixtures with various optical purities (fraction of *D* isomer = 0, 0.25, 0.5, 0.75, and 1) were used as the reference and *D*- or *L*-tyrosine was used as the analyte. As expected, the largest chiral discrimination was observed when pure *D*- or *L*-proline was used as the reference. There was no chiral distinction for *D*- and *L*-tyrosine when proline racemate was used



as the reference. These first results showed that the kinetic method could be applicable to measurement of enantiomeric excess.

During the last decade, tandem mass spectrometry has become an invaluable tool for identification of peptides and proteins. In this context, the most widely applied strategy is to perform low-energy CID experiments on protonated peptides ( $[M+nH]^{n+}$  ions). Not only these ions can be easily formed by several ionization methods, and especially matrix assisted laser desorption ionization (MALDI) and electrospray ionization (ESI), but they also provide primary sequence information upon activation by cleavage of the amide linkages to yield complementary  $b_n/y_n$  series of ions (Figure 26).

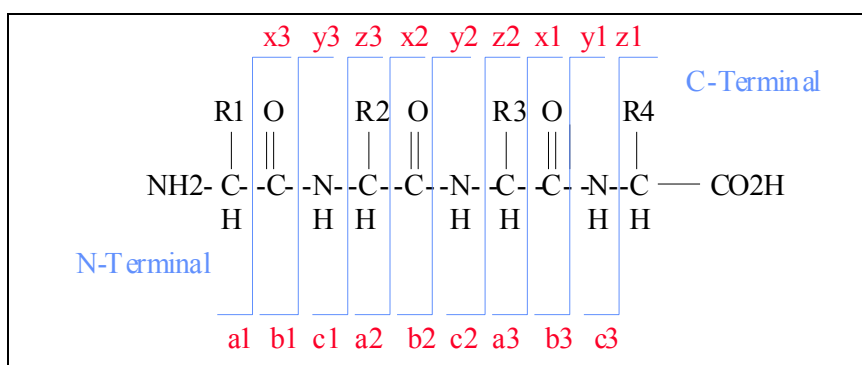


**Figure 26.** Nomenclature adopted to label fragment ions resulting from peptide backbone cleavages (From Ref. 193).

Although fragmentation of protonated peptides is highly useful, this approach suffers from several limitations. The sequence information can be limited because protonated peptides may not fragment at every amide bond, leading to incomplete sequence information. Products from only one or a few specific cleavages often dominate product ion spectra, depending upon the charge state and the primary sequence of the peptide. Finally, the location of post translational modifications (PTMs) cannot be determined. For these reasons, alternative means for deriving peptide structural information are desirable. In this context, metal-specific fragmentations can provide a useful complement toward full structural characterization of peptides.

Consequently, besides studies describing the mechanisms of interaction of copper with peptides, the reactivity of Cu(I) and Cu(II) ions has been applied for sequencing purpose, and also to distinguish isomeric peptides.

As mentioned earlier, the elimination of 46 u from  $[M+Cu]^+$  ions is commonly observed for amino acids. On the other hand, this fragmentation is not observed for peptides. Instead, Shields et al.<sup>194</sup> have shown that the metastable ion spectra of  $[M+Cu]^+$  complexes obtained with small peptides containing a N-terminal arginine, are characterized by loss of neutral fragments such as water, formaldehyde, acetaldehyde when peptides include a serine, threonine or glutamic acid residue, and ammonia or guanidine for peptides containing basic residues such as lysine or arginine. Unlike the  $[M+H]^+$  ions, immoniums ions and internal fragments were practically not detected. Interestingly, series of ions of general formula  $[a_n+Cu-H]^+$ ,  $[b_n+Cu-H]^+$ , and  $[c_n+Cu+H]^+$ , resulting from the cleavage of the peptidic chain are also particularly abundant. Such ions have also been observed with alkali metals<sup>195</sup> and  $Ag^{+196}$ , and provide interesting sequence information. Authors also noticed that the dissociation processes of  $[M+Cu]^+$  ions were governed by the presence and the position of the arginine residue. All the fragment ions of peptides containing a N-terminal arginine contained the arginine residue and  $Cu^+$ .

$[b_n + Cu - H]^+$  ions are formed by cleavage of peptide backbone amide bonds associated with the migration of hydrogen to the neutral leaving group. Several mechanisms have been proposed in the literature in order to explain their formation, one involving the transfer of a hydrogen from the  $C\alpha$ -carbon to the neutral leaving group,<sup>197</sup> and two involving instead a hydrogen from the amide NH group.<sup>198,199</sup> Data obtained with glycine-containing peptides suggested that the proton transferred to the leaving group does not originate from the side chain as glycine does not have a side chain.

Furthermore, results deduced from H/D exchange experiments indicated that the hydrogen transferred is an amide nitrogen from the N-terminal side of the cleavage. Consequently, to interpret the difference of reactivity between  $[M+H]^+$  and  $[M+Cu]^+$  ions, authors proposed that the  $Cu^+$  ion is anchored at the N-terminal arginine, and that  $[b_n+Cu-H]^+$  fragment ions are formed via a mobile proton transferred from the N-terminus to other amide nitrogens along the peptide backbone. The results obtained during this particular study also showed that the  $[a_n+Cu-H]^+$  ion were either generated directly from the precursor ions, or by loss of CO from the corresponding  $[b_n+Cu-H]^+$  species. A second study<sup>200</sup> confirmed that the side chains of the basic amino acids arginine and, to a lesser extent, histidine and lysine were the  $Cu^+$  binding sites within peptides. B3LYP calculations have also been performed in order to establish a relative copper affinity scale for monodentate and bidentate interactions. Relative binding energies of the model monodentate ligand- $Cu^+$  systems were as follows: Arg> His> Lys> Cys> Ser. A slightly different order has been found for bidentate  $Cu^+$  binding energies (Arg>Lys>His>Gln>Asn>Glu>Asp), indicating the importance of multidentate  $Cu^+$  coordination. In a MALDI study published several years ago,<sup>201</sup> it was deduced from the analysis of the interactions with sixteen synthetic peptides that the compounds containing no histidine did not form stable metal complexes under MS conditions, whereas all histidine containing sequences formed metal complexes. This confirms histidine as an important binding site of copper in proteins.

The use of metallation by divalent metal ions for investigating peptide structures has not been widely explored under negative ESI conditions so far. One reason could be the relatively low yield of negative-ion complexes generated under ESI conditions in comparison with those achieved in positive-ion mode. However, the group of Tabet has demonstrated that the copper reactivity can be successfully applied for the

differentiation of isomeric peptides.<sup>202,203</sup> By mixing various modified enkephalins (YGGFX, X=I, L, M, Q, K) and copper chloride, pseudo-molecular ions such as [(M-3H)+Cu(II)]<sup>-</sup>, [M-H]<sup>-</sup> and [M-2H+CuCl]<sup>-</sup> can be generated in the gas phase by electrospray. The cationisation yield strongly depends on the concentration metal/ligand ratio and by using a ratio 10/1, the [(M-3H)+Cu(II)]<sup>-</sup> complex can be produced in significant abundance.

The major pathway observed in the low-energy CID spectra of [(M-3H)+Cu(II)]<sup>-</sup> corresponds to the loss of carbon dioxide. This differs strongly from the reactivity observed for binary complexes involving either of the other first-row transition metal ions, as with Mn<sup>2+</sup>, Fe<sup>2+</sup>, Co<sup>2+</sup>, Ni<sup>2+</sup> or Zn<sup>2+</sup> there is no loss of CO<sub>2</sub> (or it is very weak) and H<sub>2</sub>O elimination appears to be preferred. Formation of the [(M-3H)+Cu(II)]<sup>-</sup> complexes requires removal of three labile protons, e.g., from the amide and/or the carboxylic groups as well as the phenol group of the tyrosine side chain. The elimination of CO<sub>2</sub> strongly suggests that the terminal carboxylic site is deprotonated and does not coordinate the metallic centre.

The distinction of the C-terminal YGGFL and YGGFI (I and L at the C-terminal position) isomers by MS/MS experiments is possible neither from [M-H]<sup>-</sup> ions nor from [M+H]<sup>+</sup> species. On the other hand, these two peptides can be unambiguously distinguished by fragmentation of the [(M-3H)+Cu(II)]<sup>-</sup> complexes (Figure 27).

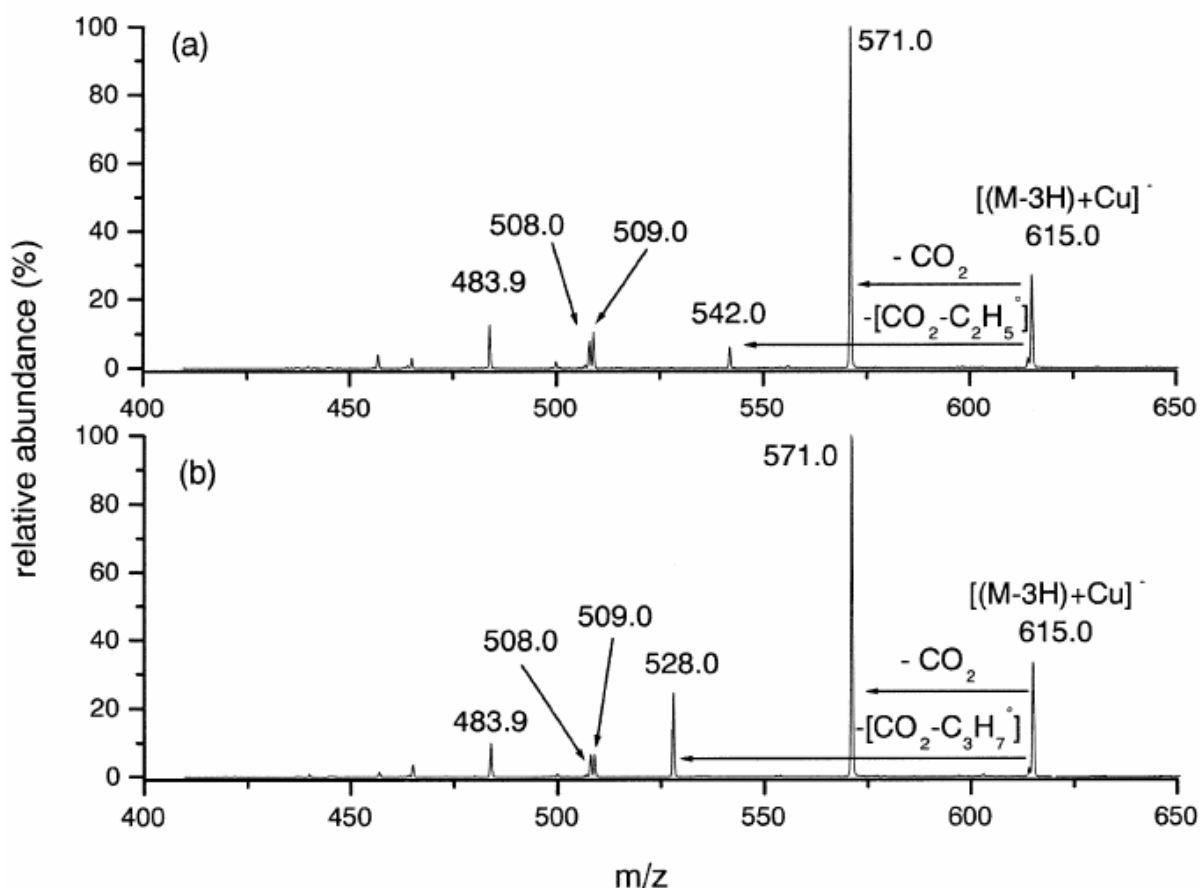


**Figure 27.** Low-energy CID spectrum of  $[M-3H+Cu(II)]^-$  complexes obtained for **a)** YGGFI and **b)** YGGFL. (taken from Bossée et al. *Rapid Communications in Mass Spectrometry* 17, 1229 (2003), Wiley; reprinted with permission)

Following decarboxylation, the loss of a  $C_2H_5$  radical, is indeed characteristic of YGGFI loss while elimination of  $C_3H_7$  is specific of YGGFL. Other transition metal ions (e.g.  $Mn^{2+}$ ,  $Fe^{2+}$ ,  $Co^{2+}$ ,  $Ni^{2+}$  or  $Zn^{2+}$ ) did not lead to such diagnostic ions. Such radical losses (produced by  $\beta$ - $\gamma$  bond cleavages) were observed only with  $Cu^{2+}$  ions and indicate the reduction of copper occurred during the decomposition process. Note however that such a distinction is not achieved when the I and L residues occupy internal position along the peptidic chain. It should also be pointed out that under high-energy CID, radical losses have been observed from anionic binary complexes containing alkali-earth metals.<sup>204,205</sup> However,  $\alpha$ - $\beta$  bond cleavages take place rather

than  $\beta$ - $\gamma$  bond cleavages. Such  $\alpha$ - $\beta$  bond cleavages did not allow the Leu/Ile isomers to be distinguished.

The two isobaric peptides, namely YGGFK and YGGFQ were also studied.<sup>203</sup> Both spectra exhibits losses of  $\text{CO}_2$  and  $\text{CH}_2=\text{C}_6\text{H}_4=\text{O}$ . Interestingly, YGGFQ exhibits an abundant additional product ion attributed to the loss of  $\text{H}_2\text{NCOCH}_2$  (Gln side-chain radical), again leading to the distinction of C-terminal Gln/Lys residues.

Isomeric peptide distinction can also be achieved through the use of the kinetic method, by a strategy similar to that presented for the distinction of enantiomeric amino acids (*vide supra*). More precisely, Cooks and co-workers evaluated the capacity of the kinetic method for the differentiation of isomeric dipeptides and for the quantitation of mixtures of isomers.<sup>206</sup> Six pairs of isomeric dipeptides (X-Y/Y-X) were successfully distinguished, by using an appropriate reference, and the relative amount of each partner in binary mixtures could be determined. This approach is particularly powerful because the spectra are simple and therefore easy to interpret. Although the information content is low, the fragmentation abundances are dependent on stereochemical interactions that are very sensitive to isomeric form. More recently, the kinetic method has been applied to differentiate isomeric tripeptides<sup>207</sup> and was extended further to determine compositions of ternary mixtures of the isomers Gly-Gly-Ala (GGA), Ala-Gly-Gly (AGG), and Gly-Ala-Gly (GAG). Different metals ions were tested and among the first-row transition metal ions, Cu(II) yields remarkably effective isomeric differentiation for both the isobaric tripeptides, GGI/GGL using GAG as the reference ligand, and the positional isomers GAG/GGA using GGI as the reference ligand. The procedure also allowed to perform chiral quantification of a ternary mixture of optical isomers.

Finally, complexation by  $\text{Fe}^{2+}$  and  $\text{Cu}^{2+}$  metal ions was successfully used to differentiate diastereomeric YAGFL,  $\text{Y}^{(\text{D})}\text{AGFL}$  and  $\text{Y}^{(\text{D})}\text{AGF}^{(\text{D})}\text{L}$  pentapeptides.<sup>208</sup> Binary

$[\text{Metal(II)(M-H)}]^+$  metal–peptide complexes were generated by ESI in the positive-ion mode. Their fragmentations were studied under low-energy collision conditions in an ion trap mass spectrometer. Again, with copper, the decarboxylation process is common to the three systems, but a careful examination of the CID spectra showed interesting differences. Indeed elimination of  $\text{CH}_2=\text{C}_6\text{H}_4=\text{O}$  is characteristic of the YAGFL peptide, therefore allowing its distinction from its  $\text{Y}^{(\text{D})}\text{AGFL}$  isomer. Concerning  $\text{Y}^{(\text{D})}\text{AGFL}$  and  $\text{Y}^{(\text{D})}\text{AGF}^{(\text{D})}\text{L}$  pentapeptides, their distinction is less straightforward and is based on the intensity of the fragment ion resulting from the decarboxylation. These distinctions was attributed to the stereochemical effects due to the  $^{(\text{D})}\text{Leu}/^{(\text{L})}\text{Leu}$  and the  $^{(\text{D})}\text{Ala}/^{(\text{L})}\text{Ala}$  residues yielding various steric interactions which direct relative dissociation rate constants of the binary  $[\text{M-H+Metal(II)}]^+$  complexes.

## ***2. Ternary complexes***

As biomolecules such as amino acids and peptides are practically always polydentate ligands, metal ions may interact with a variety of binding sites and coordination numbers, therefore resulting in a multitude of possible structures. In addition, numerous computational studies of transition metal ion complexes have shown that these structures are often very close in energy, and that the most stable forms in the gas phase do not necessarily correspond to the most stable forms in solution. Consequently, the actual structures generated in the gas phase by simply mixing the metal ion and the ligand of interest, are often unknown. A way to circumvent this problem is to use an auxiliary organic ligand that occupies some coordination sites in the metal ion ligand sphere and thus direct the coordination of the biomolecule to involve only one or two of its functional groups. In solution, copper(II) ions form stable complexes with multidentate polar molecules, such as

diimines, nitrogen heterocycles, amino acids, peptides or nucleosides. Very stable complexes self-assemble in solution when Cu(II) salts are mixed with an equivalent of the analyte and an aromatic diimine, for example, 2,2'-bipyridine (bpy) or 1,1'-phenanthroline (phen) (Figure 28) and the pioneering work of the Tureček's group has demonstrated that these solutions results in the production by electrospray of very abundant gaseous  $[\text{Cu(II)(ligand)(Analyte-H)}]^+$  ternary complexes.

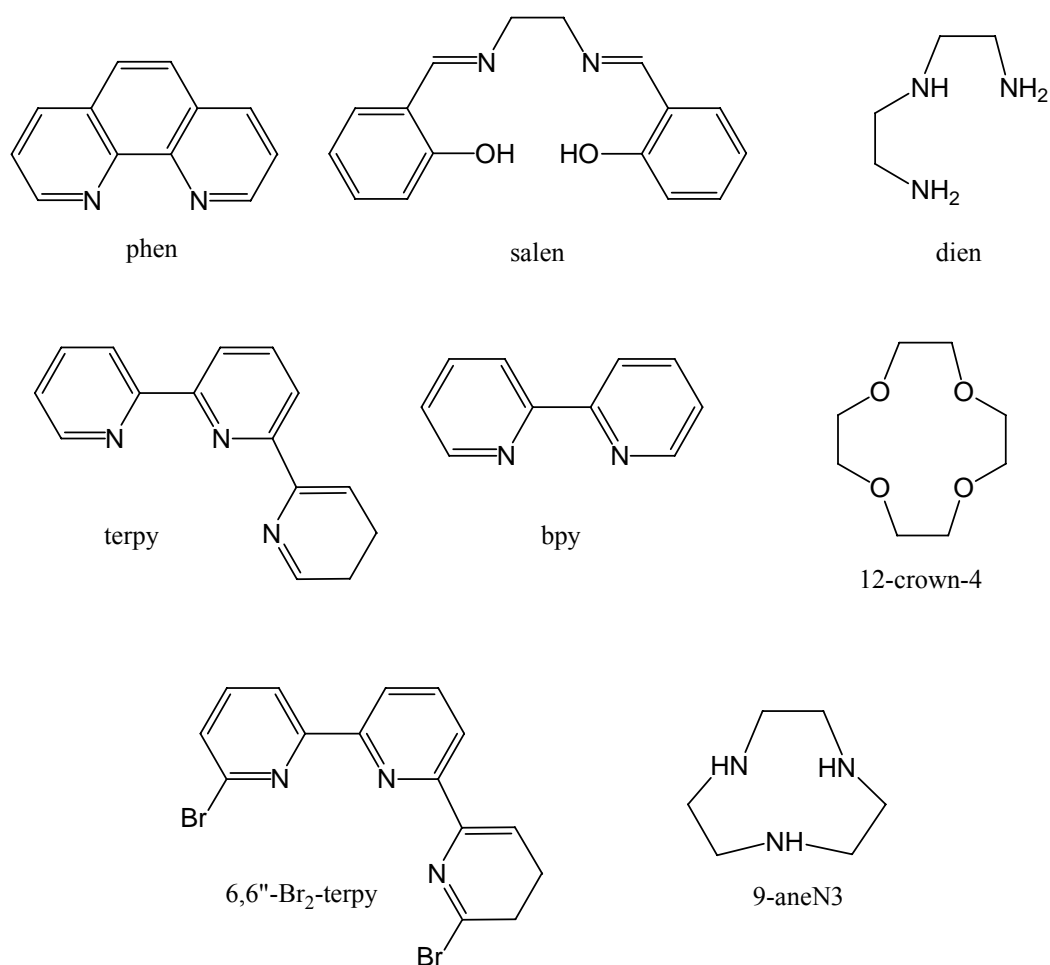


**Figure 28.** Auxiliary ligands typically used for the formation of ternary Cu(II) complexes.

Amino acids were the first biomolecules studied by this group<sup>61,153,154</sup> and the structure of these ternary complexes has been characterized by combining mass spectrometry and theoretical calculations (Figure 29).



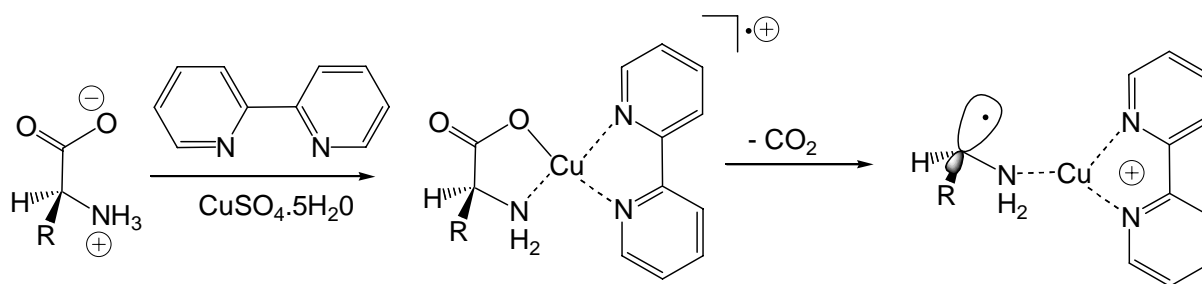


**Figure 29.** Structure of ternary Cu(II) complexes obtained with amino acids and the auxiliary ligand bipyridine.

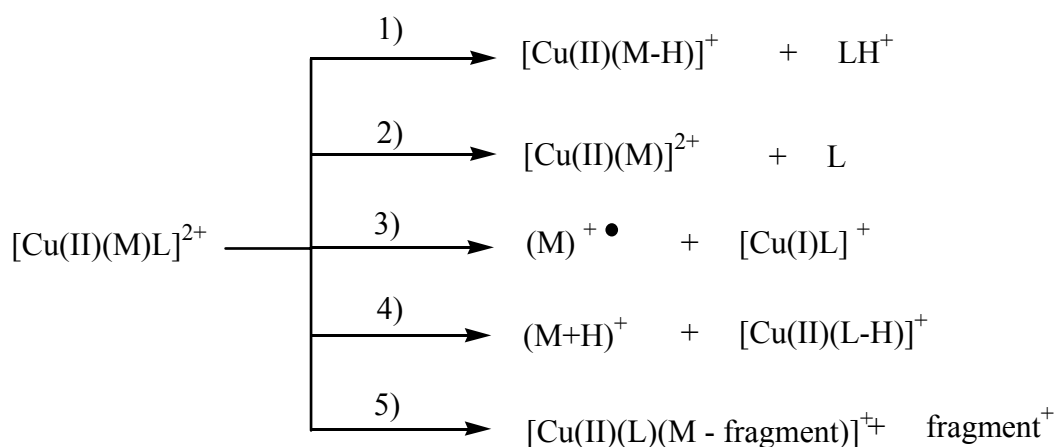
Experiments have shown that amino acids bind to Cu(II) by deprotonated carboxylate groups. Blocking the carboxylic group as a methyl ester practically prevents the complexes from being formed by electrospray.<sup>61,209</sup> The ternary complexes are odd-electron species showing a tetracoordinated Cu(II) with a square planar geometry. The bpy and amino acid amine nitrogens form regular Cu–N bonds with lengths. Analysis of the electron density reveals that most of the positive charge is located on the auxiliary ligand.

Upon collision, these singly charged ternary complexes undergo facile decarboxylation (Figure 29) yielding an amino acid C<sub>α</sub> radical. In turn, this ion undergoes the cleavage of the C<sub>β</sub>–C<sub>γ</sub> bond resulting in the loss of a radical from the side chain. Consequently, these ternary complexes allow notably to distinguish leucine from isoleucine, and lysine from glutamine.<sup>210</sup> Isomeric amino acids leucine and isoleucine could also be quantified in 90:10 to 10:90 binary mixtures, Tureček and co-workers also studied a series of tripeptides (GGA, LGG, GGL, GGI, FGG, GGF, LGF, GLF, GFL, GYA and GAY).<sup>211</sup> CID spectra of ternary complexes showed fragments that were indicative of the amino acid sequence in the peptide. The CID spectra of GGL and GGI complexes exhibit diagnostic peaks allowing C-terminal leucine and isoleucine to be distinguished. Interestingly, the formation of the [Cu(bpy)peptide]<sup>2+</sup> ternary complexes is also

observed when adopting mild electrospray ionization conditions. Their MS/MS spectra are clearly distinct for peptide isomers. Their fragmentation proceeds from both the *N*- and *C*-termini. Dissociations starting from the *N*-terminus are analogous to those in protonated peptides and produce b- and a-type ions. The complementary Cu-containing singly charged ions are analogous to ternary complexes of dipeptides or amino acids and are useful for structure elucidation of the *C*-termini in the peptides. The reader will find a complete description of these studies in a review published in 2007 by F. Tureček.<sup>12</sup>

An new type of redox reactions involving Cu(II) ions was discovered by Siu and co-workers for ternary complexes containing peptides and diethylenetriamine (dien) as auxiliary ligand (L).<sup>212</sup> By mixing in methanol the Cu(II)dien(NO<sub>3</sub>)<sub>2</sub> complex and a peptide M, [Cu(II)(dien)(M)]<sup>2+</sup> ions could be produced by electrospray. Upon collision, this complex dissociates according a charge transfer process to give rise to the radical cation of the peptide, M<sup>+•</sup>. The product ion spectra of M<sup>+•</sup> appeared very different from those of the corresponding (M+H)<sup>+</sup> and display a rich fragmentation chemistry, providing complementary structural information. This new reaction has attracted a considerable attention because of the unique fragmentation behavior of such radical cations. Indeed, while the fragmentation of even-electron peptide ions is dominated by the cleavage of amide bonds, radical cations are also characterized by cleavages of N–C $\alpha$  bonds, leading to c and z product ions (Figure 26). Consequently, many studies have been published over the last eight years and nowadays the use of ternary complexes is a well-established approach, besides electron capture dissociation (ECD) and electron transfer dissociation (ETD), to produce gaseous radical cation of amino acids and peptides. However, the charge transfer reaction is not the only dissociation

observed. By using enkephalin derivatives<sup>213</sup>, the following dissociation scheme could be established:



In order to favor the charge transfer process, many efforts have been devoted to the choice of the auxiliary ligand (Figure 28). The first experiments were carried out by using dien as auxiliary ligand.<sup>212,213</sup> However, with dien, this particular methodology was only applicable to peptides containing tyrosyl or tryptophanyl residues. Attempts to produce radical cation of peptides including basic amino acids failed. NH-containing ligands such as dien indeed promote proton transfer reactions to the peptide (channel 4). Several studies have extended this approach to the use of terpy (terpy=2,2':6',2''-terpyridine) for generating peptide radical cations.<sup>214-216</sup> In addition to peptides with tyrosyl and tryptophanyl residues, the  $[\text{Cu(II)(terpy)(M)}]^{2+}$  complex was also found capable of generating radical cations of oligopeptides containing basic amino acid residues such as arginine, lysine and histidine. It was also established that the abundance of the peptide radical cation could depend on the sequence of the peptide. By using simple di- and tripeptides GX, GGX, GXG, XG and XGG, the influence of the position of the basic residue, X (X=R, K and H) on the formation of peptide radical cations was probed,<sup>217</sup> and it was found that  $\text{M}^+$  is formed with greatest abundance when the basic residue is at the C-terminus. In order to gain some insights into the binding modes of these peptides to  $[\text{Cu(II)(terpy)}]^{2+}$ , the formation and

fragmentation of copper(II) complexes of tripeptides protected as their carboxy methyl/ethyl esters (M-OCH<sub>3</sub> or M-OC<sub>2</sub>H<sub>5</sub>) were also studied. For lysine and arginine, no ternary complexes were observed, suggesting that arginine- and histidine-containing peptides bind to [Cu(II)(terpy)]<sup>2+</sup> as zwitterions. By using terpy as auxiliary ligand, it was still not possible to generate radical cations containing only aliphatic amino acid residues, which is a very challenging problem due to the relatively high ionization energies (IEs) of aliphatic amino acids. Recently, Chu et al.<sup>218-220</sup> reported the benefits of sterically encumbered auxiliary ligands. They demonstrated that it was indeed possible to generate molecular radical cations of a series of aliphatic tripeptides GGX (W=G, A, P, I, K, L and V), by using either 12-crown-4, 6,6''-Br<sub>2</sub>-terpy or 9-aneN3 ligands (Chart 6). 12-Crown-4 is a cyclic polyether ligand that has no exchangeable protons, and therefore competitive proton transfer can be avoided during the formation of radical cations of M. The enhancement in the formation of peptide radical cations observed with Cu(II)(9-aneN3) is at first glance surprising, because both 9-aneN3, like dien, contain three amino nitrogen atoms and acidic hydrogen (NH) atoms. The facile formation of GGK<sup>•+</sup> ions from [Cu(II)(9-aneN3)GGK]<sup>2+</sup> complex ions presumably occurs because of inefficient proton transfer between the peptide and the sterically constrained 9-aneN3 ligand. For the whole series of GGX tripeptides, use of 12-crown-4 ligand resulted in more abundant peptide radical cations. The reasons for the enhanced peptide radical cation formation when using sterically encumbered ligands, relative to their open-chain analogs, are not obvious. It was suggested that presence of a constrained macrocyclic ligand could weaken metal-peptide chelation through steric repulsion between the ligand and the peptide, a situation which may lead to more favorable peptide radical cation formation.

Finally, Chu and Lam have recently shown that the formation of hydrogen-deficient radical cations of peptides  $(M + nH)^{(n+1)+\bullet}$  by MS/MS spectra of ternary complexes was also possible.<sup>221</sup> This had been presently achieved from triply charged  $[\text{Cu(II)(terpy)(M)}]^{3+}$  complexes.  $(M+H)^{2+\bullet}$  ions have indeed been formed in significant abundance, especially for relatively long oligopeptides that present a basic amino acid residue at either the C- or N-terminus. Dissociation of  $[M+H]^{2+\bullet}$  dications through MS<sup>3</sup> experiments leads to the formation of fragment ions  $a_n^+$ ,  $y_n^+$ ,  $[z_n + H]^+$ , and  $w_n^+$ . This fragmentation is similar to that of the dissociation of odd-electron peptide radical cations  $M^{\bullet+}$ , but is significantly different from those of the corresponding  $[M+2H]^{2+}$  and  $[M+H]^+$  ions. A very striking feature is that the differentiation between internal isomeric leucine and isoleucine residues in polypeptides is possible through the analysis of the secondary fragmentation products of the  $[z_n + H]^+$ , which generates even-electron  $w_n^+$  ions. This is illustrated by the Figure 30.

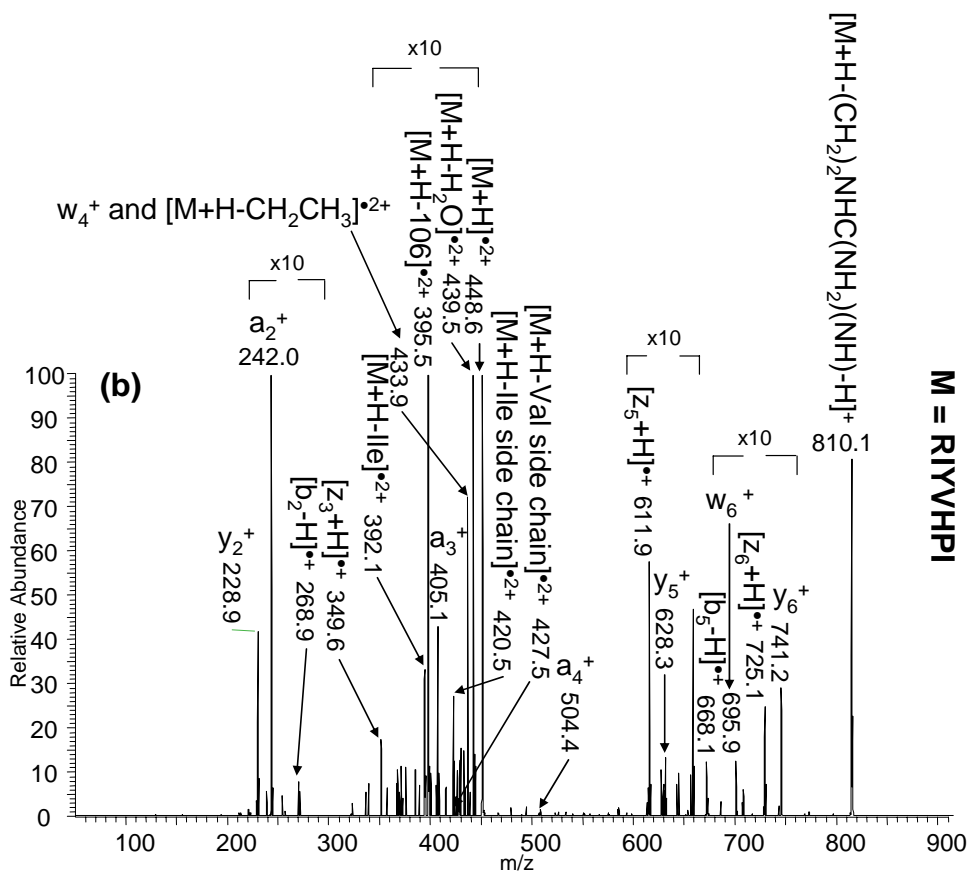
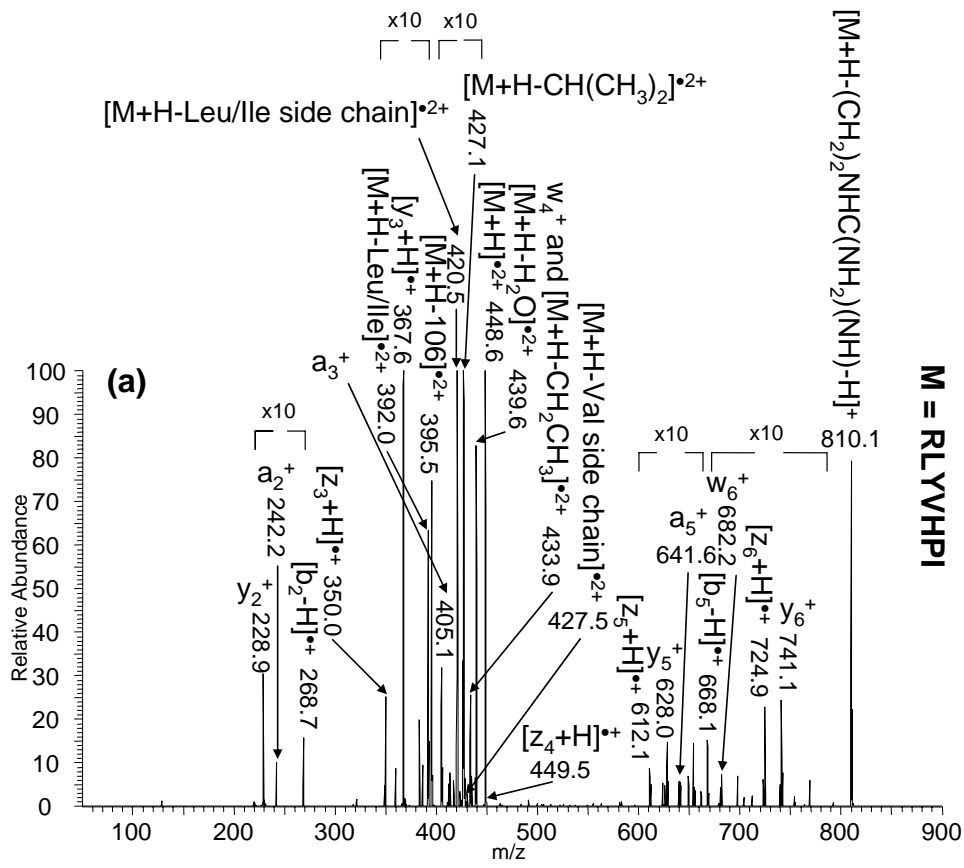


**Figure 30.** MS<sup>3</sup> spectrum of  $[M+H]^{2+}$  ions with a) M= RLYVHPI and b) M= RIYVHPI. (taken from Chu et Lam *Journal of the American Society for Mass Spectrometry* 16, 1795 (2005), ASMS; reprinted with permission)

This distinction is demonstrated by the presence of peaks associated with the loss of diagnostic neutral radicals,  $\cdot\text{CH}(\text{CH}_3)_2$  (43 u) and  $\cdot\text{CH}_2\text{CH}_3$  (29 u), for leucine and isoleucine, respectively, by inspecting the consecutive mass differences between the  $[z_6+H]^{*+}$  and  $w_6^+$  ions. This approach, although not universal, therefore appears particularly promising not only because these hydrogen-deficient radical cations are now accessible to rather cheap instruments (ion traps), but also because these ions provide particularly structural information sensibly different from that obtained from even-electron protonated ions.<sup>222,223</sup>

### 3. Interactions with Proteins

To conclude this section about peptides and proteins, it is worth noting that several studies dealt with the interaction of copper ions with large proteins,<sup>224-230</sup> and notably metallothioneins (MTs).<sup>224,230</sup> MTs are small cysteine-rich proteins that typically comprise some 60 amino acid residues, many of which are serine and threonine. Many mono- and divalent metals have been observed to complex with MTs, including Cu(I), Ag(I), Zn(II), Cd(II), Au(I) and Hg(II).<sup>231-233</sup> Guo et al.<sup>230</sup> studied the Rabbit metallothionein MT2A and combined electrospray ionization to ion-mobility experiments to determine their binding properties towards Cd(II), Zn(II), Ag(I), Hg(II) and Cu(I) ions. They found that the number of metal ions bound by MTs depends on the pH of the solution. This number decreases as the pH is lowered. Observation of  $[\text{Cu}_4\text{MT2A}+4\text{H}]^{4+}$ ,  $[\text{Cu}_4\text{MT2A}+5\text{H}]^{5+}$ , and  $[\text{Cu}_4\text{MT2A} + 6\text{H}]^{6+}$  ions suggest a 4:1 stoichiometry. Ion-mobility measurement showed that the conformation of the ions obtained with Cu(I) are similar to those observed for Ag(I) ions and that in all case metal binding to MTs induces a conformational rigidity to the metal-MT complexes. The same stoichiometry has been observed by Jensen et al. during their study of the

metallothionein isoform 3 (MT3).<sup>224</sup> They also demonstrated that Cu(I) appears to bind preferentially to the  $\beta$  domain of MTs. As a matter of fact, addition of 2 molar equivalents of Cu(I) to the  $\beta$ MT3 domain peptide resulted in a prominent tetracopper species, while mixing Cu(I)-acetonitrile to  $\alpha$ MT3 did not generate a higher molecular weight species onto the electrospray spectrum.

Finally, one may also cite the study of Whittal et al.<sup>225</sup> about the interaction of copper ions with the Prion protein (PrP). The N-terminal side of the Syrian hamster (SHa) PrP, spanning from the 57<sup>th</sup> till the 91<sup>st</sup> residue, is highly conserved as it consists in WCQ(PHGGGWGQ)<sub>4</sub>. The repetition of the eight amino acid sequence PHGGGWGQ, each copy of which is referred to as one octarepeat, was identified as a potential Cu<sup>2+</sup> binding motif, which might induce secondary structure and protect the N-terminus against proteolysis. Whittal et al.<sup>225</sup> used ESI-MS techniques in order to evaluate the binding of Cu<sup>2+</sup> ions to the mature Prion protein (PrP), by studying synthetic peptides corresponding to sections of the sequence of the mature prion protein (PrP). This ESI-MS study demonstrated that Cu<sup>2+</sup> is unique among divalent metal ions in binding to PrP and defines the location of the major Cu<sup>2+</sup> binding site as the octarepeat region in the N-terminal domain. Furthermore, it appeared that two adjacent octarepeats were sufficient to bind one Cu<sup>2+</sup> ion, but also that the histidines were essential ligands for this. The stoichiometries of the complexes measured directly by ESI-MS were found to depend on the pH: a peptide containing four octarepeats chelates two Cu<sup>2+</sup> ions at pH 6, and four at pH 7.4. Dissociation constants ( $k_D$ 's) for each Cu<sup>2+</sup> ion binding to the octarepeat peptides were determined by electrospray. This is possible by assuming that the total signal response for each individual ion is proportional to the concentration of that species in the gas phase, and by extension, in solution. This also assumes that the free peptide and the peptide with metal bound give the same signal response. Measured  $k_D$ 's



lie mostly in the low micromolar range. Circular dichroism measurements also reveal a pH-dependent structural change. At pH 6, only a modest spectral change is induced by binding of  $\text{Cu}^{2+}$  ions, while  $\text{Cu}^{2+}$  binding at pH 7.4 induces a major conformational change.

## **B. Reactivity with saccharides and derivatives**

Carbohydrates are the most abundant biomolecules in nature. They are mainly found as polysaccharides that play a crucial role in both animal and vegetal life. Monosaccharides not only bind together to form polysaccharides, but also with purines and pyrimidines (ribose and 2-deoxy-ribose) to give nucleosides, and subsequently RNA and DNA. Moreover, most of naturally occurring proteins and lipids are glycosylated. Carbohydrates are thus involved in many biological functions, such as cell-cell recognition, cell-cell adhesion, and act also as antigens and as blood group substances. Such a variety makes carbohydrate analysis a challenging task for mass spectrometry. A complete structural description of carbohydrates implies notably exact mass measurements, determination of the sequence, sites and anomeric configuration of the glycosidic linkages, and when possible, stereochemical characterization of the different asymmetric centers of the sugar ring(s). Many studies have been carried out on those topics for more than three decades, using different ionization techniques. For many years, derivatization (methylation, permethylation and peracetylation) in conjunction with electron impact or positive-ion chemical ionization have been the primary method used. Analysis of underivatized oligosaccharides has also been performed by negative ion chemical ionization or FAB. With the advent of soft ionization methods such as FAB, or more recently ESI, the particular reactivity of the metal ions in the gas phase has been used in order to distinguish structural isomers of

mono- or polysaccharides. Among the metal ions considered, several studies published during the last ten years implied Cu(I) or Cu(II) ions, even if interactions with sugars were much less studied than interactions with amino acids or peptides.

In this context, our group compared the analytical potential of three metal ions  $\text{Ag}^+$ ,  $\text{Cu}^+$  and  $\text{Pb}^{2+}$ , by studying their interactions *D*-glucose, *D*-galactose and *D*-fructose, *O*-methyl- $\alpha$ -*D*-glucose and *O*-methyl- $\beta$ -*D*-glucose.<sup>234</sup> Mixing copper chloride and the monosaccharides in the matrix (glycerol) resulted in the formation of intense  $[\text{Cu(I)(monosaccharide)}]^+$  complexes. MIKE spectra of the  $[\text{Cu(I)(monosaccharide)}]^+$  ions are significantly different from those obtained for the silver-glycosides adducts. Similar losses are observed (dehydrogenation, dehydration), but copper cationization induces additional species. Fragmentation of the various complexes produced exclusively  $\text{Cu}^+$ -containing fragment ions. Metastable-ion fragmentation pathways common to all monosaccharides are losses of  $\text{H}_2$ , 16u and  $\text{H}_2\text{O}$ . Interestingly, the main fragmentation of the three hexoses is different for each copper complex, namely dehydration for *D*-glucose, dehydrogenation for *D*-galactose and finally loss of 16 mass units for *D*-fructose. Consequently, interactions with Cu(I) allows these three monosaccharides to be easily distinguished, experiments carried out with lead being also successful. As methylation of the anomeric hydroxyl blocks the  $\alpha\rightleftharpoons\beta$  anomerization reaction, we tried to characterize the absolute configuration of the anomeric carbon by considering the two methyl-glycosides  $\alpha$ -1-*O*-methyl-*D*-glucose and  $\beta$ -1-*O*-methyl-*D*-glucose. The distinction of these two molecules was not as straightforward as with silver cations, but the combined elimination of water and methanol appeared characteristic of the  $\beta$  anomer.

DFT calculations have been carried out to propose reliable structures for the complexes observed with *D*-glucose.<sup>235</sup> Cramer and Truhlar<sup>236</sup> have estimated in nearly 3000 the

number of possible conformers of glucopyranose. This number becomes even larger when the interaction with  $\text{Cu}^+$  is considered. In order to restrict the survey of the possible adducts to a reasonable number, Alcamí et al.<sup>235</sup> have considered only those structures in which the  $\text{Cu}^+$  is attached to at least two different oxygens of glucose, assuming that the sugar moiety retains its cyclic structure.

The calculations performed demonstrated that the most stable cyclic forms obtained for both anomers imply interaction of the metal with the hydroxymethyl group, the anomeric hydroxyl and the endocyclic oxygen (O5). (Figure 31)

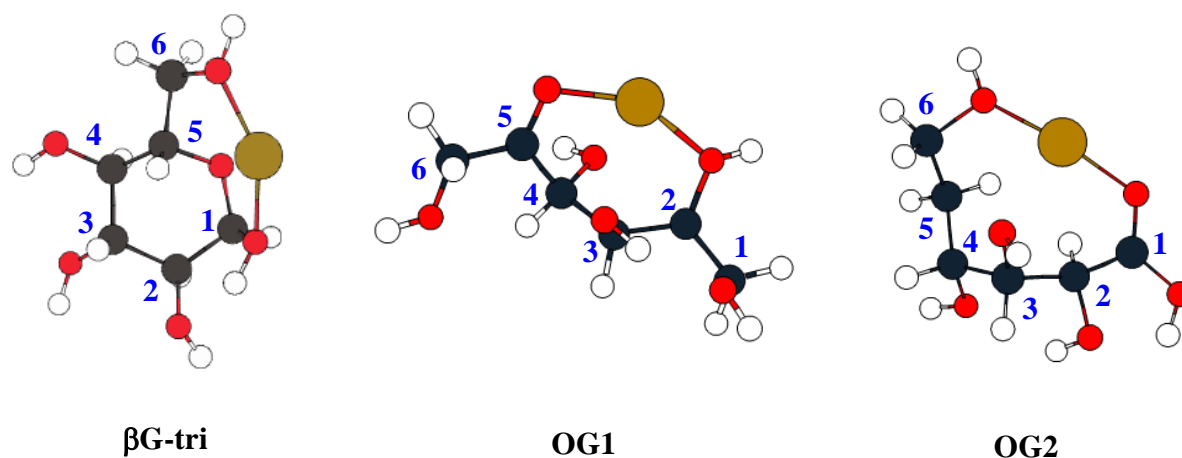


**Figure 31.** Some of the most stable cyclic and opened forms for the  $[\text{Cu}(\text{I})(D\text{-glucose})]^+$  complex

In the case of  $\beta$ -glucose it was possible to obtain a conformation in which the  $\text{Cu}^+$  is interacting with four different hydroxyl groups. Another important finding of this survey is that  $\text{Cu}^+$  association produces such important distortions of the conformation of the sugar that we cannot talk any longer of boat or chair conformations.

The AIM analysis showed that activation of the C1-O5 bond is favored in dicoordinated complexes, while the activation of the C5-O5 bond is favored in tricoordinated ones. The C1-O5 fission should be preceded by a 1,3-H shift from C5 to C1, resulting in **OG1** opened forms (Figure 31). Alternatively, a 1,3-H shift from C1 towards C5 would lead

to the C5-O5 bond fission, and to the production of **OG2** opened-structures. It is worth mentioning that the activation barriers associated with these hydrogen shifts and leading ultimately to the cleavage of the six-membered ring, although high (around 61.9 kcal mol<sup>-1</sup> at the 6-31G\* level), are still lower than the glucose-Cu<sup>+</sup> binding energy which is estimated to be 66.9 kcal mol<sup>-1</sup> at the same level of theory. Consequently, the complex formed by a direct attachment of Cu<sup>+</sup> to glucose has enough internal energy so as to overpass these activation barriers leading to opened-structures **OG1** and **OG2**. The second important quantitative result is that these opened-structures are also much more stable than the cyclic ones. The enhanced stability of the opened-structures is clearly associated with a more efficient bonding between Cu<sup>+</sup> and the oxygen atoms of the sugar moiety. In the opened-structures the O-Cu-O fragment exhibits a practically linear arrangement, while in cyclic structures this possibility is hindered by the rigidity of the ring. The potential energy surface associated with the loss of water (m/z 225, main fragmentation) was also explored and it was concluded that the most stable final product ions have their origin in opened-structures. The most stable m/z 225 product ions are those formed by a spontaneous fragmentation of the most stable opened structure **OG2**, while the less stable structures are those produced by the unimolecular dissociation of cyclic complexes.

As metastable decomposition studies showed that Ag<sup>+</sup>, Cu<sup>+</sup> and Pb<sup>2+</sup> were of potential interest in the structural characterization of isomeric glycosides, we reconsidered these systems by using electrospray ionization a couple of years later.<sup>223</sup> With the same metallic salt, ESI mass spectra showed the presence of abundant protonated and coppered species. The electrospray mass spectra CuCl<sub>2</sub>/monosaccharide mixtures are characterized by complexes in which the formal oxidation state of copper remained Cu(II) such as [Cu(II)(monosaccharide) -H]<sup>+</sup>, metallic complexes of reduced Cu(I)-

adduct ions like  $[\text{Cu(I)(monosaccharide)}]^+$  (at  $m/z$  243/245) and  $[\text{Cu(I)(monosaccharide)}_2]^+$  (at  $m/z$  423/425). Doubly-charged species were never observed. The ratio  $[\text{Cu(II)(monosaccharide) -H}]^+ / [\text{Cu(I)(monosaccharide)}]^+$  was found to depend on nozzle-skimmer voltage variations. At low cone voltage, metallic complexes involving Cu(II) are predominant. On the contrary, high cone voltage leads to an increase of the  $[\text{Cu(I)(monosaccharide)}]^+$  abundance. The formation under electrospray conditions of a mixture of organometallic species containing copper ions in two different oxidation states, already known for amino acids and peptides<sup>12</sup>, is therefore also observed with carbohydrates. Globally, positive-ion ESI spectra of coppered-complexes do not really allow the aldoses and the ketose to be differentiated. The low-energy CID spectra of  $[\text{}^{63}\text{Cu(I)(monosaccharide)}]^+$  adduct ions recorded at a collision energy of 20 eV show an amazing reactivity. The copper cation was able to induce activation of practically all C-C and C-O bonds resulting in many fragmentation pathways. Consequently, unlike in FAB conditions, the use of copper salt does not allow the distinction between *D*-glucose, *D*-galactose and *D*-fructose, neither from the positive-ion ESI spectra nor from the ESI-MS/MS spectra. Globally, lead(II) ions exhibited the greatest potential for characterizing isomeric saccharides under electrospray conditions.<sup>222,237</sup>

The ternary complex approach has also been employed in order to discriminate glucose from its aldose isomers (talose, mannose and galactose).<sup>238</sup> Ternary complexes were generated by using nickel, copper, and zinc. In addition, several auxiliary ligands were considered in order to address the effect of the size, number and coordination number of the ligands in the complex. By using a quadrupole ion trap mass spectrometer, tandem mass spectrometric experiments were performed on the electrospray-generated metal *N*-glycoside complexes. Diaminopropane (dap) and

ethylenediamine (en) were used to generate tricoordinate  $[\text{Cu}(\text{L}/\text{hexose})\text{-H}]^+$  complexes.<sup>238</sup> The product ion spectra of all tricoordinate Cu/*dap* complexes were very simple, possessing a single prominent product ion at  $m/z$  178 (elimination of  $\text{C}_4\text{H}_8\text{O}_4$  by cross-ring cleavage). Such simple spectra did not allow any stereochemical differentiation. On the other hand, the  $[\text{Cu}(\text{en}/\text{monosaccharide})\text{-H}]^+$  MS/MS spectra obtained under identical experimental conditions from all four diastereomeric Cu/*en* complexes are characterized by various cross-ring cleavages (elimination of  $\text{C}_n\text{H}_{2n}\text{O}_n$  moieties,  $n=1\text{-}3$ ) and/or loss of water, and revealed unique product ion spectra for each of these precursor ions. Whereas a full differentiation of the four diastereomeric monosaccharides was achieved with the Cu/*en* complexes, such a distinction appeared not possible with zinc. Finally, unlike the tricoordinate complexes, tetra- and pentacoordinate ions did not lead to successful distinction of the four isomers.

The gas phase reactivity of copper ions has also been applied to the structural analysis of carbohydrate derivatives, and notably flavonoids.<sup>239</sup> Flavonoids are a class of phytochemicals sharing a common chemical structure, based on a  $\text{C}_{15}$  skeleton with a chromane ring bearing a second aromatic ring B in position 2, 3 or 4, (presently 2 in that particular study, Figure 32). Their ubiquitous presence in plants makes them an integral part of the human diet. The high degree of variety in flavonoid structure makes accurate identification a difficult task.

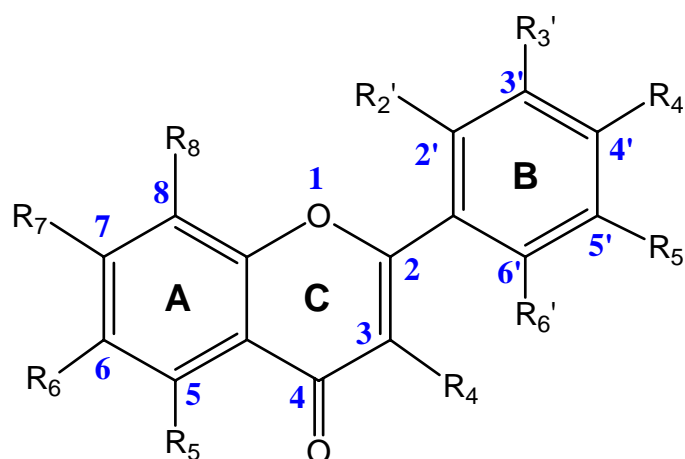


**Figure 32.** Structures of flavonoids

ESI, APCI and MALDI are used to analyse flavonoids and some significant progress has been made towards systematic structural characterization of flavonoids by mass spectrometry. However, mass spectrometric analysis is still not able to achieve de novo identification of flavonoids. Only tentative identifications generally based on collision-induced dissociations of protonated or deprotonated pseudo-molecular ions, can be made, particularly in terms of saccharide location and identity, unless complementary analytical methods, such as UV, FTIR, or NMR spectroscopy, are employed. In order to develop a simple and robust method, Davis and Brodbelt<sup>239</sup> chose to form flavonoid glucoside/metal complexes in order to get a broader array of fragments for structural analysis. Five metals, Ca(II), Mg(II), Co(II), Ni(II) and Cu(II) were evaluated for their ability to form such complexes. The complexes were produced from methanolic solutions containing 1:1 flavonoid glycoside/metal salt. No pH adjustment was performed on the analyte solutions. Under these conditions, the flavonoid glycosides formed 1:1 and 2:1 analyte/metal complexes of the type  $[M(II)(L-H)]^+$  and  $[M(II)(L)(L-H)]^+$ . The 2:1 complexes were found more abundant, and gave simple CID spectra with easily-assigned fragments and a variety of dissociation pathways for structural determination, and were therefore chosen for analytical purpose. Despite the efficient formation of transition metal complexes of the type  $[M(II)(L-H)(L)]^+$  where M=Co, Ni, or Cu, none of these complexes permitted complete identification of all glycosylation sites studied (C6, C8, O3, O7 and O4') Neither cobalt nor nickel complexation provide sufficient differentiation of 3-O- and 4'-Oglucosyl flavonoids. The copper complexes were even less useful for locating the glycosylation sites. It turned out that the Mg(II) complexes offered the best and most complete identification and differentiation of all five categories of flavonoid glucosides studied.

Numerous mass spectrometry studies on the fragmentation of polysaccharides have shown that the main fragmentation pathways consist of glycosidic cleavages (ions of the type B, C, Y or Z; Figure 33) that involve single bond rupture between the sugar rings, and cross-ring cleavages of the rings themselves (A and X ions).

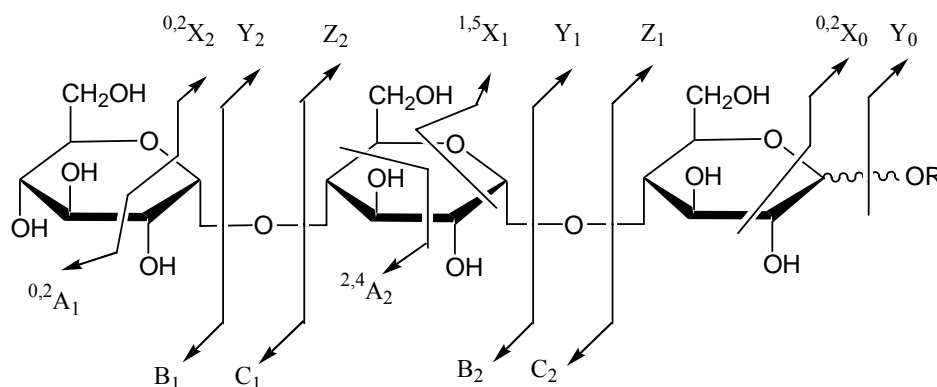


**Figure 33.** Nomenclature of the fragmentation of carbohydrates (from ref. 240)

The former predominate and provide sequence information whereas the latter yield additional information on the linkage position of one residue to the next. In the positive ion mode  $[M+H]^+$ ,  $[M+Li]^+$  and  $[M+Na]^+$  ions are often used but they mainly dissociate by glycosidic bond cleavage. Several groups have also considered other metal ions. Recently, Harvey reported the use of  $Mg^{2+}$ ,  $Ca^{2+}$ ,  $Mn^{2+}$ ,  $Co^{2+}$  and  $Cu^{2+}$  cations in order to analyse Maltoheptaose (linear  $\beta 1 \rightarrow 4$ -linked glucose) and several N-linked glycans.<sup>241</sup> Again, electrospray ionization was used and the dominant species obtained with all salts were  $[M+metal]^{2+}$  complexes. Fragmentation of the doubly charged ions became prominent as the cone voltage was increased, except those ions formed with copper. In-source fragmentation involved dissociation of the  $[M+metal]^{2+}$  ions into singly charged  $[M+metal]^+$  ions with loss of a monosaccharide residue (mannose 162 mass units). In the case of copper, the  $[M+Cu]^+$  ion was formed without apparent loss of carbohydrate indicating that its oxidation state must have changed to Cu(I).



MS/MS of the  $[M+\text{metal}]^{2+}$  ions produced both singly and doubly charged ions with the relative abundance of doubly charged ions decreasing in the order  $\text{Ca} > \text{Mg} > \text{Mn} > \text{Co} > \text{Cu}$ . Whatever the polysaccharides considered, fragmentation of  $[M+\text{Cu}]^{2+}$  or  $[M+\text{Cu}]^+$  complexes mostly corresponded to singly charged ions arising from glycosidic bond cleavages, therefore yielding useful sequence information. In the particular case of maltoheptaose, the MS/MS spectrum of the  $[M+\text{Cu}]^+$  ion was strikingly similar to that of  $[M+\text{Na}]^+$  complexes. Globally, MS/MS spectra of copper-cationized polysaccharides were devoid of cross-ring fragments, hence failing in providing position of the glycosidic linkages.

The interactions between copper and polysaccharides arising from the degradation of cellulose, chitin and chitosan were also investigated.<sup>242</sup> Chitosan is a linear homopolymer of  $\beta$ -1,4-linked *D*-glucosamine residues possessing high selectivities for transition metal ions. Chitin refers to the acetylated form of chitosan, consisting of  $\beta$ -1,4-linked *N*-acetyl-*D*-glucosamine. Owing to their abundance in the marine environment, chitosan and chitin can control metal ion equilibria in their surroundings. Cellulose was chosen as a benchmark because it does not exhibit any amino or *N*-acetylamino groups and therefore was not supposed to bind strongly copper ions. These systems were investigated by electrospray ionization and the goal of these studies was to understand the degree to which electrospray mass spectra can reflect the solution chemistry of copper–oligosaccharide complexes.<sup>242</sup> To this end, mass spectrometry data were compared with potentiometric studies. Sugar-copper complexes of general formula  $[M_2+\text{Cu}]^{2+}$ ,  $[M_3+\text{Cu}]^{2+}$  and  $[M-\text{H}+\text{Cu}]^+$  have been observed in the gas phase with the chito- and cello- tetrasaccharides. It is worth noting that  $[M+\text{Cu}]^{2+}$  were also detected, suggesting that tetrasaccharides are polarisable enough to stabilize the double charge of copper under electrospray conditions. On the other hand, the

potentiometric data revealed no copper binding for mono- and tetrasaccharides of cellulose and chitin. The complexes observed on mass spectra were therefore attributed to charge attachment phenomenon during desolvation from the highly charged electrospray droplets. In contrast, the chitosan tetrasaccharide due to its available amino groups was expected to bind copper effectively and to give intense electrospray spectra. However, no complexes were detected by mass spectrometry. Authors suggested that neutral complexes could be formed in solution. In order to check this assumption, they measured the  $[M+2H]^{2+}$  abundance as a function of the copper concentration. Its intensity declined as the  $[Cu^{2+}]$  concentration in solution was increased, suggesting removal of the free tetrasaccharide by complexation to  $Cu^{2+}$  ions. This experiment was repeated with a sodium salt but no decline in the  $[M+2H]^{2+}$  response was observed, confirming the formation of neutral and/or negatively charged Cu(II)/chitosan complexes, hence not detectable in the positive-ion mode. This result was in agreement with the potentiometric studies indicating that at pH 7 Cu(II) ions and chitosan form strong complexes which are essentially neutral or negatively charged, explaining the absence of metal species in the positive-ion ESI spectrum.

### **C. Reactivity with nucleic acid building blocks**

Metal cations can both stabilize and destabilize DNA.<sup>243</sup> The interaction of divalent cations with nucleic acids plays an important role in promoting and maintaining their functionalities.<sup>243-245</sup> As illustrated along this chapter, the open-shell  $Cu^{2+}$  cation has a rich redox chemistry and some studies have emphasized that the exposure of DNA to  $Cu^{2+}$  can have different consequences such as single and double strand cleavage, base modification, and formation of basic sites.<sup>246,247</sup>

The interactions and the coordination chemistry of metal cations with nucleic acid building blocks have been studied quite extensively in the condensed phase. By contrast, data about the intrinsic gas-phase behavior of such interactions are rather scarce. A good knowledge on the mechanisms at the molecular level is still lacking in most cases. One reasonable way of approaching this chemistry is to adopt a “bottom-up” strategy based on the gradual increase of the size and complexity of the nucleic acid building blocks. In this context, we began our gas-phase investigations with uracil, one of the five nucleobases. As mentioned in the previous parts of this chapter, we first studied in the last few years the interactions (binding, energetics) of uracil and its thio-derivatives towards proton<sup>169</sup>, copper(I)<sup>84</sup> and copper(II).<sup>125</sup> Then, we went a step further by exploring the experimental unimolecular reactivity of the complexes produced in the gas phase by electrospray ionization.<sup>151</sup>

Under electrospray conditions, interaction between copper(II) ions and uracil gave rise to different types of ions, the structure of which, as expected, clearly depended on the cone voltage applied. At low cone voltage, a pair of peaks associated to copper/uracil interaction, namely  $[\text{Cu}(\text{uracil})_n - \text{H}]^+$  complexes ( $n=1,2$ ) were observed. Increasing the cone voltage resulted in the additional apparition of  $[\text{Cu}(\text{uracil})]^+$  ions through a reduction process. No  $[\text{Cu}(\text{uracil})]^{2+}$  ions were observed, but we do neither detect higher homologues, suggesting that the source conditions were likely not mild enough to allow the production of multiply charged complexes. The  $[\text{}^{63}\text{Cu}(\text{uracil}-\text{H})]^+$  species was selected and allowed to dissociate upon collision with nitrogen. Two main fragment ions were detected at  $m/z$  130.9 and 131.9, corresponding to the loss of  $[\text{H},\text{N},\text{C},\text{O}]$  and  $[\text{N},\text{C},\text{O}]$ , respectively. A weak fragment ion at  $m/z$  145.9 attributed to the elimination of carbon monoxide was also observed. By using appropriate labeled uracils, it could be unambiguously conclude that both the loss of

NCO and HNCO involve specifically C2 and N3, whereas the loss of carbon monoxide involves only C4.

In order to rationalize these experimental findings, DFT calculation were performed on the  $[\text{Cu}(\text{uracil-H})]^+$  system. The most stable complex corresponds to a form in which  $\text{Cu}^+$  bridges between N1 and the oxygen atom of the C(2)O carbonyl group. (Figure 34)

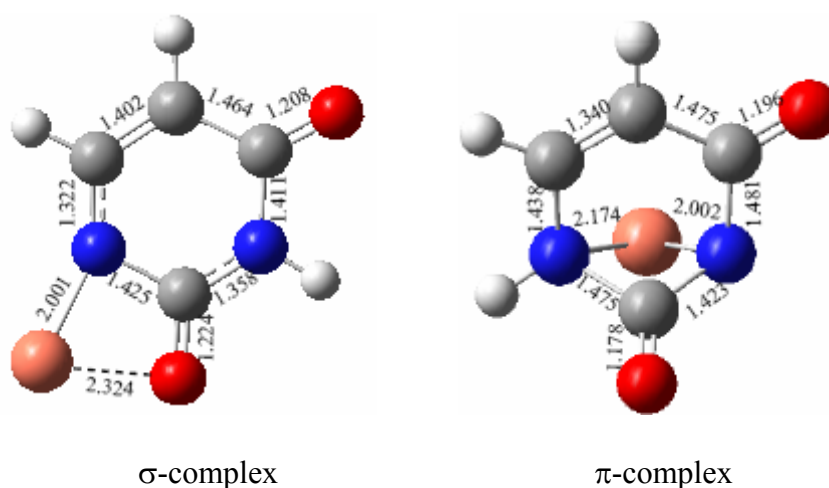


**Figure 34.** The most stable  $\sigma$ - and  $\pi$ -forms optimized for the  $[\text{Cu}(\text{uracil-H})]^+$  complex.

Conventional  $\pi$ -complexes in which the metal cation is above the plane of ring, also correspond to local minima of the potential energy surface, although they were found to be significantly less stable than  $\sigma$ -complexes.

Considering the C-N bond distances as well as the charge densities at the bond critical point deduced from an AIM analysis, the N3-C4 (scheme 5) fission seemed to be the most favorable process. A survey of the PES (See Figure 35) indicates that the loss of HNCO has its origin in the global minimum ( $\sigma$ -complex). Interestingly, the most favorable mechanism for the elimination of NCO $\cdot$  involves  $\pi$ -type complexes. This association involves specific bond activations within the ring, cleavage of which is the first step of the NCO $\cdot$  loss process. Consequently,  $\pi$ -complexes were found to play an important role in the gas-phase reactivity of  $[\text{Cu}(\text{uracil-H})]^+$  complexes. The fact that

the losses HNCO and NCO<sup>•</sup> follow complete different pathways allowed to explain that in both cases the same atoms, namely, N3 and C2 are exclusively involved.

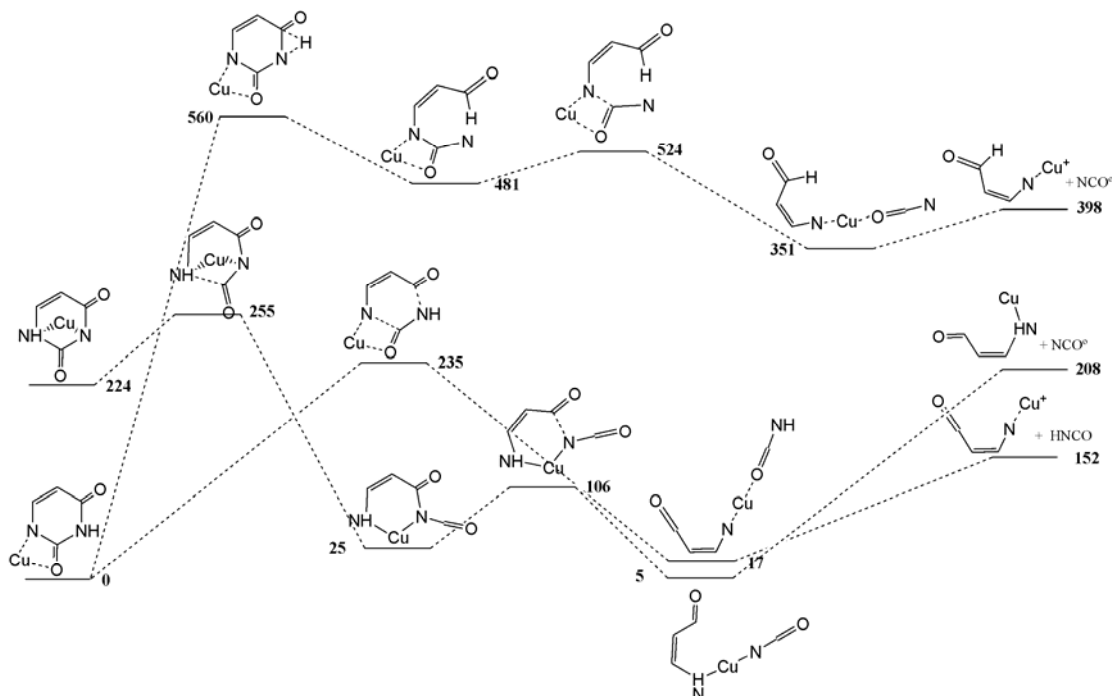


**Figure 35.** Energy profile corresponding to the loss of HNCO and NCO<sup>•</sup> from [(uracil-H)Cu]<sup>+</sup> complexes.

Recently, Rimola *et al.*<sup>184</sup> also showed the important role of  $\pi$ -complexes in the interaction of Cu<sup>+</sup> with phenylalanine, which are the precursors for the C-C insertion which triggers the fragmentation of phenylalanine-Cu<sup>+</sup> complexes.

During the last decade, electrospray ionization has also been employed to examine the formation and reactivity of [Cu(L)(N)]<sup>2+</sup> ternary complexes involving nucleic acid building blocks (N). In their study, Wee *et al.* considered both Pt(II) and Cu(II) cations, that they mixed with two possible auxiliary ligands (dien and terpy) and nucleobases, nucleosides or nucleotides.<sup>248</sup> Ternary complexes could be obtained with all the nucleic acid buildings blocks and the data obtained showed that all three components played a

role in the formation of the ternary complex. More of these complexes could be formed for Cu(II) than for Pt(II).

Like for peptides, the MS/MS spectra of the ternary complexes are characterized by different dissociation processes: a redox reaction which results in the formation of the radical cation of the nucleic acid constituent,  $N^{+\bullet}$ ; the loss of the nucleic acid constituent in its protonated form; and the fragmentation of the nucleic acid constituent.  $N^{+\bullet}$  radical cation were only observed with copper, confirming that the metal must have suitable redox properties to promote the formation of radical cations. Again, using terpy in place of dien allowed limiting the efficiency of the proton transfer process. In fact, N has the biggest influence on the fragmentations observed. Nucleobase radical cations have been solely obtained with copper and terpy ligand. The relative yield of the radical cations of each of the nucleobases from the copper ternary complexes exactly followed their relative vertical ionization potentials (IPs)  $G < A < C < T$ . Consequently, nucleobases with the lowest IPs are the most easily ionized and form the greatest yield of their radical cation upon dissociation of the metal complex. As the nucleobase was changed for the nucleosides, the redox reaction no longer occurred. Finally, changing the nucleoside to the nucleotide yields a new type of product ion in which the metal remained bound to the phosphate and the nucleobase was lost in its protonated form. In general, all of the Cu(II) complexes of the nucleotides fragmented via loss of the protonated nucleobase, suggesting the copper was bound to the phosphate. This is consistent with the known binding of copper to the phosphate moiety in nucleotides in the condensed phase.<sup>249</sup>

In a recent study of Cheng and Bohmem,<sup>250</sup> an electrosprayed water/methanol solution of guanosine and copper nitrate resulted in the formation of gas-phase copper complex of  $[CuL_n]^{2+}$ ,  $[CuL(MeOH)_n]^{2+}$ , and  $[CuG_n(NO_3)]^{+}$ , as well as the ions  $[L]^{+\bullet}$ ,  $[L+H]^+$ ,  $[G]^{+\bullet}$ , and  $[G+H]^+$  (L = guanosine, G = guanine). The observation under mild

electrospray conditions of an abundant  $[L]^{+\bullet}$  radical cation was quite unexpected and constitutes one of the very first examples of formation of radical cations of guanosine from binary mixtures. MS/MS of the  $[\text{Cu}(\text{L})_3]^{2+}$  ions suggested that the formation of  $[L]^{+\bullet}$  can be achieved through the transfer of an electron from L to  $\text{Cu}^{2+}$  within the complex before Coulomb repulsion dissociates the complex into a singly charged  $[\text{Cu}(\text{L}_2)]^+$  complex and  $[L]^{+\bullet}$ . The formation of the  $[\text{G}]^{+\bullet}$  ions observed on the MS/MS spectrum proceeds through the dissociation of the N-glycoside as confirmed by the CID spectrum of  $[L]^{+\bullet}$ . Adding or removing one L unit, resulted in very different CID spectra. The electron transfer channel disappears for  $[\text{Cu}(\text{L})_2]^{2+}$ , while a  $[\text{L}_2]^{+\bullet}$  is generated for the  $[\text{Cu}(\text{L})_4]^{2+}$  species.

Finally, bigger oligonucleotides have also been considered and Hettich published several years ago a MALDI/FTICR (Fourier Transform Ion Cyclotron Resonance) study of the interactions of transition metal ions with a series of single-stranded dinucleotides.<sup>251</sup> While metal ions such as  $\text{Na}^+$ ,  $\text{K}^+$ ,  $\text{Mg}^{2+}$ , and  $\text{Ca}^{2+}$  exhibit a strong affinity for phosphate groups, the transition metals are more likely to form covalent bonds with the nucleobases themselves. In general, the most common binding sites for heavy metal ions appear to be the N7 atoms in adenine and guanine.

Various dinucleotides were considered during this study, namely, *dTG*, *dCA*, *dCT*, *dGG* and *dAG*. Most of the results concerned the latter dinucleotide because *dAG* provides a variety of acidic protons and possible binding sites for metal ions. In the particular case of copper ions, up to three copper ions could be attached to the *dAG* dinucleotide, as attested by the presence of  $[\text{M}+\text{Cu}-2\text{H}]^-$  and  $[\text{M}+2\text{Cu}-3\text{H}]^-$  and  $[\text{M}+3\text{Cu}-4\text{H}]^-$  ions on the MALDI mass spectrum. High-resolution measurements revealed that copper is present only at the Cu(I) oxidation state. The copper ion thus appears to act similarly to the alkali metal ions, and simply displaces acidic protons of the dinucleotide.

Collisional dissociation of the  $[dAG+Cu-2H]^-$  ion revealed loss of adenine and deoxyadenosine as the primary fragment products. Collisional dissociation of the ion  $[dAG+2Cu-3H]^-$  also revealed loss of deoxyadenosine, verifying the presence of both copper ions in the remaining fragment ion. From these results, it could be deduced that at least two copper ions were associated strongly with the deoxyguanosine, replacing the 3' hydroxyl proton and/or the nucleobase protons. In order to examine this metal ion binding site with more detail, the interaction of copper with dinucleotides of varying sequences has been investigated. Up to 2, 2, 3, 3 and 4 protons could be replaced by copper for *dCA*, *dCT*, *dTG*, *dAG* and *dGG*, respectively. Because copper is present in all of these complexes as  $Cu^+$ , it does not require multisite attachment like the other multivalent metal ions examined in this article, and thus behaves like an alkali metal and simply replaces available acidic hydrogens in the dinucleotides. Consequently copper allowed the estimate of the maximum number of dinucleotide protons that can be replaced by a singly charged metal ion. As the results obtained for the series of dinucleotides suggest that the copper coordination depended primarily on the identity of the nucleobases, the author concluded that copper ions primarily replace acidic hydrogens on the nucleobases of the dinucleotides and that the involvement of the deoxyribose hydroxyl groups in metal ion binding seemed to be minimal. Based on these results, a structure (Figure 36) could be proposed for the  $[dAG+3Cu-4H]^+$  complex.



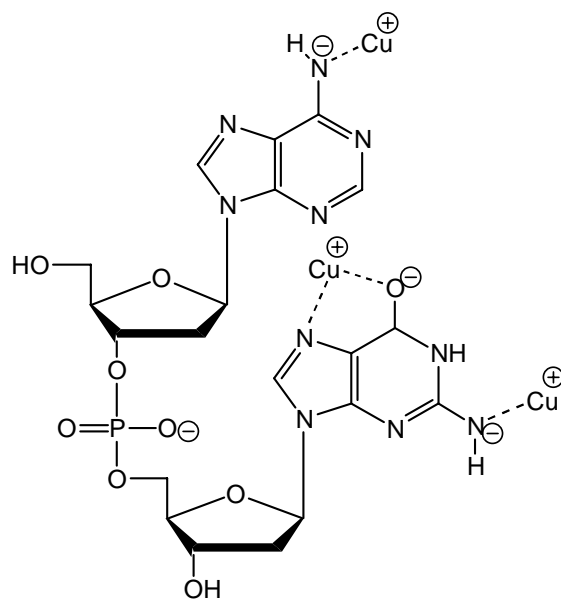


**Figure 36.** Proposed structure for the  $[dAG+3Cu-4H]^+$  complex observed by MALDI

## Appendix

Code names of the various aminoacids

Name	Code name	
	3 letters	1 letter
Alanine	Ala	A
Arginine	Arg	R
Asparagine	Asn	N
Aspartic cid	Asp	D
Cysteine	Cys	C
Glutamic acid	Glu	E
Glutamine	Gln	Q
Glycine	Gly	G
Histidine	His	H
Isoleucine	Ile	I
Leucine	Leu	L
Lysine	Lys	K
Methionine	Met	M
Phenylalanine	Phe	F
Proline	Pro	P
Serine	Ser	S
Threonine	Thr	T
Tryptophan	Trp	W
Tyrosine	Tyr	Y
Valine	Val	V

## Reference

1. M. Güell and P. E. M. Siegbahn, Theoretical study of the catalytic mechanism of catechol oxidase, *J. Biol. Inorg. Chem.*, **12**, 1251–1264 (2007).
2. S. T. Prigge, A. S. Kolhekar, B. A. Eipper, R. E. Mains and L. M. Amzel, Amidation of bioactive peptides: The structure of peptidylglycine alpha-hydroxylating monooxygenase, *Science*, **278**, 1300-1305 (1997).
3. A. Granata, E. Monzani, L. Bubacco and L. Casella, Mechanistic insight into the activity of tyrosinase from variable-temperature studies in an aqueous/organic solvent, *Chem. Eur. J.*, **12**, 2504-2514 (2006).
4. D. F. Raffa, G. A. Rickard and A. Rauk, Ab initio modelling of the structure and redox behaviour of copper(I) bound to a His–His model peptide: relevance to the  $\beta$ -amyloid peptide of Alzheimer's disease, *J. Biol. Inorg. Chem.*, **12**, 147–164 (2007).
5. R. Prabhakar and P. E. M. Siegbahn, Theoretical Study of the Mechanism for the Oxidative Half-Reaction of Copper Amine Oxidase (CAO), *J. Phys. Chem. B*, **107**, 3944-3953 (2003).
6. M. A. Kurinovich and J. K. Lee, The acidity of uracil and uracil analogs in the gas phase: Four surprisingly acidic sites and biological implications, *J. Am. Soc. Mass Spectrom.*, **13**, 985-995 (2002).
7. J. K. Lee, Insights into nucleic acid reactivity through gas-phase experimental and computational studies, *Inter. J. Mass Spectrom.*, **240**, 261-272 (2005).
8. A. C. Drohat and J. T. Stivers, NMR evidence for an unusually low N1 pK<sub>a</sub> for uracil bound to uracil DNA glycosylase: Implications for catalysis, *J. Am. Chem. Soc.*, **122**, 1840-1841 (2000).
9. S. Pan, X. J. Sun and J. K. Lee, DNA stability in the gas versus solution phases: A systematic study of thirty-one duplexes with varying length, sequence, and charge level, *J. Am. Soc. Mass Spectrom.*, **17**, 1383-1395 (2006).
10. U. Ryde, M. H. M. Olsson, B. O. Roos, J. O. D. Kerpel and K. Pierloot, On the role of strain in blue copper proteins, *J. Biol. Inorg. Chem.*, **5**, 565-574 (2000).
11. S. Pan, X. J. Sun and J. K. Lee, Stability of complementary and mismatched DNA duplexes: Comparison and contrast in gas versus solution phases, *Inter. J. Mass Spectrom.*, **253**, 238-248 (2006).

12. F. Turecek, Copper-biomolecule complexes in the gas phase. The ternary way, *Mass Spectrom. Rev.*, **26**, 563-582 (2007).
13. T. Kurikawa, H. Takeda, M. Hirano, K. Judai, T. Arita, S. Nagao, A. Nakajima and K. Kaya, Electronic Properties of Organometallic Metal-Benzene Complexes [ $M_n(\text{benzene})_m$  ( $M = \text{Sc-Cu}$ )], *Organometallics*, **18**, 1430-1438 (1999).
14. J. Miyawaki and K. Sugawara, ZEKE spectroscopy of the copper-pyridine complex, *Chem. Phys. Lett.*, **386**, 196-199 (2004).
15. M. Alcamí, O. Mó and M. Yáñez, Computational Chemistry. A useful (some times mandatory) tool in mass spectrometry studies, *Mass Spectrom. Rev.*, **20**, 195-245 (2001).
16. J. M. Mercero, J. M. Matxain, X. Lopez, D. M. York, A. Largo, L. A. Eriksson and J. M. Ugalde, Theoretical methods that help understanding the structure and reactivity of gas phase ions, *Int. J. Mass Spectrom.*, **240**, 37-99 (2005).
17. M. Pavelka and J. V. Burda, Theoretical description of copper Cu(I)/Cu(II) complexes in mixed ammine-aqua environment. DFT and ab initio quantum chemical study, *Chem. Phys.*, **312**, 193-204 (2005).
18. J. V. Burda, M. Pavelka and M. Simanek, Theoretical model of copper Cu(I)/Cu(II) hydration. DFT and ab initio quantum chemical study, *J. Mol. Struct. (Theochem)*, **683**, 183-193 (2004).
19. C. F. Schwenk and B. M. Rode, Influence of Electron Correlation Effects on the Solvation of  $\text{Cu}^{2+}$ , *J. Am. Chem. Soc.*, **126**, 12786-12787 (2004).
20. J. V. Burda, J. Sponer and P. Hobza, Ab Initio Study of the Interaction of Guanine and Adenine with Various Mono- and Bivalent Metal Cations ( $\text{Li}^+$ ,  $\text{Na}^+$ ,  $\text{K}^+$ ,  $\text{Rb}^+$ ,  $\text{Cs}^+$ ;  $\text{Cu}^+$ ,  $\text{Ag}^+$ ,  $\text{Au}^+$ ;  $\text{Mg}^{2+}$ ,  $\text{Ca}^{2+}$ ,  $\text{Sr}^{2+}$ ,  $\text{Ba}^{2+}$ ;  $\text{Zn}^{2+}$ ,  $\text{Cd}^{2+}$ , and  $\text{Hg}^{2+}$ ), *J. Phys. Chem.*, **100**, 7250-7255 (1996).
21. J. V. Burda, J. Sponer, J. Leszczynski and P. Hobza, Interaction of DNA Base Pairs with Various Metal Cations ( $\text{Mg}^{2+}$ ,  $\text{Ca}^{2+}$ ,  $\text{Sr}^{2+}$ ,  $\text{Ba}^{2+}$ ,  $\text{Cu}^+$ ,  $\text{Ag}^+$ ,  $\text{Au}^+$ ,  $\text{Zn}^{2+}$ ,  $\text{Cd}^{2+}$ , and  $\text{Hg}^{2+}$ ): Nonempirical ab Initio Calculations on Structures, Energies, and Nonadditivity of the Interaction, *J. Phys. Chem. B*, **101**, 9670-9677 (1997).
22. A. D. Becke, A new mixing of Hartree-Fock and local-density-functional theories, *J. Chem. Phys.*, **98**, 1372-1377 (1993).
23. C. Lee, W. Yang and R. G. Parr, Development of the Colle-Salvetti correlation-energy formula into a functional of the electron density, *Phys. Rev. B*, **37**, 785-789 (1988).

24. A. M. Mebel, K. Morokuma and M. C. Lin, Modification of the Gaussian-2 theoretical-model - the use of coupled-cluster energies, density-functional geometries, and frequencies, *J. Chem. Phys.*, **103**, 7414-7421 (1995).
25. A. Ricca and C. W. Bauschlicher, A Comparison of Density-Functional Theory with Ab-Initio Approaches for Systems Involving First Transition Row Metals, *Theor. Chim. Acta*, **92**, 123-131 (1995).
26. A. L. Llamas-Saiz, C. Foces-Foces, O. Mó, M. Yáñez, E. Elguero and J. Elguero, The geometry of pyrazole: a test for ab initio calculations, *J. Comput. Chem.*, **16**, 263-272 (1995).
27. J. A. Montgomery Jr., M. J. Frisch, J. Ochterski and G. A. Petersson, A complete basis set model chemistry. VI. Use of density functional geometries and frequencies, *J. Chem. Phys.*, **110**, 2822-2827 (1999).
28. L. A. Curtiss, P. C. Redfern, K. Raghavachari and J. A. Pople, Gaussian-3X (G3X) theory: Use of improved geometries, zero-point energies, and Hartree-Fock basis sets, *J. Chem. Phys.*, **114**, 108-117 (2001).
29. A. Luna, B. Amekraz and J. Tortajada, A theoretical study on the complexation of sp, sp<sup>2</sup> and sp<sup>3</sup> nitrogen-containing species by Cu<sup>+</sup>, *Chem. Phys. Lett.*, **266**, 31-37 (1997).
30. S. Hoyau and G. Ohanessian, Absolute Affinities of  $\alpha$ -Amino Acids for Cu<sup>+</sup> in the Gas Phase. A Theoretical Study, *J. Am. Chem. Soc.*, **119**, 2016-2024 (1997).
31. A. Rimola, E. Constantino, L. Rodríguez-Santiago and M. Sodupe, Binding properties of Cu<sup>+2+</sup>-(glycyl)<sub>n</sub> glycine complexes (n = 1-3), *J. Phys. Chem. A*, **112**, 3444-3453 (2008).
32. A. Luna, M. Alcamí, O. Mó and M. Yáñez, Cu<sup>+</sup> binding energies. Dramatic failure of the G2 method vs. good performance of the B3LYP approach, *Chem. Phys. Lett.*, **320**, 129-138 (2000).
33. G. Corongiu and P. Nava, Gas-Phase Geometries and Energies of bis(2,2'-Bipyridine) Interacting Either with Cu(I) or Ag(I): Computational Study, *Inter. J. Quant. Chem.*, **93**, 395-404 (2003).
34. T. Marino, N. Russo and M. Toscano, Gas-phase metal ion (Li<sup>+</sup>, Na<sup>+</sup>, Cu<sup>+</sup>) affinities of glycine and alanine, *J. Inorg. Bio.*, **79**, 179-185 (2000).
35. T. Marino, N. Russo and M. Toscano, Interaction of Cu<sup>+</sup> and Cu<sup>2+</sup> ions with  $\alpha$ -alanine. A density functional study, *J. Mass. Spect.*, **37**, 786-791 (2002).

36. S. J. Klippenstein and C. N. Yang, Density functional theory predictions for the binding of transition metal cations to pi systems: from acetylene to coronene and tribenzocyclyne, *Inter. J. Mass Spectrom.*, **201**, 253-267 (2000).
37. I. Georgieva, N. Trendafilova, L. Rodríguez-Santiago and M. Sodupe, Coordination properties of the oxime analogue of glycine to Cu(II), *J. Phys. Chem. A*, **109**, 5668-5676 (2005).
38. J. Poater, M. Solà, A. Rimola, L. Rodríguez-Santiago and M. Sodupe, Ground and Low-Lying States of  $\text{Cu}^{2+}$ - $\text{H}_2\text{O}$ . A Difficult Case for Density Functional Methods, *J. Phys. Chem. A*, **1008**, 6072-6078 (2004).
39. T. K. Dargel, R. H. Hertwig and W. Koch, How do coinage metal ions bind to benzene?, *Mol. Phys.*, **96**, 583-591 (1999).
40. I. Corral, O. Mo and M. Yanez,  $\text{Li}^+$  vs  $\text{Cu}^+$  association to toluene, phenylsilane and phenylgermane. Conventional vs non-conventional  $\pi$ -complexes, *Eur. J. Mass Spectrom.*, **10**, 921-929 (2004).
41. I. Corral, O. Mó and M. Yáñez,  $\text{Cu}^+$  association to some Ph-X (X=OH,  $\text{NH}_2$ , CHO, COOH,  $\text{CF}_3$ ) phenyl derivatives. A comparison with  $\text{Li}^+$  complexes, *Inter. J. Mass Spectrom.*, **255-256**, 20-27 (2006).
42. P. Milko, J. Roithová, D. S. Schröder, J. Lemaire, H. Schwarz and M. C. Holthausen, The Phenoxy/Phenol/Copper Cation: A Minimalistic Model of Bonding Relations in Active Centers of Mononuclear Copper Enzymes, *Chem. Eur. J*, **14**, 10 (2008).
43. T. K. Ghanty and E. R. Davidson, Theoretical Investigation of Electronic Structure and ESR Hyperfine Parameters for the  $\text{CuH}^+$  Molecule., *Int. J. Quantum Chem.*, **77**, 291-300 (2000).
44. M. J. Frisch, G. W. Trucks, H. B. Schlegel, G. E. Scuseria, M. A. Robb, J. R. Cheeseman, V. G. Zakrzewski, J. J. A. Montgomery, T. Vreven, K. N. Kudin, J. C. Burant, J. M. Millam, S. S. Iyengar, J. Tomasi, V. Barone, B. Mennucci, M. Cossi, G. Scalmani, N. Rega, G. A. Petersson, H. Nakatsuji, M. Hada, M. Ehara, K. Toyota, R. Fukuda, J. Hasegawa, M. Ishida, T. Nakajima, Y. Honda, O. Kitao, C. Adamo, J. Jaramillo, R. Gomperts, R. E. Stratmann, O. Yazyev, J. Austin, R. Cammi, C. Pomelli, J. Ochterski, P. Y. Ayala, K. Morokuma, G. A. Voth, P. Salvador, J. J. Dannenberg, V. G. Zakrzewski, S. Dapprich, A. D. Daniels, M. C. Strain, O. Farkas, D. K. Malick, A. D. Rabuck, K. Raghavachari, J. B. Foresman, J. V. Ortiz, Q. Cui, A. G. Baboul, S. Clifford, J. Cioslowski, B. B. Stefanov, G. Liu, A. Liashenko, P. Piskorz, I. Komaromi,

- R. L. Martin, D. J. Fox, T. Keith, M. A. Al-Laham, C. Y. Peng, A. Nanayakkara, M. Challacombe, P. M. W. Gill, B. Johnson, W. Chen, M. W. Wong, C. Gonzalez and J. A. Pople, "Gaussian03, Revision E.01," (Gaussian, Inc., Wallingford CT, 2003).
45. B. J. Lynch and D. G. Truhlar, Obtaining the right orbitals is the first step to calculating accurate binding energies for  $\text{Cu}^+$  ion, *Chem. Phys. Lett.*, **361**, 251-258 (2002).
46. D. Cremer and Z. He, Sixth-Order Moller-Plesset Perturbation Theory-On the Convergence of the MPn Series, *J. Phys. Chem.*, **100**, 6173-6188 (1996).
47. A. Ricca and C. W. Bauschlicher, Jr., Successive OH Binding Energies of  $\text{M}(\text{OH})_n^+$  for  $n = 1-3$  and  $\text{M} = \text{Sc}, \text{Ti}, \text{V}, \text{Co}, \text{Ni},$  and  $\text{Cu}$ , *J. Phys. Chem. A*, **101**, 8949-8955 (1997).
48. A. Luna, M. Alcamí, O. Mó, M. Yáñez and J. Tortajada, A theoretical study of the interaction between  $\text{Ni}^+$  and small oxygen and nitrogen containing bases, *Int. J. Mass Spectrom.*, **217**, 119-129 (2002).
49. C. Trujillo, A. M. Lamsabhi, O. Mó and M. Yáñez, The importance of the oxidative character of doubly charged metal cations in binding neutral bases. [Urea- $\text{M}^{2+}$ ] and [thiourea- $\text{M}^{2+}$ ] ( $\text{M} = \text{Mg}, \text{Ca}, \text{Cu}$ ) complexes, *Phys. Chem. Chem. Phys.*, **10**, 3229-3235 (2008).
50. M. Alcamí, O. Mó, M. Yáñez and I. L. Cooper, The performance of density-functional theory in challenging cases: Halogen oxides, *J. Chem. Phys.*, **112**, 6131-6140 (2000).
51. P. Su, F. Lin and C. S. Yeh, Photodissociation Studies of  $\text{M}(\text{Furan})^+$  ( $\text{M} = \text{Cu}, \text{Ag},$  and  $\text{Au}$ ) and  $\text{Au}(\text{C}_3\text{H}_4)^+$  Complexes, *J. Phys. Chem. A*, **105**, 9643-9648 (2001).
52. Y. S. Yang, W. Y. Hsu, H. F. Lee, Y. C. Huang, C. S. Yeh and C. H. Hu, Experimental and Theoretical Studies of Metal Cation-Pyridine Complexes Containing  $\text{Cu}$  and  $\text{Ag}$ , *J. Phys. Chem. A*, **103**, 11287 - 11292 (1999).
53. *NIST Chemistry Webbook. Standard Reference Database Number 69. Eds. P.J. Linstrom and W.G. Mallard, Release June 2005, National Institute of Standards and Technology, Gaithersburg MD, 20899 (<http://webbook.nst.gov>). (2005).*
54. L. Puskar and A. J. Stace, UV photofragmentation of gas phase  $\text{M}^+$  and  $\text{M}^{2+}$  complexes with ketones, where  $\text{M} = \text{Cu}$  and  $\text{Ag}$ , *Mol. Phys.*, **103**, 1829-1835 (2005).
55. K. F. Willey, P. Y. Cheng, M. B. Bishop and M. A. Ducan, Charge-Transfer Photochemistry in Ion Molecule Cluster Complexes of Silver, *J. Am. Chem. Soc.*, **113**, 4721-4728 (1991).

56. M. T. Rodgers, J. R. Stanley and R. Amunugama, Periodic Trends in the Binding of Metal Ions to Pyridine Studied by Threshold Collision-Induced Dissociation and Density Functional Theory, *J. Am. Chem. Soc.*, **122**, 10969 - 10978 (2000).
57. N. S. Rannulu and M. T. Rodgers, Noncovalent interactions of Cu<sup>+</sup> with N-donor ligands (pyridine, 4,4-dipyridyl, 2,2-dipyridyl, and 1,10-phenanthroline): collision-induced dissociation and theoretical studies, *J. Phys. Chem. A*, **111**, 3465-3479 (2007).
58. D. Wu, B. Ren, Y. Jiang, X. Xu and Z. Tian, Density Functional Study and Normal-Mode Analysis of the Bindings and Vibrational Frequency Shifts of the Pyridine-M (M = Cu, Ag, Au, Cu<sup>+</sup>, Ag<sup>+</sup>, Au<sup>+</sup>, and Pt) Complexes, *J. Phys. Chem. A*, **106**, 9042 (2002).
59. J. Miyawaki and K. Sugawara, ZEKE photoelectron spectroscopy of the silver- and copper-ammonia complexes, *J. Chem. Phys.*, **119**, 6539-6545 (2003).
60. T. G. Spence, B. T. Trotter and L. A. Posey, Ligand-field photochemistry of the [Cu<sup>II</sup>(bpy)(serine-H)]<sup>+</sup> complex in the gas phase, *Inter. J. Mass Spectrom.*, **177**, 187-196 (1998).
61. C. L. Gatlin, F. Turecek and T. Vaisar, Gas-Phase Complexes of Amino-Acids with Cu(II) and Diimine Ligands .2. Amino-Acids with O, N and S Functional-Groups in the Side-Chain, *J. Mass. Spect.*, **30**, 1617-1627 (1995).
62. L. Puskar, P. E. Barran, R. R. Wright, D. A. Kirkwood and A. J. Stace, The ultraviolet photofragmentation of doubly charged transition metal complexes in the gas phase: Initial results for [Cu.(pyridine)<sub>n</sub>]<sup>+2</sup> and [Ag.(pyridine)<sub>n</sub>]<sup>+2</sup> ions *J. Chem. Phys.*, **112**, 7751-7754 (2000).
63. L. Puskar and A. J. Stace, Gas phase ligand field photofragmentation spectroscopy, *J. Chem. Phys.*, **114**, 6499-6501 (2001).
64. L. Puskar, H. Cox, A. Goren, G. Aitken and A. J. Stace, Ligand field spectroscopy of Cu(II) and Ag(II) complexes in the gas phase: theory and experiment, *Faraday Disc.*, **124**, 259 (2003).
65. R. R. Wright, N. R. Walker, S. Firth and A. J. Stace, Coordination and Chemistry of Stable Cu(II) Complexes in the Gas Phase, *J. Phys. Chem. A*, **105**, 54-64 (2001).
66. G. Wu, J. Guan, G. Aitken, H. Cox and A. J. Stace, Infrared multiphoton spectra from metal dication complexes in the gas phase, *J. Chem. Phys.*, **124**, 201103 (2006).



67. M. Chachisvilis and A. H. Zewail, Femtosecond dynamics of pyridine in the condensed phase: Valence isomerization by conical intersections, *J. Phys. Chem. A*, **103**, 7408-7418 (1999).
68. A. J. Stace, Metal ions in hydrogen bonded solvents: a gas phase perspective, *Phys. Chem. Chem. Phys.*, **3**, 1935-1941 (2001).
69. A. B. P. Lever, *Inorganic Electronic Spectroscopy*, 2nd ed, Elsevier, Amsterdam, 1984.
70. D. L. Leussing and R. C. Hansen, The Copper(II)-Pyridine Complexes and Their Reaction with Hydroxide Ions, *J. Am. Chem. Soc.*, **79**, 4270-4273 (1957).
71. K. Ozutsumi and T. Kawashima, Exafs and Spectrophotometric Studies on the Structure of Pyridine Complexes with Copper(II) and Copper(I) Ions in Aqueous-Solution, *Polyhedron*, **11**, 169-175 (1992).
72. L. Petit, C. Adamo and N. Russo, Absorption spectra of first-row transition metal complexes of bacteriochlorins: a theoretical analysis, *J. Phys. Chem. B*, **109**, 12214-12221 (2005).
73. A. D. Quartarolo, N. Russo, E. Sicilia and F. Lejl, Absorption Spectra of the Potential Photodynamic Therapy Photosensitizers Texaphyrins Complexes: A Theoretical Analysis, *J. Chem. Theory Comput.*, **3**, 860-869 (2007).
74. B. S. Freiser, *Organometallic Ion Chemistry*, Kluwer Academic Publishers, Dordrecht, 1996.
75. C. H. Ruan, Z. B. Yang and M. T. Rodgers, Influence of the d orbital occupation on the nature and strength of copper cation- $\pi$  interactions: threshold collision-induced dissociation and theoretical studies, *Phys. Chem. Chem. Phys.*, **9**, 5902-5918 (2007).
76. B. A. Cerda and C. Wesdemiotis, The Relative Copper(I) Ion Affinities of Amino Acids in the Gas Phase, *J. Am. Chem. Soc.*, **117**, 9734-9739 (1995).
77. T. Shoeib, C. Rodriguez, K. Michael Siu and A. C. Hopkinson, A comparison of copper(I) and silver(I) complexes of glycine, diglycine and triglycine, *Phys. Chem. Chem. Phys.*, **3**, 853-861 (2001).
78. M. Belcastro, T. Marino, N. Russo and M. Toscano, Interaction of cysteine with  $\text{Cu}^{2+}$  and group IIb ( $\text{Zn}^{2+}$ ,  $\text{Cd}^{2+}$ ,  $\text{Hg}^{2+}$ ) metal cations: a theoretical study, *J. Mass. Spect.*, **40**, 300-306 (2005).
79. D. Schröder, R. Wesendrup, R. H. Hertwig, T. K. Dargel, H. Grauel, W. Koch, B. R. Bender and H. Schwarz, Equilibrium isotope effects in cationic transition-metal(I)

ethene complexes  $M(C_2X_4)^+$  with  $M = Cu, Ag, Au$  and  $X = H, D$ , *Organometallics*, **19**, 2608-2615 (2000).

80. A. W. Ehlers, C. G. d. Koster, R. J. Meier and K. Lammertsma, MALDI-TOF-MS of Saturated Polyolefins by Coordination of Metal Cations: A Theoretical Study, *J. Phys. Chem. A*, **105**, 8691-8695 (2001).

81. J. Bertrán, L. Rodríguez-Santiago and M. Sodupe, The Different Nature of Bonding in  $Cu^+$ -Glycine and  $Cu^{2+}$ -Glycine, *J. Phys. Chem. B*, **103**, 2310-2317 (1999).

82. M. T. Rodgers and P. B. Armentrout, Influence of *d* Orbital Occupation on the Binding of Metal Ions to Adenine, *J. Am. Chem. Soc.*, **124**, 2678-2691 (2002).

83. N. Russo, M. Toscano and G. A., Gas-phase theoretical prediction of the metal affinity of copper(I) ion for DNA and RNA bases, *J. Mass. Spect.*, **38**, 265-270 (2003).

84. A. M. Lamsabhi, M. Alcamí, O. Mó and M. Yáñez, Gas-Phase Reactivity of Uracil, 2-Thiouracil, 4-Thiouracil, and 2,4-Dithiouracil towards the  $Cu^+$  Cation :A DFT Study, *ChemPhysChem*, **4**, 1011-1016 (2003).

85. A. Luna, M. Alcamí, O. Mó and M. Yáñez,  $Cu^+$  reactivity trends in  $sp$ ,  $sp^2$ , and  $sp^3$  nitrogen, phosphorus and arsenic containing bases, *Int. J. Mass Spectrom.*, **201**, 215-231 (2000).

86. L. Galiano, M. Alcamí, O. Mó and M. Yáñez, Gas-Phase Chemistry of Ethyl and Vinyl Amines, Phosphines, and Arsines: A DFT Study of the Structure and Stability of Their  $Cu^+$  Complexes, *J. Phys. Chem. A*, **106**, 9306-9312 (2002).

87. L. Galiano, M. Alcamí, O. Mó and M. Yáñez, Gas-Phase Chemistry of Ethynylamine, -Phosphine and -Arsine. Structure and Stability of their  $Cu^+$  and  $Ni^+$  Complexes, *ChemPhysChem*, **4**, 72-78 (2003).

88. G. Vitale, A. B. Valina, H. Huang, R. Amunugama and M. T. Rodgers, Solvation of Copper Ions by Acetonitrile. Structures and Sequential Binding Energies of  $Cu^+(CH_3CN)_x$ ,  $x = 1-5$ , from Collision-Induced Dissociation and Theoretical Studies, *J. Phys. Chem. A*, **105**, 11353-11364 (2001).

89. E. R. Fisher and P. B. Armentrout, Reactions of  $Co^+$ ,  $Ni^+$ , and  $Cu^+$  with Cyclopropane and Ethylene-Oxide - Metal Methylidene Ion Bond-Energies, *J. Phys. Chem.*, **94**, 1674-1683 (1990).

90. R. H. Hertwig, W. Koch, D. Schroder, H. Schwarz, J. Hrusak and P. Schwerdtfeger, A comparative computational study of cationic coinage metal-ethylene complexes  $(C_2H_4)M^+$  ( $M=Cu, Ag, Au$ ), *J. Phys. Chem.*, **100**, 12253-12260 (1996).

91. C. W. Bauschlicher, Jr., S. R. Langhoff and H. Partridge, The binding energies of copper<sup>+</sup>-water and copper<sup>+</sup>-ammonia complexes (Cu<sup>+</sup>-(H<sub>2</sub>O)<sub>n</sub> and Cu<sup>+</sup>-(NH<sub>3</sub>)<sub>n</sub> (n = 1-4)), *J. Chem. Phys.*, **94**, 2068-2072 (1991).
92. M. R. Sievers, L. M. Jarvis and P. B. Armentrout, Transition-Metal Ethene Bonds: Thermochemistry of M<sup>+</sup>(C<sub>2</sub>H<sub>4</sub>)<sub>n</sub> (M = Ti-Cu, n = 1 and 2) Complexes, *J. Am. Chem. Soc.*, **120**, 1891-1899 (1998).
93. J. Bera, A. Samuelson and J. Chandrasekhar, Ab Initio Study of Structures, Energetics, and Bonding in Formally High-Oxidation-State Copper Organometallics, *Organometallics*, **17**, 4136-4145 (1998).
94. C. N. Yang and S. J. Klippenstein, Theory and modeling of the binding in cationic transition-metal-benzene complexes, *J. Phys. Chem. A*, **103**, 1094-1103 (1999).
95. R. C. Dunbar, D. Solooki, C. A. Tessier, W. J. Youngs and B. Asamoto, Gas-Phase Synthesis of Metallocyclotriynes, *Organometallics*, **10**, 52-54 (1991).
96. R. C. Dunbar, G. T. Uechi, D. Solooki, C. A. Tessier, W. Youngs and B. Asamoto, Reactions of Gas-Phase Atomic Metal-Ions with the Macrocyclic Ligand Tribenzocyclotriyne, *J. Am. Chem. Soc.*, **115**, 12477-12482 (1993).
97. F. Meyer, F. A. Khan and P. B. Armentrout, Thermochemistry of Transition-Metal Benzene Complexes - Binding-Energies of M(C<sub>6</sub>H<sub>6</sub>)<sub>X</sub><sup>+</sup> (X=1, 2) for M=Ti to Cu, *J. Am. Chem. Soc.*, **117**, 9740-9748 (1995).
98. R. Amunugama and M. T. Rodgers, Periodic Trends in the Binding of Metal Ions to Pyrimidine Studied by Threshold Collision-Induced Dissociation and Density Functional Theory, *J. Phys. Chem. A*, **105**, 9883-9892 (2001).
99. H. Koizumi and P. B. Armentrout, Collision-Induced Dissociation and Theoretical Studies of Cu<sup>+</sup>-Dimethoxyethane Complexes, *J. Am. Soc. Mass Spectrom.*, **12**, 480-489 (2001).
100. H. Koizumi, X. Zhang and P. B. Armentrout, Collision-Induced Dissociation and Theoretical Studies of Cu<sup>+</sup> Dimethyl Ether Complexes, *J. Phys. Chem. A*, **105**, 2444-2452 (2001).
101. M. Porento and P. Hirva, Theoretical studies on the interaction of anionic collectors with Cu<sup>+</sup>, Cu<sup>2+</sup>, Zn<sup>2+</sup> and Pb<sup>2+</sup> ions, *Theor. Chem. Acc.*, **107**, 200-205 (2002).
102. D. W. Fuerstenau, R. Herrera-Urbina and D. W. McGlashan, Studies on the applicability of chelating agents as universal collectors for copper minerals, *Int. J. Miner. Process.*, **58**, 15-33 (2000).

103. I. Georgieva and N. Trendafilova, Bonding analyses, formation energies, and vibrational properties of M-R<sub>2</sub>dtc complexes (M=Ag(I), Ni(II), Cu(II), or Zn(II)), *J. Phys. Chem. A*, **111**, 13075-13087 (2007).
104. I. Corral, O. Mó and M. Yáñez, Binding energies of Cu<sup>+</sup> to saturated and  $\alpha,\beta$ -unsaturated alkanes, silanes and germanes. The role of agostic interactions., *Int. J. Mass Spectrom.*, **107**, 1370-1376 (2003).
105. I. Corral, O. Mó and M. Yáñez, Agostic vs.  $\pi$ -interactions in complexes of ethynyl-silanes and ethynyl-germanes with Cu<sup>+</sup> in the gas phase, *J. Phys. Chem. A*, **107**, 1370-1376 (2003).
106. N. S. Rannulu and M. T. Rodgers, Solvation of copper ions by imidazole: Structures and sequential binding energies of Cu<sup>+</sup>(imidazole)<sub>x</sub>, x = 1–4. Competition between ion solvation and hydrogen bonding, *Phys. Chem. Chem. Phys.*, **7**, 1014-1025 (2005).
107. Y. D. Hill, B. S. Freiser and C. W. Bauschlicher, Unexpected Displacement of Alkenes by Alkanes in the Reactions of Y(Alkene)<sup>2+</sup> : An Experimental and Theoretical-Study, *J. Am. Chem. Soc.*, **113**, 1507-1510 (1991).
108. E. D. Glendening, A. E. Reed and F. Weinhold, "NBO version 3.1."
109. M. Brookhart and M. L. H. Green, Carbon-Hydrogen-Transition Metal Bonds, *J. Organomet. Chem.*, **250**, 395-408 (1983).
110. M. J. S. Dewar, A review of pi complex theory, *Bull. Soc. Chim. Fr.*, **C79**, 18 (1951).
111. J. Chatt and L. A. Duncanson, Olefin Co-Ordination Compounds .3. Infra-Red Spectra and Structure - Attempted Preparation of Acetylene Complexes, *J. Chem. Soc.* , 2939-2947 (1953).
112. T. Ziegler and A. Rauk, Theoretical-Study of the Ethylene-Metal Bond in Complexes between Cu<sup>+</sup>, Ag<sup>+</sup>, Au<sup>+</sup>, Pt<sup>0</sup>, or Pt<sup>2+</sup> and Ethylene, Based on the Hartree-Fock-Slater Transition-State Method, *Inorg. Chem.*, **18**, 1558-1565 (1979).
113. D. Feller and D. A. Dixon, Metal Ion Binding: An Electronic Structure Study of M(Dimethyl Ether)<sub>n</sub>, M = Cu, Ag, and Au and (n = 1–4), Complexes, *J. Phys. Chem. A*, **106**, 5136-5143 (2002).
114. J. V. Burda, M. K. Shukla and J. Leszczynski, Theoretical model of the aqua-copper [Cu(H<sub>2</sub>O)<sub>5</sub>]<sup>+</sup> cation interactions with guanine, *J. Mol. Model.*, **11**, 362-369 (2005).

115. M. Pavelka, M. K. Shukla, J. Leszczynski and J. V. Burda, Theoretical study of hydrated copper(II) interactions with guanine: a computational density functional theory study, *J. Phys. Chem. A*, **112**, 256-267 (2008).
116. Y. Yoshioka, H. Kawai, T. Sato, K. Yamaguchi and I. Saito, Ab Initio Molecular Orbital Study on the G-Selectivity of GGG Triplet in Copper(I)-Mediated One-Electron Oxidation, *J. Am. Chem. Soc.*, **125**, 1968-1974 (2003).
117. L. Rulisek and J. Sponer, Outer-shell and inner-shell coordination of phosphate group to hydrated metal ions ( $Mg^{2+}$ ,  $Cu^{2+}$ ,  $Zn^{2+}$ ,  $Cd^{2+}$ ) in the presence and absence of nucleobase. The role of nonelectrostatic effects, *J. Phys. Chem. B*, **107**, 1913-1923 (2003).
118. Z. Yang, N. S. Rannulu, Y. Chu and M. T. Rodgers, Bond dissociation energies and equilibrium structures of  $Cu^+(MeOH)_x$ ,  $x = 1-6$ , in the gas phase: competition between solvation of the metal ion and hydrogen-bonding interactions, *J. Phys. Chem. A*, **112**, 388-401 (2008).
119. Y. Chu, Z. Yang and M. T. Rodgers, Solvation of Copper Ions by Acetone. Structures and Sequential Binding Energies of  $Cu^+(acetone)_x$ ,  $x = 1-4$  from Collision-Induced Dissociation and Theoretical Studies, *J. Am. Soc. Mass Spectrom.*, **13**, 453-468 (2002).
120. M. Y. Combariza and R. W. Vachet, Effect of Coordination Geometry on the Gas-Phase Reactivity of Four-Coordinate Divalent Metal Ion Complexes, *J. Phys. Chem. A*, **108**, 1757-1763 (2004).
121. A. Luna, B. Amekraz, J. P. Morizur, J. Tortajada, O. Mó and M. Yáñez, Reactions of Urea with  $Cu^+$  in the Gas Phase: An Experimental and Theoretical Study, *J. Phys. Chem. A*, **104**, 3132-3141 (2000).
122. M. Rosi and C. W. Bauschlicher, Jr., The binding energies of one and two water molecules to the first transition row metal positive ions, *J. Chem. Phys.*, **90**, 7264-7272 (1989).
123. M. Rosi and C. W. Bauschlicher, Jr., The binding energies of one and two water molecules to the first-row transition metal positive ions. II, *J. Chem. Phys.*, **92**, 1876-1878 (1990).
124. C. W. Bauschlicher, S. R. Langhoff and H. Partridge, The Binding-Energies of  $Cu^+(H_2O)_n$  and  $Cu^+(NH_3)_n$  ( $n = 1-4$ ), *J. Chem. Phys.*, **94**, 2068-2072 (1991).

125. A. M. Lamsabhi, M. Alcamí, O. Mó, M. Yáñez and J. Tortajada, Association of  $\text{Cu}^{2+}$  with Uracil and its Thio Derivatives : A Theoretical Study, *ChemPhysChem*, **5**, 1871-1879 (2004).
126. S. Pulkkinen, M. Noguera, L. Rodríguez-Santiago, M. Sodupe and J. Bertran, Gas Phase Intramolecular Proton Transfer in Cationized Glycine and Chlorine Substituted Derivatives (M-Gly, M= $\text{Na}^+$ ,  $\text{Mg}^+$ ,  $\text{Cu}^+$ ,  $\text{Ni}^+$  and  $\text{Cu}^{2+}$ ): Existence of Zwitterionic Structures ?, *Chem. Eur. J*, **6**, 4393-4399 (2000).
127. C. Sivasankar, N. Sadhukhan, J. Bera and A. Samuelson, Is copper(I) hard or soft? A density functional study of mixed ligand complexes, *New J. Chem*, **31**, 385 (2007).
128. X. Wang, B. Sohnlein, S. Li, J. Fuller and D. Yang, Pulsed-field ionization electron spectroscopy and molecular structures of copper-(pyridine)<sub>n</sub> (n = 1, 2) complexes, *Can. J. Chem.*, **85**, 714-723 (2007).
129. B. Ni, J. R. Kramer and N. H. Werstiuk, Density functional theory and QT atoms-in-molecules study on the hydration of CuI and AgI ions and sulfides, *J. Phys. Chem. A*, **109**, 1548-1558 (2005).
130. D. Feller, E. D. Glendening and W. A. d. Jong, Structures and binding enthalpies of  $\text{M}^+(\text{H}_2\text{O})_n$  clusters, M=Cu, Ag, Au, *J. Chem. Phys.*, **110**, 1475-1491 (1999).
131. D. Caraiman, T. Shoeib, K. M. Siu, A. C. Hopkinson and D. K. Bohme, Investigations of the gas-phase reactivity of  $\text{Cu}^+$  and  $\text{Ag}^+$  glycine complexes towards CO, D<sub>2</sub>O and NH<sub>3</sub>, *Inter. J. Mass Spectrom.*, **228**, 629-646 (2003).
132. N. R. Walker, S. Firth and A. J. Stace, Stable Cu(II) co-ordination complexes in the gas phase, *Chem. Phys. Lett.*, **292**, 125-132 (1998).
133. A. Bérces, T. Nukada, P. Margl and T. Ziegler, Solvation of  $\text{Cu}^{2+}$  in Water and Ammonia. Insight from Static and Dynamical Density Functional Theory, *J. Phys. Chem. A*, **103**, 9693-9701 (1999).
134. G. W. Marini, K. R. Liedl and B. M. Rode, Investigation of  $\text{Cu}^{2+}$  Hydration and the Jahn-Teller Effect in Solution by QM/MM Monte Carlo Simulations, *J. Phys. Chem. A*, **103**, 11387-11393 (1999).
135. H. D. Pranowo, A. H. B. Setiaji and B. M. Rode,  $\text{Cu}^+$  in Liquid Ammonia and in Water: Intermolecular Potential Function and Monte Carlo Simulation, *J. Phys. Chem. A*, **103**, 11115-11120 (1999).

136. C. F. Schwenk and B. M. Rode, Extended ab initio quantum mechanical/molecular mechanical molecular dynamics simulations of hydrated  $\text{Cu}^{2+}$ , *J. Chem. Phys.*, **119**, 9523-9531 (2003).
137. C. F. Schwenk and B. M. Rode, New Insights into the Jahn-Teller Effect through ab initio Quantum-Mechanical/Molecular-Mechanical Molecular Dynamics Simulations of Cu(II) in Water, *ChemPhysChem*, **4**, 931-943 (2003).
138. C. F. Schwenk and B. M. Rode, Cu(II) in Liquid Ammonia : An Approach by Hybrid Quantum-Mechanical/Molecular-Mechanical Molecular Dynamics Simulation, *ChemPhysChem*, **5**, 342-348 (2004).
139. H. D. Pranowo and B. M. Rode, Solvation of  $\text{Cu}^{2+}$  in Liquid Ammonia: Monte Carlo Simulation Including Three-Body Corrections, *J. Phys. Chem. A*, **103**, 4298-4302 (1999).
140. C. F. Schwenk and B. M. Rode, The influence of the Jahn-Teller effect and of heteroligands on the reactivity of  $\text{Cu}^{2+}$ , *Chem. Commun.*, 1286-1287 (2003).
141. T. Marino, M. Toscano, N. Russo and A. Grand, Structural and electronic characterization of the complexes obtained by the interaction between bare and hydrated first-row transition-metal ions ( $\text{Mn}^{2+}$ ,  $\text{Fe}^{2+}$ ,  $\text{Co}^{2+}$ ,  $\text{Ni}^{2+}$ ,  $\text{Cu}^{2+}$ ,  $\text{Zn}^{2+}$ ) and glycine, *J. Phys. Chem. B*, **110**, 24666-24673 (2006).
142. D. F. Raffa, R. Gomez-Balderas, P. Brunelle, G. A. Rickard and A. Rauk, Ab initio model studies of copper binding to peptides containing a His-His sequence: relevance to the  $\beta$ -amyloid peptide of Alzheimer's disease, *J. Biol. Inorg. Chem.*, 887-902 (2005).
143. R. Gómez-Balderas, D. F. Raffa, G. A. Rickard, P. Brunelle and A. Rauk, Computational studies of Cu(II)/Met and Cu(I)/Met binding motifs relevant for the chemistry of Alzheimer's disease, *J. Phys. Chem. A*, **109**, 5498-5508 (2005).
144. M. H. M. Olsson, U. Ryde, B. O. Roos and K. Pierloot, On the relative stability of tetragonal and trigonal Cu(II) complexes with relevance to the blue copper proteins, *J. Biol. Inorg. Chem.*, **3**, 109-125 (1998).
145. M. H. M. Olsson and U. Ryde, The influence of axial ligands on the reduction potential of blue copper proteins, *J. Biol. Inorg. Chem.*, **4**, 654-663 (1999).
146. K. Paraskevopoulos, M. Sundararajan, R. Surendran, M. Hough, R. Eady, I. Hillier and S. Hasnain, Active site structures and the redox properties of blue copper proteins: atomic resolution structure of azurin II and electronic structure calculations of azurin, plastocyanin and stellacyanin, *Dalton Trans.*, 3067 (2006).

147. I. Corral, O. Mó and M. Yáñez, Bonding and Bonding Perturbation in Ion-Molecule Interactions in the Gas Phase, in *Encyclopedia of Computational Chemistry*. URL: <http://www.mrw.interscience.wiley.com/eccarticles/cn0062/frame.html>, 2004.
148. D. Cremer and E. Kraka, Chemical bonding without binding electron densities: Is differential density analysis sufficient for bonding description?, *Angew. Chem.*, **96**, 612-614 (1984).
149. J. Zhang, V. Frankevich, R. Knochenmuss, S. D. Friess and R. Zenobi, Reduction of Cu(II) in Matrix-Assisted Laser Desorption/Ionization Mass Spectrometry, *J. Am. Soc. Mass Spectrom.*, **14**, 42-50 (2003).
150. A. M. Lamsabhi, M. Alcamí, O. Mó, M. Yáñez and J. Tortajada, Gas-phase deprotonation of uracil-Cu<sup>2+</sup> and thiouracil-Cu<sup>2+</sup> complexes, *J. Phys. Chem. A*, **110**, 1943-1950 (2006).
151. A. M. Lamsabhi, M. Alcamí, O. Mó, M. Yáñez, J. Tortajada and J. Y. Salpin, Unimolecular Reactivity of Uracil-Cu<sup>2+</sup> Complexes in the Gas Phase, *ChemPhysChem*, **8**, 181-187 (2007).
152. D. Xing, X. Tan, X. Chen and Y. Bu, Theoretical study on the gas-phase acidity of multiple sites of Cu<sup>+</sup>-adenine and Cu<sup>2+</sup>-adenine complexes, *J. Phys. Chem. A*, **112**, 7418-7425 (2008).
153. C. L. Gatlin, F. Turecek and T. Vaisar, Gas-Phase Complexes of Amino-Acids with Cu(II) and Diimine Ligands .1. Aliphatic and Aromatic-Amino-Acids, *J. Mass. Spect.*, **30**, 1605-1616 (1995).
154. C. L. Gatlin, F. Turecek and T. Vaisar, Copper(II) Amino-Acid Complexes in the Gas-Phase, *J. Am. Chem. Soc.*, **117**, 3637-3638 (1995).
155. H. Lavanant, E. Hecquet and Y. Hoppilliard, Complexes of L-histidine with Fe<sup>2+</sup>, Co<sup>2+</sup>, Ni<sup>2+</sup>, Cu<sup>2+</sup>, Zn<sup>2+</sup> studied by electrospray ionization mass spectrometry, *Inter. J. Mass Spectrom.*, **185/186/187**, 11-23 (1999).
156. M. Noguera, J. Bertran and M. Sodupe, A quantum chemical study of Cu<sup>2+</sup> interacting with guanine-cytosine base pair. Electrostatic and oxidative effects on intermolecular proton-transfer processes, *J. Phys. Chem. A*, **108**, 333-341 (2004).
157. M. Noguera, J. Bertran and M. Sodupe, Cu<sup>2+/+</sup> cation coordination to adenine-thymine base pair. Effects on intermolecular proton-transfer processes, *J. Phys. Chem. B*, **112**, 4817-4825 (2008).
158. N. R. Walker, R. R. Wright, P. E. Barran, J. N. Murrell and A. J. Stace, Comparisons in the Behavior of Stable Copper(II), Silver(II), and Gold(II) Complexes



in the Gas Phase: Are There Implications for Condensed-Phase Chemistry?, *J. Am. Chem. Soc.*, **123**, 4223-4227 (2001).

159. J. Allison, R. B. Freas and D. P. Ridge, Cleavage of alkanes by transition-metal ions in the gas-phase, *J. Am. Chem. Soc.*, **101**, 1332-1333 (1979).

160. P. B. Armentrout and J. L. Beauchamp, The chemistry of atomic transition-metal ions - insight into fundamental-aspects of organometallic chemistry, *Acc. Chem. Res.*, **22**, 315-321 (1989).

161. P. B. Armentrout, Electronic state-specific transition-metal ion chemistry, *Ann. Rev. Phys. Chem.*, **41**, 313-344 (1990).

162. K. Eller and H. Schwarz, Organometallic chemistry in the gas-phase, *Chem. Rev.*, **91**, 1121-1177 (1991).

163. J. C. Weisshaar, Control of transition-metal cation reactivity by electronic state selection, *Adv. Chem. Phys.*, **82**, 213-262 (1992).

164. P. B. Armentrout, Thermochemical Measurements by Guided Ion Beam Mass Spectrometry, in *Selective Hydrocarbons Activation: Principles and Progress*, edited by J. A. Davis, P. L. Watson, A. Greenberg and J. F. Liebman VCH, New York, 1993.

165. J. C. Weisshaar, Bare transition metal atoms in the gas phase: reactions of M, M<sup>+</sup>, and M<sup>2+</sup> with hydrocarbons, *Acc. Chem. Res.*, **26**, 213-219 (1993).

166. G. A. Somorjai, *Introduction to Surface Chemistry and Catalysis*, John Wiley & Sons, New York, 1994.

167. P. B. Armentrout and B. L. Kickel, Gas-Phase Thermochemistry of Transition Metal Ligand Systems: Reassessment of Values and Periodic Trends, in *Organometallic Ion Chemistry*, edited by B. S. Freiser Kluwer, Dordrecht, The Netherlands, 1996.

168. P. B. Armentrout, Organometallic Bonding and Reactivity, in *Topics in Organometallics Ion Chemistry, Vol. 4. Gas-Phase Organometallic Chemistry*, edited by J. Brown and P. Hofman Spring-Verlag, Berlin, 1999.

169. A. M. Lamsabhi, M. Alcamí, O. Mó, W. Bouab, M. Esseffar, J. L. Abboud and M. Yáñez, Are the Thiouracils Sulfur Bases in the Gas-phase?, *J. Phys. Chem. A*, **104**, 5122-5130 (2000).

170. M. Esseffar, W. Bouab, A. M. Lamsabhi, J. L. Abboud, R. Notario and M. Yáñez, An Experimental and Theoretical Study on Some Thiocarbonyl-I<sub>2</sub> Molecular Complexes, *J. Am. Chem. Soc.*, **122**, 2300-2308 (2000).

171. A. Luna, B. Amekraz, J. Tortajada, J. P. Morizur, M. Alcamí, O. Mó and M. Yáñez, Modeling the Interactions between Peptide Functions and Cu(I): Formamide-Cu<sup>+</sup> Reactions in the Gas Phase, *J. Am. Chem. Soc.*, **120**, 5411-5426 (1998).
172. A. Luna, J. P. Morizur, J. Tortajada, M. Alcamí, O. Mó and M. Yáñez, Role of Cu<sup>+</sup> Association on the Formamide --> Formamidic Acid -->(Aminohydroxy)carbene Isomerizations in the Gas Phase, *J. Phys. Chem. A*, **102**, 4652-4659 (1998).
173. D. S. Schroder, T. Weiske and H. Schwarz, Dissociation behavior of Cu(urea)<sup>+</sup> complexes generated by electrospray ionization, *Inter. J. Mass Spectrom.*, 729-738 (2002).
174. A. Luna, B. Amekraz, J. Morizur, J. Tortajada, O. Mó and M. Yáñez, Reactions between Guanidine and Cu<sup>+</sup> in the Gas Phase. An Experimental and Theoretical Study, *J. Phys. Chem. A*, **101**, 5931-5941 (1997).
175. Y. Huang, P. Su and C. S. Yeh, Gas-Phase Studies of Group-11 Cation (Cu<sup>+</sup>, Ag<sup>+</sup>, and Au<sup>+</sup>) Reactions with 2-Propanol in a Supersonic Beam-Expansion Source, *Bull. Chem. Soc. Jpn.*, **74**, 677-688 (2001).
176. M. Cheng and C. H. Hu, Reactions of 2-Propanol with Cu<sup>+</sup> in the Gas Phase: A Density Functional Theory Study, *J. Phys. Chem. A*, **106**, 11570-11580 (2002).
177. M. Alcamí, A. Luna, O. Mó, M. Yáñez, J. Tortajada and B. Amekraz, Unimolecular Reactivity of Strong Metal-Cation Complexes in the Gas Phase: Ethylenediamine-Cu<sup>+</sup>, *Chem. Eur. J.*, **10**, 2927-2934 (2004).
178. A. Luna, O. Mó, M. Yáñez, J. P. Morizur, E. Leclerc, B. Desmazières, V. Haldys, J. Chamot-Rooke and J. Tortajada, Specific reactivity of 1-alkenes with transition metal cations 1-Pentene- and 1-octene-Cu<sup>+</sup> reactions in the gas phase, *Inter. J. Mass Spectrom.*, **228**, 359-371 (2003).
179. P. J. Fordham, J. Chamot-Rooke, E. Giudice, J. Tortajada and J. P. Morizur, Analysis of Alkenes by Copper Ion Chemical Ionization Gas Chromatography/Mass Spectrometry and Gas Chromatography/Tandem Mass Spectrometry, *J. Mass. Spect.*, **34**, 1007-1017 (1999).
180. D. S. Schroder, H. Schwarz, J. Wu and C. Wesdemiotis, Long-lived dications of Cu (H<sub>2</sub>O)<sup>2+</sup> and Cu(NH<sub>3</sub>)<sup>2+</sup> do exist!, *Chem. Phys. Lett.*, **343**, 258-264 (2001).
181. J. A. Stone, T. Su and D. Vukomanovic, A collisionally activated dissociation (CAD) and computational investigation of doubly and singly charged DMSO complexes of Cu<sup>2+</sup>, *Can. J. Chem.*, **83**, 1921-1935 (2005).

182. H. Lavanant and Y. Hoppilliard, Formation and fragmentation of alpha-amino acids complexed by  $\text{Cu}^+$ , *J. Mass. Spect.*, **32**, 1037-1049 (1997).
183. Y. Hoppilliard, G. Ohanessian and S. Bourcier, Fragmentation Mechanisms of Glycine- $\text{Cu}^+$  in the Gas Phase. An Experimental and Theoretical Study, *J. Phys. Chem. A*, **108**, 9687-9696 (2004).
184. A. Rimola, M. Sodupe, J. Tortajada and L. Rodríguez-Santiago, Gas phase reactivity of  $\text{Cu}^+$ -aromatic amino acids. An experimental and theoretical study, *Inter. J. Mass Spectrom.*, **257**, 60-69 (2006).
185. E. R. Talaty, B. A. Perera, A. L. Gallardo, J. M. Barr and M. J. Van Stipdonk, Elucidation of Fragmentation Pathways for the Collision-Induced Dissociation of the Binary Ag(I) Complex with Phenylalanine, *J. Phys. Chem. A*, **105**, 8059-8068 (2001).
186. C. Seto and J. A. Stone, Low energy collisionally activated dissociation of  $\text{Cu}^{2+}(\text{glycine})(\text{H}_2\text{O})$ ,  $\text{Cu}^{2+}(\text{glycine})(\text{H}_2\text{O})_2$ ,  $\text{Cu}^{2+}(\text{glycine})_2$ , and  $\text{Cu}^{2+}(\text{glycylglycine})_2$ , *Inter. J. Mass Spectrom.*, **192**, 289-302 (1999).
187. R. Tauler and B. M. Rode, Reactions Of Cu(II) With Glycine And Glycylglycine In Aqueous-Solution At High-Concentrations Of Sodium-Chloride, *Inorg. Chim. Acta*, **173**, 93-98 (1990).
188. K. R. Liedl and B. M. Rode, Ab initio Calculations Concerning The Reaction-Mechanism Of The Copper(II) Catalyzed Glycine Condensation In Aqueous Sodium-Chloride Solution, *Chem. Phys. Lett.*, **197**, 181-186 (1992).
189. S. A. McLuckey, D. Cameron and R. G. Cooks, Proton Affinities from Dissociations of Proton-Bound Dimers, *J. Am. Chem. Soc.*, **103**, 1313-1317 (1981).
190. W. A. Tao, D. Zhang, E. N. Nikolaev and R. G. Cooks, Copper(II)-Assisted Enantiomeric Analysis of D,L-Amino Acids Using the Kinetic Method: Chiral Recognition and Quantification in the Gas Phase, *J. Am. Chem. Soc.*, **122**, 10598-10609 (2000).
191. R. G. Cooks, J. S. Patrick, T. Kotiaho and S. A. McLuckey, Thermochemical Determinations by the Kinetic Method, *Mass Spectrom. Rev.*, **13**, 287-339 (1994).
192. W. A. Tao, D. Zhang, F. Wang, P. D. Thomas and R. G. Cooks, Kinetic Resolution of D,L-Amino Acids Based on Gas-Phase Dissociation of Copper(II) Complexes, *Anal. Chem.*, **71**, 4427-4429 (1999).
193. P. Roepstorff and J. Fohlman, Proposal For A Common Nomenclature For Sequence Ions In Mass-Spectra Of Peptides, *Biomed. Mass Spectrom.*, **11**, 601-601 (1984).

194. S. J. Shields, B. K. Bluhm and D. H. Russell, Fragmentation chemistry of  $[M+Cu]^+$  peptide ions containing an N-terminal arginine, *J. Am. Soc. Mass Spectrom.*, **11**, 626-638 (2000).
195. T. Lin, A. H. Payne and G. L. Glish, Dissociation pathways of alkali-cationized peptides: Opportunities for C-terminal peptide sequencing, *J. Am. Soc. Mass Spectrom.*, **12**, 497-504 (2001).
196. I. K. Chu, X. Guo, T. C. Lau and K. W. M. Siu, Sequencing of argenitinated peptides by means of electrospray tandem mass spectrometry, *Anal. Chem.*, **71**, 2364-2372 (1999).
197. L. M. Teesch and J. Adams, Fragmentations Of Gas-Phase Complexes Between Alkali-Metal Ions And Peptides - Metal-Ion Binding To Carbonyl Oxygens And Other Neutral Functional-Groups, *J. Am. Chem. Soc.*, **113**, 812-820 (1991).
198. T. Yalcin, C. Khouw, I. G. Csizmadia, M. R. Peterson and A. G. Harrison, Why are B ions stable species in peptide spectra?, *J. Am. Soc. Mass Spectrom.*, **6**, 1165-1174 (1995).
199. T. Yalcin, I. G. Csizmadia, M. R. Peterson and A. G. Harrison, The structure and fragmentation of  $B_n$  ( $n \geq 3$ ) ions in peptide spectra, *J. Am. Soc. Mass Spectrom.*, **7**, 233-242 (1996).
200. B. K. Bluhm, S. J. Shields, C. A. Bayse, M. B. Hall and D. H. Russell, Determination of copper binding sites in peptides containing basic residues: a combined experimental and theoretical study, *Inter. J. Mass Spectrom.*, **204**, 31-46 (2001).
201. S. Kuenzel, D. Pretzel, J. Andert, K. Beck and S. Reissmann, Synthesis and characterization of metal binding pseudotripeptides, *J. Peptide Sci.*, **9**, 502-509 (2003).
202. A. Bossée, F. Fournier, O. Tasseau, B. Bellier and J. Tabet, Electrospray mass spectrometric study of anionic complexes of enkephalins with Cu(II): regioselective distinction of Leu/Ile at the C-terminus induced by metal reduction, *Rapid Commun. Mass Spectrom.*, **17**, 1229-1239 (2003).
203. A. Bossée, C. Afonso, F. Fournier, O. Tasseau, C. Pepe, B. Bellier and J. Tabet, Anionic copper complex fragmentations from enkephalins under low-energy collision-induced dissociation in an ion trap mass spectrometer, *J. Mass. Spect.*, **39**, 903-912 (2004).
204. P. Hu and M. L. Gross, Strong interactions of anionic peptides and alkaline earth metal ions: metal-ion-bound peptides in the gas phase, *J. Am. Chem. Soc.*, **114**, 9153-9160 (1992).

205. P. Hu and M. L. Gross, Strong interactions of anionic peptides and alkaline earth metal ions: bis(peptide) complexes in the gas phase, *J. Am. Chem. Soc.*, **114**, 9161-9169 (1992).
206. W. A. Tao, L. Wu and R. G. Cooks, Differentiation and Quantitation of Isomeric Dipeptides by Low-Energy Dissociation of Copper(II)-Bound Complexes, *J. Am. Soc. Mass Spectrom.*, **12**, 490-496 (2001).
207. L. Wu, K. Lemr, T. Aggerholm and R. G. Cooks, Recognition and Quantification of Binary and Ternary Mixtures of Isomeric Peptides by the Kinetic Method: Metal Ion and Ligand Effects on the Dissociation of Metal-Bound Complexes, *J. Am. Soc. Mass Spectrom.*, **14**, 152-160 (2003).
208. M. Lagarrigue, A. Bossée, C. Afonso, F. Fournier, B. Bellier and J. Tabet, Diastereomeric differentiation of peptides with Cu<sup>II</sup> and Fe<sup>II</sup> complexation in an ion trap mass spectrometer, *J. Mass. Spect.*, **41**, 1073-1085 (2006).
209. T. Vaisar, J. Heinecke, J. Seymour and F. Turecek, Copper-mediated intra-ligand oxygen transfer in gas-phase complexes with 3-nitrotyrosine, *J. Mass. Spect.*, **40**, 608-614 (2005).
210. J. Seymour and F. Turecek, Distinction and quantitation of leucine – isoleucine isomers and lysine – glutamine isobars by electrospray ionization tandem mass spectrometry (MS<sub>n</sub>, n = 2, 3) of copper(II) – diimine complexes, *J. Mass. Spect.*, **35**, 566-571 (2000).
211. T. Vaisar, C. L. Gatlin, R. D. Rao, J. Seymour and F. Turecek, Sequence information, distinction and quantitation of C-terminal leucine and isoleucine in ternary complexes of tripeptides with Cu(II) and 2,2' -bipyridine, *J. Mass. Spect.*, **36**, 306-316 (2001).
212. I. K. Chu, C. Rodriguez, T. Lau, A. C. Hopkinson and K. W. M. Siu, Molecular Radical Cations of Oligopeptides, *J. Phys. Chem. B*, **104**, 3393-3397 (2000).
213. I. K. Chu, C. F. Rodriguez, F. Rodriguez, A. C. Hopkinson and K. W. M. Siu, Formation of molecular radical cations of enkephalin derivatives via collision-induced dissociation of electrospray-generated copper (II) complex ions of amines and peptides, *J. Am. Soc. Mass Spectrom.*, **12**, 1114-1119 (2001).
214. S. Wee, R. A. J. O'Hair and W. D. McFadyen, Side-chain radical losses from radical cations allows distinction of leucine and isoleucine residues in the isomeric peptides Gly-XXX-Arg, *Rapid Comm. Mass Spectrom.*, **16**, 884-890 (2002).

215. S. Wee, R. A. J. O'Hair and W. D. McFadyen, Comparing the gas-phase fragmentation reactions of protonated and radical cations of the tripeptides GXR\*1, *Inter. J. Mass Spectrom.*, **234**, 101-122 (2004).
216. E. Bagheri-Majdi, Y. Ke, G. Orlova, I. K. Chu, A. C. Hopkinson and K. W. M. Siu, Copper-Mediated Peptide Radical Ions in the Gas Phase, *J. Phys. Chem. B*, **108**, 11170-11181 (2004).
217. S. Wee, R. A. J. O'Hair and W. D. McFadyen, The role of the position of the basic residue in the generation and fragmentation of peptide radical cations, *Inter. J. Mass Spectrom.*, **249-250**, 171-183 (2006).
218. I. K. Chu, S. Siu, C. Lam, J. Chan and C. Rodriguez, Formation of molecular radical cations of aliphatic tripeptides from their complexes with Cu<sup>II</sup>(12-crown-4), *Rapid Commun. Mass Spectrom.*, **18**, 1798-1802 (2004).
219. I. K. Chu, C. N. W. Lam and S. O. Siu, Facile Generation of Tripeptide Radical Cations In Vacuo via Intramolecular Electron Transfer in Cu<sup>II</sup> Tripeptide Complexes Containing Sterically Encumbered Terpyridine Ligands, *J. Am. Soc. Mass Spectrom.*, **16**, 763-771 (2005).
220. C. Lam, S. Siu, G. Orlova and I. K. Chu, Macrocyclic effect of auxiliary ligand on the gas-phase dissociation of ternary copper(II)-GGX complexes, *Rapid Commun. Mass Spectrom.*, **20**, 790-796 (2006).
221. I. K. Chu and C. N. W. Lam, Generation of Peptide Radical Dications via Low-Energy Collision-Induced Dissociation of [Cu<sup>II</sup>(terpy)(M + H)]<sup>3+</sup>, *J. Am. Soc. Mass Spectrom.*, **16**, 1795-1804 (2005).
222. J. Y. Salpin and J. Tortajada, Structural characterization of hexoses and pentoses using lead cationization. An electrospray ionization and tandem mass spectrometric study, *J. Mass. Spect.*, **37**, 379-388 (2002).
223. L. Bouteau, E. Leon, J. Y. Salpin, B. Amekraz, C. Moulin and J. Tortajada, Gas-phase reactivity of silver and copper coordinated monosaccharide cations studied by electrospray ionization and tandem mass spectrometry, *Eur. J. Mass Spectrom.*, **9**, 377-390 (2003).
224. L. T. Jensen, J. M. Peltier and D. R. Winge, Identification of a four copper folding intermediate in mammalian copper metallothionein by electrospray ionization mass spectrometry, *J. Biol. Inorg. Chem.*, **3**, 627 (1998).

225. R. M. Whittal, H. L. Ball, F. E. Cohen, A. L. Burlingame, S. B. Prusiner and M. A. Baldwin, Copper binding to octarepeat peptides of the prion protein monitored by mass spectrometry, *Protein Sci.*, **9**, 332-343 (2000).
226. T. Kurahashi, A. Miyazaki, S. Suwan and M. Isobe, Extensive Investigations on Oxidized Amino Acid Residues in H<sub>2</sub>O<sub>2</sub>-Treated Cu,Zn-SOD Protein with LC-ESI-Q-TOF-MS, MS/MS for the Determination of the Copper-Binding Site, *J. Am. Chem. Soc.*, **123**, 9268-9278 (2001).
227. A. Urvoas, B. Amekraz, C. Moulin, L. Le Clainche, R. Stöcklin and M. Moutiez, Analysis of the metal-binding selectivity of the metallochaperone CopZ from *Enterococcus hirae* by electrospray ionization mass spectrometry, *Rapid Commun. Mass Spectrom.*, **17**, 1889-1896 (2003).
228. R. Nagane, T. Koshigoe and M. Chikira, Interaction of Cu(II)-Arg-Gly-His-Xaa metallopeptides with DNA: effect of C-terminal residues, Leu and Glu, *J. Inorg. Bio.*, **93**, 204-212 (2003).
229. A. Sinz, A. J. Jin and O. Zschornig, Evaluation of the metal binding properties of a histidine-rich fusogenic peptide by electrospray ionization Fourier transform ion cyclotron resonance mass spectrometry, *J. Mass. Spect.*, **38**, 1150-1159 (2003).
230. Y. Guo, Y. Ling, B. A. Thomson and K. W. M. Siu, Combined Ion-Mobility and Mass-Spectrometry Investigations of Metallothionein Complexes Using a Tandem Mass Spectrometer with a Segmented Second Quadrupole, *J. Am. Soc. Mass Spectrom.*, **16**, 1787-1794 (2005).
231. A. Arseniev, P. Schultze, E. Worgotter, W. Braun, G. Wagner, M. Vasak, J. H. R. Kagi and K. Wuthrich, 3-Dimensional Structure Of Rabbit Liver [Cd7]Metallothionein-2a In Aqueous-Solution Determined By Nuclear Magnetic-Resonance, *J. Mol. Biol.*, **201**, 637-657 (1988).
232. H. Li and J. D. Otvos, HPLC characterization of Ag<sup>+</sup> and Cu<sup>+</sup> metal exchange reactions with Zn- and Cd-metallothioneins, *Biochemistry*, **35**, 13937-13945 (1996).
233. M. J. Stillman, Spectroscopic Studies of Copper and Silver Binding to Metallothioneins, *Metal-Based Drugs*, **6**, 277-290 (1999).
234. J. Y. Salpin, L. Boutreau, V. Haldys and J. Tortajada, Gas-phase reactivity of glycosides and methyl glycosides with Cu<sup>+</sup>, Ag<sup>+</sup> and Pb<sup>2+</sup> ions by fast-atom bombardment and tandem mass spectrometry, *Eur. J. Mass Spectrom.*, **7**, 321-330 (2001).

235. M. Alcamí, A. Luna, O. Mó, M. Yáñez, L. Bouteau and J. Tortajada, Experimental and Theoretical Investigation of the Reactions between Glucose and  $\text{Cu}^+$  in the Gas Phase, *J. Phys. Chem. A*, **106**, 2641-2651 (2002).
236. C. J. Cramer and D. G. Truhlar, Quantum-Chemical Conformational-Analysis of Glucose in Aqueous-Solution, *J. Am. Chem. Soc.*, **115**, 5745-5753 (1993).
237. A. El Firdoussi, M. Lafitte, J. Tortajada, O. Kone and J.-Y. Salpin, Characterization of the glycosidic linkage of underivatized disaccharides by interaction with  $\text{Pb}^{2+}$  ions, *J. Mass. Spect.*, **42**, 999-1011 (2007).
238. G. Smith, A. Kaffashan and J. A. Leary, Influence of coordination number and ligand size on the dissociation mechanisms of transition metal monosaccharide complexes, *Inter. J. Mass Spectrom.*, **183**, 299-310 (1999).
239. B. D. Davis and J. S. Brodbelt, Determination of the Glycosylation Site of Flavonoid Monoglucosides by Metal Complexation and Tandem Mass Spectrometry, *J. Am. Soc. Mass Spectrom.*, **15**, 1287-1299 (2004).
240. B. Domon and C. E. Costello, A Systematic Nomenclature for Carbohydrate Fragmentations in Fab-MS MS Spectra of Glycoconjugates, *Glycoconjugate J.*, **5**, 397-409 (1988).
241. D. J. Harvey, Ionization and collision-induced fragmentation of N-linked and related carbohydrates using divalent cations, *J. Am. Soc. Mass Spectrom.*, **12**, 926-937 (2001).
242. M. Shahgholi, J. H. Callahan, B. J. Rappoli and D. A. Rowley, Investigation of Copper-Saccharide Complexation Reactions using Potentiometry and Electrospray Mass Spectrometry, *J. Mass. Spect.*, **32**, 1080-1093 (1997).
243. B. Lippert, Multiplicity of metal ion binding patterns to nucleobases, *Coord. Chem. Rev.*, **200**, 487-516 (2000).
244. C. Harford and B. Sarkar, Amino terminal Cu(II)- and Ni(II)-binding (ATCUN) motif of proteins and peptides: Metal binding, DNA cleavage, and other properties, *Acc. Chem. Res.*, **30**, 123-130 (1997).
245. C. J. Burrows and J. G. Muller, Oxidative nucleobase modifications leading to strand scission, *Chem. Rev.*, **98**, 1109-1151 (1998).
246. B. Halliwell and O. I. Aruoma, DNA Damage By Oxygen-Derived Species - Its Mechanism And Measurement In Mammalian Systems, *Febs Letters*, **281**, 9-19 (1991).
247. R. Drouin, H. Rodriguez, S. W. Gao, Z. Gebreyes, T. R. Oconnor, G. P. Holmquist and S. A. Akman, Cupric ion ascorbate hydrogen peroxide-induced DNA



damage: DNA-bound copper ion primarily induces base modifications, *Free Radical Biol. Med.*, **21**, 261-273 (1996).

248. S. Wee, R. A. J. O'Hair and W. D. Mcfadyen, Can radical cations of the constituents of nucleic acids be formed in the gas phase using ternary transition metal complexes?, *Rapid Commun. Mass Spectrom.*, **19**, 1797-1805 (2005).

249. R. Cini and C. Pifferi, Supramolecular networks via hydrogen bonding and stacking interactions for adenosine 5'-diphosphate. Synthesis and crystal structure of diaqua(2,2':6',2''-terpyridine)copper(II) [adenosine 5'-diphosphato(3-)](2,2':6',2''-terpyridine)cuprate(II) adenosine 5'-diphosphate(1-) hexadecahydrate and density functional geometry optimization analysis of copper(II)- and zinc(II)pyrophosphate complexes, *J. Chem. Soc. Dalton Trans.*, 699-710 (1999).

250. P. Cheng and D. K. Bohme, Gas-phase formation of radical cations of monomers and dimers of guanosine by collision-induced dissociation of Cu(II)-guanosine complexes, *J. Phys. Chem. B*, **111**, 11075-11082 (2007).

251. R. L. Hettich, Investigating the effect of transition metal ion oxidation state on oligodeoxyribonucleotide binding by matrix-assisted laser desorption/ionization Fourier transform ion cyclotron resonance mass spectrometry, *Inter. J. Mass Spectrom.*, **204**, 55-57 (2001).